Dissertation

Submitted to the

Combined Faculties for the Natural Sciences and for Mathematics

of the Ruperto-Carola University of Heidelberg, Germany

for the degree of

Doctor of Natural Sciences

presented by

Carolin Blattner (M.Sc.)

Born in Schwetzingen, Germany

Oral examination: 21.09.2016

The Role of CCR5 in the Recruitment of MDSC to the Tumor Microenvironment

Referees:

Prof. Dr. Viktor Umansky

PD Dr. Adelheid Cerwenka

Declaration according to § 8 (3) b) and c) of the doctoral degree regulations:

b) I hereby declare that I have written the submitted dissertation myself and in this process have used no other sources or materials than those expressly indicated,

c) I hereby declare that I have not applied to be examined at any other institution, nor have I used the dissertation in this or any other form at any other institution as an examination paper, nor submitted it to any other faculty as a dissertation.

Heidelberg,

Name

The work described in this thesis was started in October 2013 and completed in July 2016 under the supervision of Prof. Dr. Viktor Umansky at the Research Group “Clinical Cooperation Unit Dermato-Oncology“ of the German Cancer Research Center (DKFZ), Heidelberg and the University Medical Center Mannheim.

I. Publications

Publication during the PhD studies:

Jacquelot, N., Enot, D.P., Flament, C., Vimond, N., Blattner, C., Pitt, J.M., Yamazaki, T., Roberti, M.P., Daillere, R., Vetizou, M., Poirier-Colame, V., Semeraro, M., Caignard, A., Slingluff Jr., C. L., Sallusto, F., Rusakiewicz, S., Weide, B., Marabelle, A., Kohort, H., Dalle, S., Cavalcanti, A., Kroemer, G., Di Giacomo, A. M., Maio, M., Wong, P., Yuan, J., Wolchok, J., Umansky, V., Eggermont, A., Zitvogel, L. (2016). Chemokine receptor patterns in lymphocytes mirror metastatic spreading in melanoma. The Journal of clinical investigation *126*, 921-937.

Conference and workshop presentations:

Blattner C.

Oral presentation: “Chemokine receptor CCR5 in the recruitment of myeloid-derived suppressor cells to melanoma microenvironment” DKFZ-MOST Workshop; 04/2015; Heidelberg, Germany

Blattner C.

Oral presentation: “CCR5 in the recruitment of myeloid-derived suppressor cells to the tumor microenvironment” Immuno Retreat DKFZ; 06/2015; Rothenfels, Germany

Blattner C.

Oral presentation: “Role of CCR5 in the recruitment of immunosuppressive cells into the melanoma microenvironment” DKFZ-MOST Workshop, 04/2016; Rehovot, Israel

Blattner C.

Poster Presentation: “Chemokine receptor CCR5 in the recruitment of myeloid-derived suppressor cells to melanoma microenvironment” CITIM 2015; 04/2015; Lubljiana, Slowenia

Blattner C.

Poster Presentation: “The role of CCR5 on MDSC in their recruitment and activation in melanoma microenvironment” CIMT 2016; 05/2016; Mainz, Germany

II. Table of Contents

I. Publications III

II. Table of Contents IV

III. Summary VIII

IV. Zusammenfassung X

1 Introduction 1

1.1 Immune system 1

1.1.1 Innate immune system 1

1.1.2 Adaptive immune system 2

1.2 The immune system and cancer immunoediting 5

1.3 MDSC 5

1.3.1 Ontogeny of MDSC 6

1.3.2 MDSC subsets in mice 7

1.3.3 MDSC subsets in human 7

1.3.4 MDSC expansion and activation 8

1.3.5 MDSC-mediated suppression of T cell function 9

1.3.6 Therapeutic targeting of MDSC 11

1.4 C-C chemokine receptor 5 12

1.4.1 CCR5 in HIV 12

1.4.2 The role of CCR5 in cancer 13

1.5 Malignant Melanoma 13

1.6 Melanoma therapy 14

1.6.1 Conventional therapy 14

1.6.2 Targeted therapies 14

1.6.3 Negative checkpoint inhibitors 15

1.7 *Ret* transgenic mouse melanoma model 15

2 Aim of the project 17

3 Materials and Methods 18

3.1 Materials 18
3.1.1 Mouse strains 18
3.1.2 Cell culture products 18
3.1.3 Cell culture media 19
3.1.4 Magnetic cell sorting (MACS) 19
3.1.5 Kits 19
3.1.6 Antibodies 20
3.1.7 Chemicals and biological reagents 21
3.1.8 Solutions 21
3.1.9 Dextramers 22
3.1.10 Routine laboratory material 22
3.1.11 Laboratory equipment 22
3.1.12 Software for data analysis 23
3.3 Methods 24
3.3.1 Determination of cell numbers 24
3.3.2 Organ preparation and single cell suspension from *ret* transgenic mice 24
3.3.3 Fluorescence activated cell sorting (FACS) 25
3.3.4 Surface staining 25
3.3.5 Intracellular staining 25
3.3.6 Bio-plex assay 25
3.3.7 Proliferation Assay 26
3.3.8 MHC dextramer staining of TRP-2 specific $CD8^+$ T cells 27
3.3.9 Analysis of MDSC migration capacity 27
3.3.10 Therapy of *ret* transgenic mice with the mCCR5-Ig fusion protein 28
3.3.11 Characteristics of melanoma patients at different stages 28
3.3.12 PBMC isolation from human peripheral blood samples 29
3.3.13 Preparation of tumor samples from melanoma patients 30
3.3.14 Statistical analysis 30

4 Results 31

4.1 The role of CCR5-CCR5 ligand interaction in melanoma-bearing mice 31

4.1.1 CCR5 expression on MDSC in melanoma-bearing mice 31

4.1.2 CCR5 expression pattern on MDSC subsets in tumor bearing mice 34

4.1.3 Increased production of chronic inflammatory mediators in melanoma lesions 36

4.1.4 Production of chronic inflammatory mediators in melanoma lesions during tumor development 38

4.1.5 Immunosuppressive activity of $CCR5^+$ MDSC in tumor bearing mice 40

4.1.6 Immunosuppressive effect of $CCR5^+$ MDSC on $CD8^+$ T cells 44

4.1.7 Chemokine-mediated migration capacity of MDSC 45

4.1.8 Role of CCR5 on various T cell subsets in melanoma-bearing mice 47

4.2 Treatment of *ret* transgenic tumor bearing mice with mCCR5-Ig 53

4.2.1 Effect of soluble CCR5-Ig on survival of *ret* transgenic mice 53

4.2.2 Analysis of immune cells in mCCR5-Ig treated tumor bearing mice 54

4.3 CCR5 expression on MDSC in melanoma patients 57

4.3.1 Elevated CCR5 expression on Mo-MDSC and Gr-MDSC in melanoma patients during tumor progression 57

4.3.2 Immunosuppressive phenotype of $CCR5^+$ Mo-MDSC and $CCR5^+$ Gr-MDSC in melanoma patients 60

4.3.3 Accumulation of $CCR5^+$ Mo-MDSC in skin tumors of melanoma patients 64

4.3.4 Increased concentration of chronic inflammatory mediators in tumors 65

4.3.5 CCR5 is highly expressed on Treg 67

5 Discussion 71

5.1 Expression of CCR5 on murine MDSC 71

5.2 Inflammatory factors in migration, accumulation and activity of MDSC 73

5.3 Pattern of CCR5 expression on Treg and non-regulatory T cells in mice 74

5.4 The role of CCR5 on MDSC in melanoma patients 75

5.5 Modulation of MDSC by chronic inflammatory factors in cancer patients 76

5.6 CCR5 expression on Treg in cancer patients 77

5.7 The role of CCR5 in anti-cancer therapy 78

5.8 Conclusion 79

6 References 80

7 Abbreviation 92

8 List of Figures 94

9 Acknowledgements 96

III. Summary

The aim of the study was to analyze the recruitment and accumulation of MDSC in the tumor microenvironment via C-C chemokine receptor type 5 (CCR5)/CRR5 ligand interaction, as well as immunosuppressive activity of CCR5-expressing tumor-infiltrating MDSC. We demonstrated that $CCR5^+$ Mo-MDSC and $CCR5^+$ Gr-MDSC accumulated during tumor progression in melanoma lesions of *ret* transgenic mice, as well as in melanoma patients at different stages. In the mouse model, the frequency of $CCR5^+$ cells was higher among Gr-MDSC than among Mo-MDSC, whereas in melanoma patients, Mo-MDSC were characterized by higher frequency of $CCR5^+$ cells. $CCR5^+$ MDSC demonstrated an increased immunosuppressive phenotype reflected by enhanced NO and ROS production, as well as ARG-1 and PD-L1 expression, as compared to their $CCR5^-$ counterpart. Both in mouse model and in melanoma patients, the concentration of CCR5 ligands such as CCL3 (MIP-1α), CCL4 (MIP-1β) and CCL5 (RANTES) and inflammatory factors such as granulocyte/macrophage colony-stimulating factor (GM-CSF), vascular endothelial growth factor (VEGF), interleukin (IL)-6 and interferon-γ (IFN-γ) were increased in skin tumors as compared to the serum that allows the migration of these cells to the tumor microenvironment. Furthermore, we demonstrated that $CCR5^+$ MDSC inhibited T cell proliferation in a dose-dependent manner and showed a tendency to stronger inhibition of T cell proliferation than their $CCR5^-$ counterparts. In addition, we detected the CCR5 expression on $CD4^+$ and $CD8^+$ T cells in *ret* transgenic melanoma bearing mice. Interestingly, the frequency of $CCR5^+$ regulatory T cells (Treg) was significantly higher than that among other T cell subsets. Antigen-experienced $CCR5^+$ Treg accumulated in advanced stage melanoma patients as compared to early stage patients and healthy donor (HD). After intraperitoneal injection of mCCR5-Ig, which blocks CCR5-CCR5 ligand interactions into tumor bearing mice, we observed a significantly increase in mouse survival as compared to the control group. Moreover, the frequency of MDSC and Treg decreased in skin tumors after mCCR5-Ig therapy. NO production by MDSC in skin tumors and the frequency of CD69 expression, reduced activated Treg in metastatic lymph nodes (LN), which indicates the therapeutic effect of mCCR5-Ig.

In summary, we demonstrated that during melanoma progression, CCR5 expressing MDSC accumulated in the tumor microenvironment and exerted strong immunosuppressive activity. This accumulation was mediated by CCR5 ligands and other inflammatory factors. Blockage of CCR5-CCR5 ligand interactions induced the prolongation of the survival of tumor bearing mice mediated by a reduced migration and immunosuppressive activity of MDSC and Treg at the tumor site. Our findings define a critical role for CCR5 in recruiting MDSC and Treg,

which can be used for the development of novel immunotherapeutic strategies for melanoma patients.

IV. Zusammenfassung

Das Ziel der Studie bestand darin, die Rekrutierung und Akkumulierung der MDSC in das Tumormilieu über die CC-Motiv-Chemokin-Rezeptor 5 (CCR5)/CCR5 Liganden Interaktion und der immunsuppressiven Aktivität der CCR5-exprimierenden, tumor-infiltrierenden MDSC zu analysieren. Unsere Untersuchungen zeigten, dass $CCR5^+$ Mo-MDSC und $CCR5^+$ Gr-MDSC in den Melanomläsionen der *ret* transgenen Mäuse sowie in Melanompatienten unterschiedlicher Stadien während der Tumorprogression akkumulieren. Die Anzahl der $CCR5^+$ Zellen war im Mausmodel unter Gr-MDSC höher also unter Mo-MDSC, wohingegen Mo-MDSC in Melanompatienten eine höhere Anzahl an $CCR5^+$ Zellen aufwiesen. $CCR5^+$ MDSC zeigten einen stärkeren immun-suppressiven Phänotyp, der sich im Vergleich zu ihrem $CCR5^-$ Gegenpart durch eine erhöhte ROS und NOS Produktion sowie ARG-1 und PD-L1 Expression auszeichnete. Sowohl im Mausmodel als auch in den Melanompatienten waren die Konzentrationen der CCR5 Liganden CCL3 (MIP-1α), CCL4 (MIP-1β) und CCL5 (RANTES), sowie die Inflammationsfaktoren granulocyte/macrophage colony-stimulating factor (GM-CSF), vascular endothelial growth factor (VEGF), interleukin (IL)-6 und interferon-γ (IFN-γ), welche die Migration dieser Zellen ins Tumormilieu ermöglichen, in Hauttumoren höher als im Serum. Weiterhin war zu beobachten, dass $CCR5^+$ MDSC die Proliferation der T Zellen zellzahl-abhängig blockieren und die T Zell Proliferation stärker inhibieren als ihr $CCR5^-$ Gegenpart. Des Weiteren wurde die CCR5 Expression auf $CD4^+$ und $CD8^+$ T Zellen in *ret* transgenen Melanom-tragenden Mäusen untersucht. Interessanterweise war die Anzahl an $CCR5^+$ regulatorischen T Zellen (Treg) signifikant höher als bei anderen T Zell Subtypen. Antigen-erfahrene $CCR5^+$ Treg akkumulierten in Melanompatienten fortgeschrittenen Stadiums im Vergleich zu Melanompatienten der frühen Phase und gesunden Spendern. Nach intraperitonealer Injektion des mCCR5-Ig, welches die CCR5-CCR5 Liganden Interaktion in Tumor-tragenden Mäusen blockiert, war bei den Mäusen im Vergleich zur Kontrollgruppe eine signifikant verlängerte Überlebensrate zu beobachten. Außerdem war die Anzahl an MDSC und Treg im Hauttumor nach der mCCR5-Ig Therapie geringer. Die NO Produktion der MDSC im Hauttumor und die Anzahl der CD69 exprimierenden, aktivierten Treg waren in den metastatischen Lymphknoten vermindert, was auf den therapeutischen Effekt von mCCR5-Ig hinweist.

Zusammenfassend wurde gezeigt, dass während der Melanom Progression CCR5-exprimierender MDSC im Tumormilieu akkumulieren und eine starke immunsuppressive Aktivität ausüben. Diese Akkumulierung wurde durch CCR5 Liganden und andere Inflammationsfaktoren vermittelt. Die Blockierung der CCR5-CCR5 Liganden

Interaktion verlängerte das Überleben der Tumor-tragenden Mäuse, welches durch eine geringere Migration und immunsuppressorische Aktivität der MDSC und Treg im Tumor einherging. Unsere Ergebnisse deuten darauf hin, dass CCR5 eine entscheidende Rolle bei der Rekrutierung von MDSC und Treg spielt, welche für die Entwicklung neuer immuntherapeutischer Strategien an Melanompatienten verwendet werden könnte.

1 Introduction

1.1 Immune system

The immune system consists of cells, tissues and organs and is responsible for the protection against various foreign pathogens like viruses, bacteria, fungi, parasites and tumors. It distinguishes between self and non-self or altered self-structures on cells. Therefore, the defense mechanism of the immune system is based on detecting structural features of the invading pathogens. It recognizes, attacks and kills pathogens. Pathogens can thereby adapt in order to escape the immune system. Some parts of the immune system also play a role in the cases of auto-immune and cancer diseases, as well as allergy (Murphy et al., 2009). In vertebrates, there are two arms of the immune system: innate immune system, which is responsible for a broad spectrum of unspecific, pathogen structures, and adaptive immune system, which is specific for particular non-self-antigens (Alberts et al., 2015).

1.1.1 Innate immune system

The innate immune system is hereditary and serves as the first-line defense against pathogens with the epithelial barrier. This part of the immune system does not need a sensitization to antigens. The innate immune system consists of granulocytes, macrophages, dendritic cells (DC), natural killer (NK) cells and plasma proteins called the complement system.

The recognition of an infectious agent is based on germline-encoded receptors. These receptors are called pattern recognition receptors (PRR) and recognize pathogen-associated molecular patterns (PAMPS). These PAMPS are conserved repeating patterns from microorganisms, e.g. lipopolysaccharide (LPS) of gram negative bacteria, lipoteichoic acid (LTA) of gram-positive bacteria, mannose and glycan of fungi, bacterial CpG DNA or double-stranded viral RNA (Mogensen, 2009). The best characterized PRRs are toll-like receptors (TLR). Their activation leads to pathogen uptake by phagocytic cells. As a result of the uptake, the phagocytic cells secret pro-inflammatory cytokines and chemokines which are important for the recruitment of other immune cells (Kawai and Akira, 2010). The most efficient phagocytic cells are DCs. After pathogen uptake, they mature, migrate to the local lymph nodes (LN), where they secret factors that are important for the innate immune system and induce the adaptive immune response (Murphy et al., 2009). In such way they connect the innate and adaptive immune systems.

1.1.2 Adaptive immune system

The adaptive immune system needs to be activated by the innate immune system. It is classified in cellular and humoral immunity. Cellular immunity consists of T cells with antigen-specific T cell receptors (TCR) that recognize short antigen fragments bound to MHC molecules. The humoral immunity consists of B cells which express antigen-specific receptors that recognize antigenic determinants. The receptors of T cells and B cells are random products of somatic gene rearrangement during maturation (Murphy et al., 2009).

Extracellular pathogens are recognized by B cells that originate from the bone marrow (BM). During maturation, they express membrane-bound immunoglobulins (B cell receptor, BCR). After activation, they differentiate into either memory or antibody-secreting plasma cells.

Intracellular pathogens are detected by T cells via cell-mediated immune response. T cells are generated in the BM and migrate to the thymus for their maturation. Their TCRs recognize peptides only when they are presented by MHC molecules. When they bind to MHC class I, they are $CD8^+$ T cells, whereas $CD4^+$ T cells bind to MHC class II. For the complete activation, T cells need costimulatory signals from antigen-presenting cells (APC). After elimination of their targets, effector cells undergo apoptosis or build up the immunological memory that is responsible for a rapid reinduction of memory cells after the reentering of the same pathogen. This immunological memory mediates a long lasting protection against diseases (Murphy et al., 2009).

1.1.2.1 T cells

Hematopoietic precursors of T cells are generated in the bone marrow (BM) and migrate to the thymus, where they mature into naïve T cells. Through somatic recombination naïve T cells get TCR for specific antigens for a huge variety of peptide-major histocompatibility complex (MHC) complexes (Murphy et al., 2009). They become activated upon their stimulation with tumor-associated antigens presented by APC like DC, macrophages and B cells. In general, APC take up, process and present tumor antigens to T cells in the context of MHC class I or class II. In the thymus, T cells specific for endogenous MHC molecules are separated from cells that bind self-antigens. Afterwards, antigen-experienced T cells are capable of directly recognizing antigens bound to MHC molecules on tumor cells. T cells can be divided into $CD4^+$ and $CD8^+$ T cells for effective immune response (Murphy et al., 2009).

The activation of antigen-specific T cells leads to their clonal expansion and gain the effector function of cytotoxic T cells. These cells specifically eliminate their target cells, in addition to include cancer cells. It comes to a dysfunction of these cells during prolonged antigen exposure. Then T cells are not able to proliferate anymore and fail to eliminate target cells (Murphy et al., 2009).

$CD4^+$ T helper cells are responsible for the cytokine-mediated activation of the humoral response and for the prolonged function of the cytotoxic $CD8^+$ T cell response. The first classification divided $CD4^+$ T cells into two subsets; type 1 T helper cells (Th1) and type 2 T helper cells (Th2) (Mosmann et al., 1986). After binding to the peptide-MHC II complex on APC, Th1 cells produce interferon-γ (IFN-γ) and activate the cellular immunity against intracellular microorganisms. Th2 cells secret interleukin (IL)-4, IL-5 and IL-13, which promote humoral immune response against extracellular pathogens (Zhou et al., 2009).

Cytotoxic T lymphocytes (CTL) are responsible for the elimination of damaged or infected cells. After binding to the peptide-MHC I complex on APC, CTL secret perforin and granzymes and induce apoptosis in target cells. After completing this function the CLT undergo cell death. Remarkably, some of them survive and persist as memory T cells, reacting quicker upon reinduction with the same antigen as compared to the first antigen contact and providing long-term immunity. Memory T cells are divided into resident memory (T_{RM}), effector memory (T_{EM}) and central memory (T_{CM}) T cells according to their localization, their recall ability and effector functions (Laidlaw et al., 2016).

1.1.2.1.1 Regulatory T cells (Treg)

Treg were described in 1995 independently by Sakaguchi *et al.* (Sakaguchi et al., 1995) and Shevach (Bonomo et al., 1995). Treg are characterized by the expression of the transcription factor forkhead-box-protein P3 (FoxP3) and the IL-2 receptor α-chain (CD25). FoxP3 is a member of the forkhead family of deoxyribonucleic acid (DNA)-binding transcription factors that are required for Treg development, maintenance and function (Fontenot et al., 2003; Ziegler, 2006). Treg can suppress the activity of other cell types like $CD4^+$, $CD8^+$ T cells, DC, B cells, monocytes/macrophages and DC (Schmidt et al., 2012). They maintain peripheral tolerance, prevent autoimmune diseases and limit chronic inflammatory diseases (Vignali et al., 2008). There are various mechanisms of Treg-mediated suppression (Fig. 1).

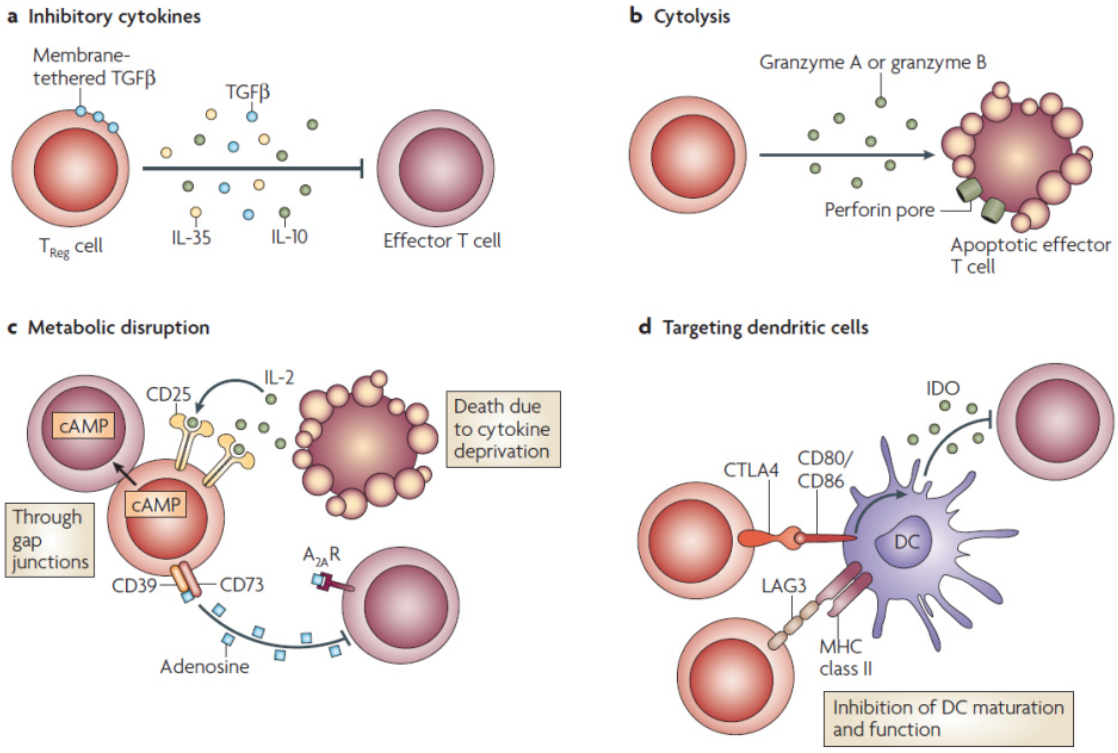

Figure 1: Suppression mechanisms of Treg: **a)** suppression by inhibitory cytokines, **b)** suppression by cytolysis, **c)** suppression by metabolic disruption and **d)** suppression by modulation of DC maturation or function (Vignali et al., 2008).

Treg produce inhibitory cytokines such as transforming growth factor β (TGF-β) and IL-10. They can directly induce cytolysis in granzyme A/B or perforin-dependent manner. Furthermore, Treg express CD25 and thus compete with effector T cells (Teff) for IL-2. The deprivation of IL-2 hampers Teff in their proliferation. The expression of the inhibitory co-receptor cytotoxic T-lymphocyte-associated Protein 4 (CTLA-4) on Treg and the binding of this molecule with the co-stimulatory molecules B7-1 (CD80) and B7-2 (CD86) on DC results in an upregulation of indolamin-2,3-dioxygenase (IDO), which inhibits T cell activation and function (Vignali et al., 2008).

Two populations of Tregs are known: natural Treg (nTreg) and adaptive or induced Treg (iTreg). At the moment, there are no specific markers to distinguish between the two subsets. nTreg development is promoted by self-peptide-MHC interaction in the thymus, independent of DC during T lymphocyte development (Stritesky et al., 2012). These Treg enter then in the peripheral circulation and distribute in peripheral reservoirs like LN and the spleen (Toda and Piccirillo, 2006). The conversion of naïve T cells into iTreg occurs in peripheral lymphoid

organs by interactions with DC under the influence of inductive signals such as TGF-β and IL-10 (Toda and Piccirillo, 2006; Pletinckx et al., 2011).

Several publications show that Treg are important pro-tumorigenic cells in the tumor microenvironment that inhibit anti-tumor immunity and correlate with reduced overall survival (Quail and Joyce, 2013). T cells with regulatory function in patients with cancer were first reported in 2001 (Woo et al., 2001). In this study, they found an elevated frequency of Treg in patients suffering from lung or ovarian cancer. The depletion of Treg leads to an improved anti-tumor response in tumor-bearing mice (Nishikawa and Sakaguchi, 2010), but mice that lack FoxP3 due to a loss-of-function mutation die of multi-organ autoimmune reactions very early (Josefowicz et al., 2012).

1.2 The immune system and cancer immunoediting

The process of immunoediting is composed of three phases: elimination, equilibrium and escape. In the first phase, immune cells fight against arising tumors. The tumor is either eradicated or persists and enters equilibrium. The second phase is the stage of immune-mediated latency. The cancer and immune cells stay in balance. Incomplete tumor destruction and escape result in an immune resistant tumor growth. When the tumor increases and metastasis develop, the escape phase is reached (Dunn et al., 2002). Mostly, the tumor escapes one or both arms of the immune system. In 2011, a new hallmark of cancer “Avoiding of immune destruction” by Hanahan and Weinberg emerged (Hanahan and Weinberg, 2011). There are several mechanisms for how tumors escape from the immune system. One of them is dealt with the recruitment of immunosuppressive cells such as myeloid-derived suppressor cells (MDSC) or Treg to the tumor microenvironment, which can affect the anti-tumor immune response.

1.3 MDSC

The reason why immunotherapeutic clinical studies often fail is that the tumors build up an immunosuppressive microenvironment to escape the immune response and to create an immunosuppressive network that negatively influences the immunotherapy. T cells, for example, are able to infiltrate into the site of a tumor but they are often unable to attack cancer cells. This is due to the fact that tumor cells downregulate specific antigens or MHC molecules and secret inhibitory molecules (Vinay et al., 2015). Furthermore, myeloid precursor cells are converted into MDSC in the tumor microenvironment (Talmadge and Gabrilovich, 2013).

MDSC represent a heterogeneous population of immature myeloid cells (IMC). They were first described more than 25 years ago in mice with cancer. Only some years ago, MDSC contribution to the negative regulation of immune responses during pathological conditions was demonstrated (Talmadge and Gabrilovich, 2013). All MDSC have in common their myeloid origin, the immature state and their ability to suppress T cell responses.

1.3.1 Ontogeny of MDSC

Hematopoietic stem cells differentiate in the BM via common myeloid progenitor cells into IMC. In healthy individuals, IMC are released in the peripheral blood and migrate to peripheral lymphoid organs, where they mature into macrophages, DC or granulocytes. Different pathological conditions, including cancer, chronic inflammation, trauma or autoimmune disorders can inhibit the differentiation of IMC and promote the expansion of this population. Subsequently, IMCs become activated by tumor-derived factors and cytokines, which lead to the generation of MDSC with potent immunosuppressive potential (Lindau et al., 2013).

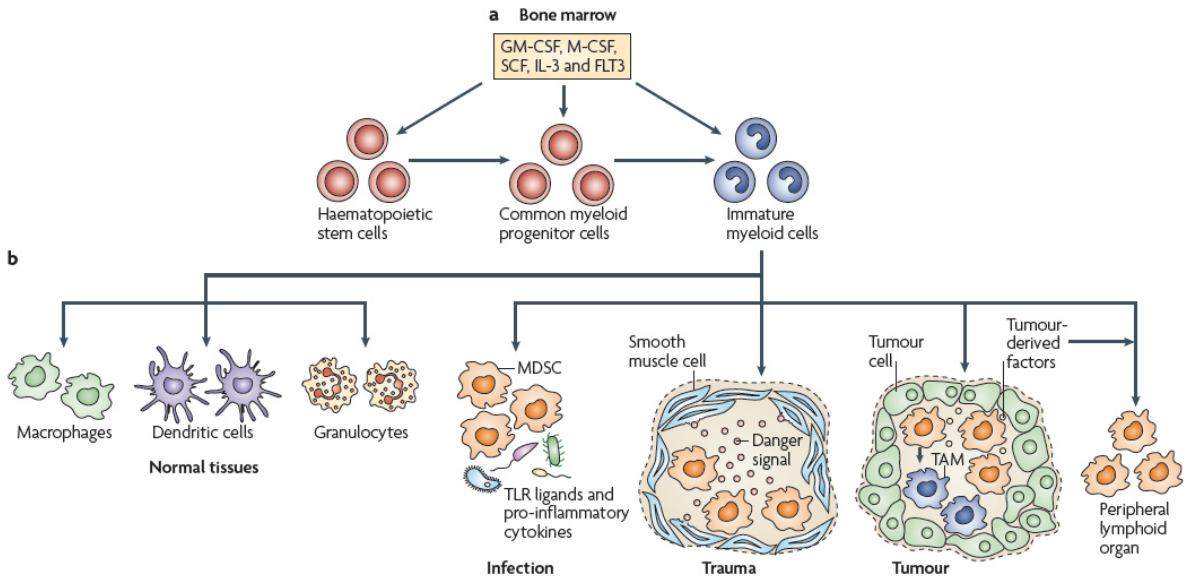

Figure 1: Generation and accumulation of MDSC. IMC are generated in the BM. Under healthy conditions, they differentiate into macrophages, DC and granulocytes. During infection, trauma or cancer, several cytokines are secreted. The differentiation of IMC is partially blocked and MDSC are accumulated and migrated to the site of inflammation, where they exert immunosuppressive functions (Gabrilovich and Nagaraj, 2009).

1.3.2 MDSC subsets in mice

Mouse MDSC are characterized by the coexpression of CD11b and the lineage differentiation antigen Gr-1 (Stromnes et al., 2014). Gr-1 contains the Ly6C and Ly6G epitopes, which enable differentiation between two morphological and functional distinct MDSC subpopulations: monocytic MDSC ($CD11b^{+}Ly6C^{high}Ly6G^{-}$) with monocytic phenotype and granulocytic MDSC ($CD11b^{+}Ly6C^{low}Ly6G^{+}$) that morphologically resemble polymorphonuclear granulocytes (Youn et al., 2008; Zhou et al., 2010; Monu and Frey, 2012; Stromnes et al., 2014). $CD11b^{+}Gr\text{-}1^{+}$ monocytic and granulocytic (polymorphonuclear) subsets have been found in mice. Both subsets are able to inhibit T cells; however, MDSC have more potent suppressive activity in tumor than in peripheral lymphoid organs (Kumar et al., 2016). Studies in tumor-bearing mice have shown that MDSC inhibit T cell function and stimulate the development of Treg in an IFN-γ and IL-10 dependent way (Kumar et al., 2016). The frequency of MDSC subsets seems to be influenced by the cancer type.

1.3.3 MDSC subsets in human

Since Gr-1 marker is not expressed in humans, MDSC from cancer patients were characterized as $Lin^{-}HLA\text{-}DR^{-}CD33^{+}$ or $CD14^{-}CD11b^{+}CD33^{+}$ cells (Marvel and Gabrilovich, 2015). Monocytic MDSC were characterized as $CD11b^{+}HLA\text{-}DR^{-/low}CD14^{+}CD15^{-}$ whereas granulocytic MDSC were $CD11b^{+}HLA\text{-}DR^{-/low}CD14^{-}CD15^{+}$ cells (Filipazzi et al., 2012). Some studies defined Gr-MDSC as $CD14^{-}CD11b^{+}$ or $CD33^{+}HLA\text{-}DR^{-}$ without expression of mature myeloid and lymphoid markers (Nagaraj and Gabrilovich, 2010; Stromnes et al., 2014). Under healthy conditions, the peripheral blood of healthy individuals contains 0.5 % IMC (Gabrilovich and Nagaraj, 2009). It has been described that patients with different cancer types possess about 75 % Gr-MDSC and 25 % Mo-MDSC among total MDSC (Kusmartsev et al., 2004; Gabrilovich and Nagaraj, 2009). It was found that the MDSC elimination with 5-fluorouracil (5-FU) results in an increased frequency of intratumoral $CD8^{+}$ T cells (Vincent et al., 2010). High frequencies of Gr-MDSC correlate with poor prognosis in patients with breast or colorectal cancer (Solito et al., 2011; Zhang et al., 2013). The number of MDSC in cancer patients increased during tumor development. However, 3-4 weeks after surgical resection of the tumor, the frequency of these cells decreased. These findings were consistent with the fact that the generation of MDSC is due to the higher production of soluble factors secreted by the tumor, and a reduction of these cells results in an increased frequency of T cells (Jayaraman et al., 2012; Talmadge and Gabrilovich, 2013).

1.3.4 MDSC expansion and activation

$CD11b^+Gr\text{-}1^+$ cells make up 20-30 % of cells in the BM of healthy mice. However, the spleen contains only 2-4 % $CD11b^+Gr\text{-}1^+$ cells, whereas in LN, they are almost absent (Gabrilovich and Nagaraj, 2009). Upon tumor development in mice, the frequency of MDSC increase by 10 fold; a similar increase could be detected in the peripheral blood of patients with various cancer types (Ochoa et al., 2007). These immunosuppressive cells are also found in tumors (Marvel and Gabrilovich, 2015).

There are several factors that influence the expansion, activation and accumulation of MDSC in tumors (Monu and Frey, 2012). Soluble factors, which are responsible for the expansion of MDSC, are mostly secreted by tumor cells and inhibit the maturation of IMC like prostaglandins, stem-cell factor (SCF), macrophage-stimulating factor (M-CSF), IL-6, granulocyte/macrophage colony-stimulating factor (GM-CSF) and vascular endothelial growth factor (VEGF) (Gabrilovich and Nagaraj, 2009; Stromnes et al., 2014). Most of these factors are inducers for the Janus kinase (JAK) and signal transducer and activator of transcription (STAT) 3 signaling pathway involved in the survival, proliferation and differentiation of myeloid progenitor cells. A permanent activation of the STAT3 pathway in myeloid progenitor cells leads to higher production of S100 calcium-binding protein A8 (S100A8) and S100 calcium-binding protein A9 (S100A9), resulting in the inhibition of the differentiation and promoting of MDSC expansion in the spleen of tumor bearing mice (Cheng et al., 2008; Marvel and Gabrilovich, 2015). Since S100A8 and S100A9 play a critical role in the induction of inflammation and could induce MDSC expansion, these molecules connect the inflammation with immune suppression in cancer.

The second group of factors stimulating MDSC is mainly produced by immune cells and fibroblasts such as IFN-γ, TLRs, IL-13, IL-4, TGF-β and IL-1β (Marvel and Gabrilovich, 2015). Without these factors, MDSC would not be able to exert their immunosuppressive function (Gabrilovich and Nagaraj, 2009). They induce STAT6, STAT1 and nuclear factor kappa B (NF-κB). STAT1 is activated by IFN-γ and IL-1β and leads to the upregulation of arginase (ARG-1) and inducible nitric oxide synthase (iNOS) expression (Marvel and Gabrilovich, 2015). Therefore, STAT1 deficient mice fail to suppress T cell proliferation (Kusmartsev and Gabrilovich, 2005). In addition, signaling via CD124 has been reported to induce STAT6, as well as ARG-1 and iNOS expression (Condamine and Gabrilovich, 2011). Moreover, both IL-4 and IL-13 can upregulate ARG-1 activity in MDSC and enhance their immunosuppressive function (Gabrilovich and Nagaraj, 2009).

It has been demonstrated that the recruitment of MDSC to the tumor microenvironment is mediated by such factors as CC-chemokine ligand (CCL)-2, chemokine (C-X-C motif) ligand

(CXCL)-5, CXCL8, CCL15 and CXCL12 (Kumar et al., 2016). In breast, ovarian and gastric human tumors, the migration of MDSC has been shown to be driven by the CCR2/CCL2 axis (Kumar et al., 2016). The migration of MDSC subsets into the tumor is thereby determined by the histology and the chemokines produced by the tumor. CCL2 and CCL5 have been reported to be the main chemokines for Mo-MDSC recruitment to the tumor (Kumar et al., 2016).

Several studies indicate that tumor-infiltrating MDSC can convert into tumor-associated macrophages (TAM) under hypoxia in the tumor microenvironment (Schouppe et al., 2012; Solito et al., 2014; Kumar et al., 2016). MDSC can also skew macrophages towards an M2 phenotype (Sinha et al., 2007; Ugel et al., 2015). Increasing numbers of TAMs is associated with poor prognosis in patients with lung cancer (Quatromoni and Eruslanov, 2012). High levels of TAM correlate with a bad prognosis in different cancer types (Gwak et al., 2015; Wang et al., 2015)

It has been shown that MDSC stimulate the expansion and activation of Treg (Pan et al., 2010; Marvel and Gabrilovich, 2015). Treg induction is based on IL-10 and TGF-β production by MDSC (Ostrand-Rosenberg and Sinha, 2009). Furthermore, it was found that C-C chemokine receptor type 5 (CCR5) ligands produced by Mo-MDSC directly recruit Treg via CCR5/CCR5-ligand interaction (Schlecker et al., 2012). Interestingly, in CCR5 deficient mice, the frequency of Treg was reduced and the tumor progression was delayed.

Taken together, tumor burden and other pathological conditions like chronic inflammation and infection can accelerate the expansion and activation of MDSC due to the secretion of multiple inflammatory mediators.

1.3.5 MDSC-mediated suppression of T cell function

In addition to the morphological and phenotypical distinctions, MDSC subsets use different approaches to suppress anti-tumor immunity (Lindau et al., 2013; Stromnes et al., 2014) (Fig. 3). It was found that MDSC suppress T cell proliferation and T cell cytokine production through enhanced expression of ARG-1, NOS and the elevated production of reactive oxygen species (ROS) (Kumar et al., 2016). This is associated with the loss or reduced expression of the TCR ζ-chain (Baniyash, 2004), inhibition of T cell activation, inhibition of IFN-γ production by $CD8^+$ T cells, blocking the development of CTL (Bronte et al., 2003; Kumar et al., 2016).

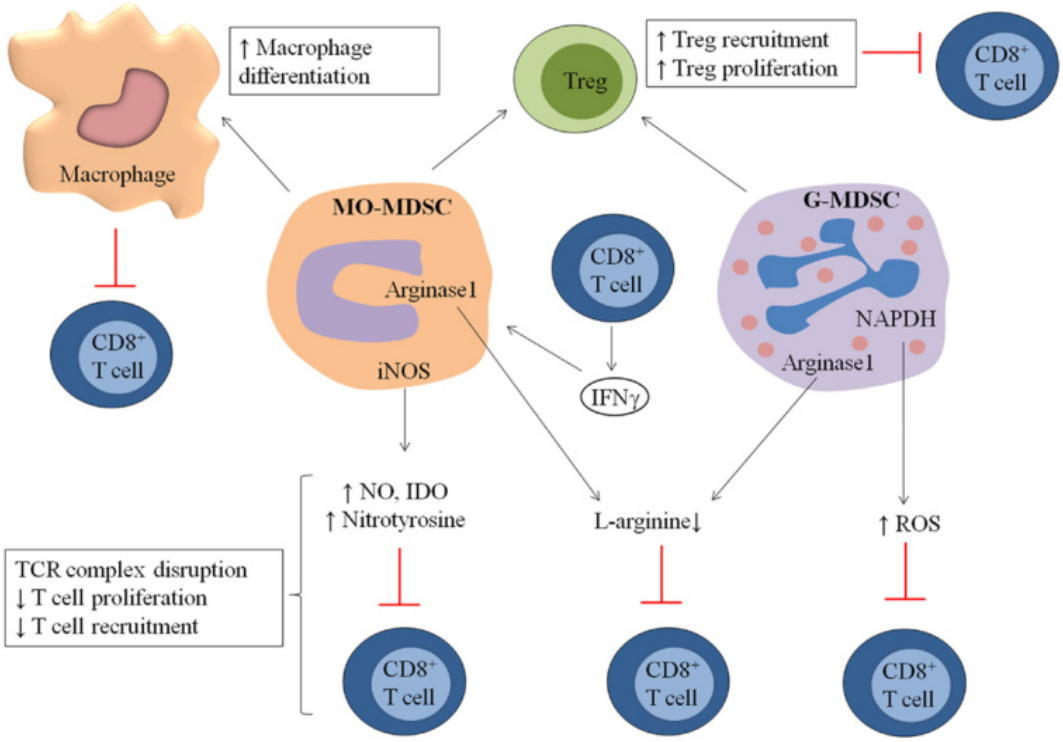

Figure 2: Suppressive effect of MDSC on immune cells. $CD11b^{+}Ly6C^{+}Ly6G^{-}$ monocytic MDSC and $CD11b^{+}Ly6C^{-}Ly6G^{+}$ granulocytic MDSC use different mechanisms to suppress the immune system such as macrophage differentiation and Treg proliferation. Further, they affect T cells by the production of NO, ROS and L-arginine (De Veirman et al., 2014).

The suppressive activity of MDSC were first associated with the degradation of L-arginine. L-arginine is metabolized by iNOS leading to nitric oxide (NO) production and by ARG-1 converting L-arginine into urea and L-ornithine. Both enzymes are highly activated in MDSC and lead to the suppression of T cell proliferation. When MDSC deplete L-arginine from the T cell microenvironment, ζ-chain expression is reduced and T cells are not able to transmit the required signals for their activation (Baniyash, 2004; Solito et al., 2014). NO induces T cell apoptosis and is responsible for the inhibition of MHC class II gene expression (Meirow et al., 2015).

ROS production can be detected in MDSC from tumor bearing mice, as well as in cancer patients (Gabrilovich et al., 2012; Lindau et al., 2013). Increased ROS production by MDSC is associated with an enhanced NADPH oxidase NOX2 activity (Solito et al., 2014). Peroxynitrite leads to the nitrosylation of the TCR of $CD8^{+}$ T cells and prevents interactions with peptide-MHC complex (Gabrilovich and Nagaraj, 2009). This leads to the inhibition of antigen-specific T cell responses through the downregulation of the ζ-chain expression in tumor bearing mice

(Baniyash, 2004). The tumor-induced ROS production by MDSC is an important process by tumors to stimulate MDSC proliferation and to block differentiation into APC (Kusmartsev and Gabrilovich, 2003). *In vitro* studies showed that the inhibition of ROS in MDSC isolated from mice or patients inhibit the suppressive function of MDSC (Gabrilovich and Nagaraj, 2009).

Programmed cell death protein 1 (PD-1) is a type I transmembrane protein with two known ligands: programmed death-ligand 1 (PD-L1) and programmed death-ligand 2 (PD-L2). PD-1 is expressed on activated T cells, B cells, NK cells and DC whereas PD-L1 is expressed on cancer cells, Treg, MDSC, T cells, B cells and DC. Treg in melanoma bearing mice were described to stimulate MDSC to express PD-L1 and to produce IL-10 (Fujimura et al., 2012). Hypoxic conditions inside the tumor upregulate PD-L1 expression on tumor-infiltrating MDSC resulting in more potent suppressive activity as compared to splenic MDSC (Noman et al., 2014).

Moreover, MDSC have been reported to deplete cysteine from the T cell environment (Solito et al., 2014). Cysteine is essential for the activation, differentiation and proliferation of T cells. Under normal conditions, APC provide T cells with cysteine by importing cystine, converting it into cysteine and then exporting it with ASC transporters (Srivastava et al., 2010). MDSC compete with T cells for cysteine thus preventing the generation of cysteine on their own (Monu and Frey, 2012). This leads to the depletion of cysteine from the tumor microenvironment and the inhibition of T cell activation and function (Srivastava et al., 2010; Kumar et al., 2016).

1.3.6 Therapeutic targeting of MDSC

MDSC accumulation is correlated with tumor progression and associated with T cell suppression (Ugel et al., 2015). It has been demonstrated that the reduction of frequencies or immunosuppressive functions of MDSC in the tumor microenvironment significantly improves anti-tumor immunity (Umansky and Sevko, 2012; Wesolowski et al., 2013; Stromnes et al., 2014). Several approaches were developed for targeting MDSC including:

- Neutralization of tumor-derived factors that induce the development and expansion of MDSC
- Induction of MDSC differentiation in macrophages, DC and granulocytes
- Elimination of MDSC by chemotherapeutic drugs
- Blockage of the suppressive function by MDSC
- Inhibition of MDSC migration by blocking the interaction between chemokines and their receptors on MDSC surface

1.4 C-C chemokine receptor 5

Chemokines are small 8-14 kDa chemoattractant cytokines for leukocyte trafficking to the site of inflammation through interactions with specific transmembrane, G protein-coupled receptors (GPCR). 50 endogenous chemokines binding to 20 GPCR were described (Palomino and Marti, 2015). A few of the chemokines bind to more than one receptor. Chemokines are known to be involved in inflammatory diseases and cancer. In cancer, chemokines are secreted by tumor cells to attract immune cells by binding onto their receptors. These receptors in general are members of the seven transmembrane receptors and signal through the heterotrimeric G proteins upon ligand binding (Jo and Jung, 2016).

CCR5 is a member of the trimeric guanine nucleotide-binding-protein-coupled seven-transmembrane receptor superfamily that acts via G proteins. It is composed of 352 amino acids and has a molecular mass of 40.6 kDa (Barmania and Pepper, 2013). The ligands of CCR5 named CCL3 (MIP-1α), CCL4 (MIP-1β) and CCL5 (RANTES) are secreted by tumor cells, T cells, monocytes/ macrophages, DC and MDSC. CCR5 is expressed on memory and effector T cells, monocytes, macrophages, immature DC and MDSC. Its ligands enable CCR5-expressing cells to migrate to the site of inflammation (Barmania and Pepper, 2013).

1.4.1 CCR5 in HIV

CCR5 and CXCR4 were shown to be key receptors for the entry of human immunodeficiency virus (HIV). Individuals exhibiting a 32 bp deletion in the CCR5 gene produce a non-functional protein which is not expressed on the surface. The mutated allele contains 215 amino acids in comparison to 352 amino acids of the wild type (WT) CCR5. The protein finally lacks the last three transmembrane domains and regions, which are crucial for interaction with the G-protein and signal transduction (Barmania and Pepper, 2013). In northern Europe, around 20 % of the population have a CCR5Δ32 polymorphism whereas the deletion is almost absent in African, Middle Eastern and American Indian populations (Bryant and Slade, 2015). Homozygote people with a depletion of 32 bp in the CCR5 gene (Δ32 mutation) do not express the receptor whereas heterozygotes express it partially as compared to WT homozygotes (Bhatia et al., 2009). Individuals harboring homozygous mutant allele (Δ32/Δ32) are highly resistant to HIV-1 infection, whereas heterozygotes (Δ32/wt) can delay progression of HIV infection (Harper et al., 2015).

It has been recently found that patients with a functional mutated CCR5 are resistant to prostate cancer (Balistreri et al., 2009). Moreover, it has been demonstrated that melanoma patients with a CCR5Δ32 deletion showed a decreased overall survival following immunotherapy as compared to patients with WT alleles (Ugurel et al., 2008).

1.4.2 The role of CCR5 in cancer

Since it was shown that CCR5 might play a role in cancer, the study of CCR5-CCR5 ligand axis revealed that melanoma growth is delayed in CCR5-deficient mice (Aldinucci and Colombatti, 2014). In a transplantable B16 melanoma model, it was found that CCR5 expression on stromal cells is necessary for the spread of melanoma cells to the lungs (van Deventer et al., 2005).

Inhibition of CCR5-CCR5 ligand interaction by maraviroc has been recently shown to delay the tumor growth in colorectal cancer patients, although the number of Treg was not reduced (Ward et al., 2015). On the other side, the CCR5 inhibitor TAL-779 blocked the migration of Treg to the tumor microenvironment and thereby resulted in a reduced tumor growth in the mouse model of pancreatic cancer (Tan et al., 2009). Furthermore, it could be shown that CCL5 enhances the proliferative and invasive capacity of prostate cancer cells *in vitro*, an effect which could be abolished by the CCR5 antagonist TAK-779 (Vaday et al., 2006). Another group found that the treatment with Met-CCL5, an antagonist of CCR5 and CCR1, decreased the tumor growth in a breast cancer mouse model (Robinson et al., 2003).

CCR5 deficient mice, which were injected with B16 melanoma cells, showed a delayed tumor growth and a better response to cancer vaccines (Ng-Cashin et al., 2003). However, the role of the CCR5-CCR5 ligand interactions in MDSC accumulation in tumor microenvironment during melanoma progression needs to be clarified.

1.5 Malignant Melanoma

Malignant melanoma is an aggressive malignancy of transformed melanocytes that is resistant to standard therapy, e.g. chemo-radiotherapy. In the United States, melanoma is the fifth and sixth most common type of cancer in males and females expected to be diagnosed in 2016 (Siegel et al., 2016). Only 5 % of all skin cancers account for melanoma, but it is responsible for 90 % of skin cancer deaths. In terms of incident, malignant melanoma is the most rapidly increasing malignancy in Western population (Garbe et al., 2010) due to improved life standard, e.g. travelling to sunny resorts and get tanned and due to the higher life average of the people. Mostly effected are young and middle-aged Caucasians triggered by solar UV radiation, fair skin, red or blond hairs, blue eyes or family history of melanoma (MacKie et al., 2009).

Melanoma arises from the transformation of melanin-producing melanocytes in the skin and rarely in non-cutaneous melanocytes like retina or mucosal surfaces. Patients suffering from melanoma can be divided into different groups according to the TNM classification. This

classification considers the size of the tumor, the affection of LN and metastasis (Garbe et al., 2010). Stage I is an invasive melanoma and tumor cells spread *in situ*. In stage II, when the tumor size is 1.5 mm or bigger, patients have a 5-year survival rate of 45-79%. When the tumor starts to metastasize into regional LN and the skin, patients are in stage III. Stage IV is classified when the tumor cells from distant metastases spread through the peripheral blood, and lymphatic system into the brain, lung, liver skin and BM.

There are some gene mutations involved in melanoma development. In almost 80 % of melanoma cases, the BRAF or NRAS gene is mutated which are important for the MAP-kinase signaling pathway (Bertolotto, 2013). Mutations in these genes promote the proliferation of melanoma cells.

1.6 Melanoma therapy

1.6.1 Conventional therapy

The standard procedure for localized melanoma with adequate margins is surgical excision and the assessment of metastasis with short-term and long-term fellow-ups (Koshenkov et al., 2016). Patients with non-resectable metastasis or advanced melanoma are treated with radiotherapy (Davar and Kirkwood, 2016). This method is still in use after tumor dissection to treat left tumor tissue. Conventional chemotherapeutics such as dacarbazin and temozolomid were shown not to have a significant increase in the overall survival of patients and the number of responding patients was very low (Bhatia et al., 2009).

1.6.2 Targeted therapies

40 – 60 % of cutaneous melanoma patients have a mutation in BRAF (V600E) that constitutively activates the mitogen-activated protein (MAP) kinase pathway (Palmieri et al., 2015). In 2011, vemurafinib, a BRAFV600 kinase inhibitor was approved for patients carrying the V600E mutation with unresectable or metastatic melanoma. The disadvantage of this therapy is the short-term duration of 6-8 months of clinical response and drug resistance due to the fast development of resistances to these drugs (Chapman et al., 2011). Since the approval of a BRAF inhibitor, vemurafinib is the standard therapy for patients with the BRAF mutation (Bertolotto, 2013).

Recently, there has been shown an efficacy of trametinib and cobimetinib, two inhibitors of MEK kinase, which are located downstream of BRAF in the MAP kinase pathway. A combinatory therapy with BRAF and MEK inhibitors was shown to delay resistance development (Robert et al., 2015).

1.6.3 Negative checkpoint inhibitors

CTLA-4 is expressed on T cells and competes with CD28 for the ligands CD80 and CD86 on APC, thereby leading to an inhibition in T cell activation. Ipilimumab is a human monoclonal antibody that binds to the extracellular domain of CTLA-4 and enhances T cell activation and function promoting anti-tumor immunity (Bhatia et al., 2009). The therapy with ipilimumab resulted in an increased overall survival in melanoma patients (Redman et al., 2016). Ipilimumab has been approved in 2011.

PD-1 is another immune checkpoint molecule that is upregulated upon T cell activation. When PD-1 binds to PD-L1 (B7-H1) and PD-L2 (B7-H2), which are expressed on tumor cells and MDSC, T cell activity is blocked (He et al., 2015). Pembrolizumab, an antibody against PD-1, has been approved for the treatment of melanoma patients (Raedler, 2015). The blockage of the interaction between PD-1 and PD-L1 potentiates the immune response and mediates anti-tumor activity.

Further development of the melanoma treatment is linked with combined therapies (Ott, 2015). Thus, a triple combination therapy of BRAF and MEK inhibitors and adoptive therapy in $BRAF^{V600E}$ mutant transgenic mice resulted in increased MHC I molecule expression. These led to increased T cell infiltration to the tumor associated with complete tumor regression (Hu-Lieskovan et al., 2015).

1.7 *Ret* transgenic mouse melanoma model

In transplantable models like B16 melanoma, the interaction of the tumor cells with the immune system and tumor stroma is not comparable with the human situation. In contrast, in *ret* transgenic mice, melanoma develops spontaneously, resembling human melanoma with regards to tumor genetics, histopathology and clinical development in more detail (Kato et al., 1998; Umansky et al., 2008). In this model, the human *ret* oncogene was fused with a methallothioneine-I promotor, leading to the overexpression of the receptor tyrosine kinase Ret in melanocytes. Activation of the kinase leads to the activation of downstream signaling molecules like mitogen-activated protein kinase (MAPK), Erk2 and c-Jun. The activation of Ret kinase promotes malignant transformation of melanocytes and tumor development. Melanoma emerges at the head, neck, back, and tail and metastasizes in LN, BM, liver, brain and lungs (Sevko et al., 2013). Melanoma lesions show characteristic melanoma morphology and express melanoma-associated antigens like S100, tyrosinase, tyrosinase related protein (TRP)-1, TRP-2 and gp100 (Abschuetz et al., 2012). The metastatic profile is similar to the metastatic pattern in patients with malignant melanoma (Houghton and Polsky, 2002).

Although the mutation of *ret* has not been detected in melanoma patients, the activation of the MAP-kinase signaling pathway is routinely seen in human melanoma (Sullivan and Flaherty, 2013).

It was previously shown that immunosuppressive cells like MDSC and Treg accumulate during tumor progression in skin tumors and metastatic LN (Kimpfler et al., 2009; Sevko et al., 2013). Furthermore, MDSC were described to inhibit T cell response, which allows a rapid tumor progression and metastasis (Umansky and Sevko, 2012). Administration of the phosphodiesterase-5 inhibitor, sildenafil, neutralizes the MDSC immunosuppressive activity, which leads then to the increased survival of melanoma-bearing mice. Furthermore, various factors that drive MDSC activation, expansion and migration were found at the site of tumor (Meyer et al., 2011; Umansky and Sevko, 2012). This complex immunosuppressive network in the tumor microenvironment could be a reason that conventional melanoma therapies are not successful and novel strategies have to be found. We propose to block the CCR5-CCR5 ligand interactions by mCCR5-Ig that binds and neutralizes CCL3, CCL4 and CCL5 thus inhibiting MDSC and Treg infiltration into the site of tumor, restoring T cell activity and finally prolonging the survival of mice.

2 Aim of the project

Patients with malignant melanoma have bad prognosis once the tumor has metastasized due to a chronic inflammation that induces strong immunosuppression. The investigation of novel therapeutic strategies is therefore very important. MDSC represent a heterogeneous population of immature macrophages, granulocytes or dendritic cells (DC) that accumulate during tumor development in cancer patients and in tumor bearing mice. CCR5 is a chemokine receptor that binds to its ligands CCL3 (MIP-1α), CCL4 (MIP-1β) and CCL5 (RANTES). Since CCR5 is reported to induce tumor growth, angiogenesis, metastasis and immune evasion, several CCR5 antagonists are already used to boost anti-tumor immune response.

The aim of the study was to characterize the recruitment and migration of human and mouse CCR5 expressing MDSC to the site of inflammation (melanoma lesions) and to investigate their phenotype and immunosuppressive activity in the tumor microenvironment. We studied the levels of factors inducing MDSC migration in melanoma lesions of *ret* transgenic mice and melanoma patients. In order to analyze the phenotype of $CCR5^+$ MDSC, immunosuppressive molecules such as ROS, NO, ARG-1 and PD-L1 were measured in *ret* transgenic tumor bearing mice and in peripheral blood from melanoma patients at different stages. Furthermore, we compared the immunosuppressive activity of $CCR5^+$ MDSC and their $CCR5^-$ counterparts. Since CCR5 is also known to be expressed on T cells, we investigated the CCR5 expression on various T cell subsets focusing on Treg, which displayed an immunosuppressive function. Based on targeting of CCR5-CCR5 ligand interaction to block the MDSC recruitment, we aimed to evaluate the possibility of neutralizing immunosuppression in the tumor microenvironment with the mCCR5-Ig fusion protein *in vivo*.

3 Materials and Methods

3.1 Materials

3.1.1 Mouse strains

3.1.1.1 Spontaneous *ret* transgenic mouse melanoma model

Mice (C57BL/6 background) expressing the human *ret* transgene in melanocytes under the control of mouse metallothionein-I promotor-enhancer were provided by Dr. I. Nakashima (Chubu University, Aichi, Japan) (Kato et al., 1998). These mice overexpress the human *Ret* proto-oncogene in melanocytes under the control of mouse metallothionein-I promoter-enhancer. The tumor develops spontaneously approximately 40 day after birth. Every second day the mice were monitored. As controls, mice without a macroscopically visible tumor and non-transgenic WT were used.

Mice were crossed and kept under pathogen-free conditions in the animal facility of the German Cancer Research Center (Heidelberg, Germany). Experiments were performed in accordance with government and institutional guidelines and regulations.

3.1.2 Cell culture products

Product	Company	Catalog No.
96-well flat bottom with lid	TPP®	92096
96-well U-bottom with lid	Sigma Aldrich	M9436-100EA
24-well flat bottom with lid	Greiner bio-one	622160
12-well flat bottom with lid	BD	353043
6-well flat bottom with lid	Thermo Scientific	140675
50 mL conical tubes	Falcon	352070
15 mL conical tubes	Falcon	352096
5 mL round-bottom polypropylene test tubes	BD	352008
5 mL round-bottom polypropylene test tubes w. cell strainer	BD	352235
serological pipettes: 5, 10 and 25 mL, sterile	Greiner bio-one	606180 607180 760180
40 µm cell strainer	BD	
Cryovial, 2 mL sterile	Sigma Aldrich	V5760-500EA
Freezing Container, "Mr. Frosty"		
Safe lock tubes: 0.5, 1.5 and 2 mL	Eppendorf	
Filter tips: 20, 200, 1000 µL	Steinbrenner	SL-GPS-L10, L250, L1000
Neubaur Zählkammer		
Cell culture flasks T75	Sigma Aldrich	C7231-120EA

Syringe 1 mL	BD
LeucoSep tubes	Greiner Bio-one

3.1.3 Cell culture media

Product	Company	Catalog No.
HEPES Buffer (1M)	Sigma Aldrich	H0887
MEM NEAA (100x)	Gibco	11140-035
UltraPure™ EDTA (0.5M, pH 8.0)	Gibco	15575
sodium pyruvate (100 mM)	Gibco	11360-039
2-βMercaptoethanol (50 mM)	Gibco	31350
RPMI Medium 1640 (1x) + GlutaMAX™	Gibco	61870-010
DPBS (1x)	Gibco	14190-094
MEM-α Medium (1x)	Gibco	22561-021
X-Vivo 20	Lonza	BE04-448Q
Ficoll	Sigma Aldrich	
Fetal Bovine Serum	PAN Biotech GmbH	3702-P260718
Bovin serum albumin	Sigma	7030-50G
Penicillin/ Streptomycin	PAA	P11-010
Dimethylsulfoxid (DMSO)	Merck	109678
0.4 % Trypan blue solution	Sigma Aldrich	T8154
Dimethylsulphoxide Hybrid Max (DMSO)	Sigma Aldrich	472301-100ML
MACS BSA Stock Solution (10 %)	Miltenyi Biotec	130-091-376
Dynabeads® Mouse T-Activator CD3/CD28	Gibco	11453D

3.1.4 Magnetic cell sorting (MACS)

Product	Company	Catalog No.
$CD8^+$ T cell isolation kit	Miltenyi Biotec	130-104-075
Myeloid-derived Suppressor cell isolation kit	Miltenyi Biotec	130-094-538
MACS Columns 25LS	Miltenyi Biotec	130-042-401
MACS Columns 25MS	Miltenyi Biotec	130-042-201

3.1.5 Kits

Product	Company	Catalog No.
BCA™ Protein Assay Kit	Thermo Scientific	23225
Bio-Plex®Cell lysis kit	Bio-Rad	171-304011
Bio-Plex® TGF-β1 Set	Bio-Rad	171-V4001M
Bio-Plex® TGF-β Standard	Bio-Rad	171-X40001
Bio-Plex® Pro™ Human Cytokine 27-plex	Bio-Rad	M500KCAF0Y
Bio-Plex® Pro™ Mouse Cytokine 23-plex	Bio-Rad	M60009RDPD
FoxP3/ Transcription Factor Fixation/ Permeabilisation Concentrate and Diluent	eBioscience	00-5521-00

Permeabilisation Buffer (10x)	eBioscience	00-8333-56

3.1.6 Antibodies

3.1.6.1 Human panel

Primary antibodies	Fluorochrom	Clone	Company	Catalog No.
CD11b	APC	ICRF44	BD	550019
HLA-DR	APC-H7	G46-6	BD	561358
CD14	PerCp Cy5.5	MΦP9	BD	345786
CD15	PE	HI98	BD	555402
PD-L1/ CD274	PE Cy7	MIH1	BD	558017
CD45	PerCp Cy5.5	HI30	Biolegend	304028
CD3	PerCp Cy5.5	HIT3a	Biolegend	300328
CD4	PE Cy7	SK3	BD	557852
CD4	APC Cy7	RPA-T4	BD	557871
CD45RA	PE Cy7	HI100	eBioscience	25-0458-42
CD8	APC Cy7	SK1	BD	557834
CD25	PE	M-A251	BD	555432
CD127	FITC	eBioRDR5	eBioscience	11-1278-42
TCR/ CD247	FITC	6B10.2	Biolegend	644104
CD8a	eFluor450	53-6.7	eBioscience	48-0081-82
CD69	PE Cy7	FN50	BD	557745
CCR5	BV421	2D7/CCR5	BD	562578
FoxP3	APC	236A/E7	eBioscience	17-4777-42

3.1.6.2 Mouse panel

Primary antibodies	Fluorochrome	Clone	Company	Catalog. No.
CD11b	APC Cy7	M1/70	BD	557657
CD11b	APC	M1/70	BD	553312
Gr-1	PE Cy7	RB6-8C5	BD	552985
Ly6C	FITC	AL-21	BD	553104
Ly6C	APC	AL-21	BD	560595
CCR5	PE	C34-3448	BD	559923
CCR5	APC	HM-CCR5	Biolegend	107012
CCR2	APC	475301	R&D	FAB5538A
PD-L1	APC	MIH5	BD	564715
PD-L1	BV421	MIH5	BD	564716
CD45.2	PerCp Cy5.5	1O4	BD	552950
CD3	PerCp Cy5.5	145-2C11	BD	551163
CD4	PE cCy7	RM4-5	BD	552775
CD8	APC Cy7	53-6.7	BD	557654
CD8	APC Cy7	YTS156.7.7	Biolegend	126620
CD25	APC Cy7	PC61	Biolegend	102026
CD25	APC	PC61	BD	557192

FoxP3	FITC	FJK-16s	eBioscience	11-5773-82
TCR/ CD247	PE	K25-407.69	BD	558448
PD-1/ CD279	BV421	J43	BD	562584
CD69	APC	H1.2F3	BD	560689

3.1.6.3 Human/mouse reagents

Primary antibodies	Fluorochrome	Clone	Company	Catalog No.
NOS Detection Kit	FITC-channel (488 nm)	production of chemical reaction	cell technologies	NOS200-2
hROS Detection Kit			cell technologies	FLAPF100-2
anti-h/m ARG-1	APC	MAB58681	R&D	IC5868A
FcR Blocking Reagent			Miltenyi	130-059-901

3.1.7 Chemicals and biological reagents

Product	Company	Catalog No.
7-AAD	BD	51-68981E
recombinant murine (CCL2)		
recombinant murine MIP-1α (CCL3)	Peprotech	250-09
recombinant murine MIP-1β (CCL4)	Peprotech	250-32
recombinant murine RANTES (CCL5)	Peprotech	250-07
recombinant mouse VEGF	Peprotech	
recombinant murine GM-CSF	Peprotech	315-03
recombinant murine IL-6	Peprotech	216-16
recombinant mouse TNF-α	Peprotech	
Carboxyfluorescein succinimidyl ester (CFSE)	Biolegend	423801
Heparin-Natrium-25000 Units	Ratiopharm	PZN-3029843
Isofluran		
RBC Lysis Buffer (10x)	Biolegend	420301

3.1.8 Solutions

Solution	Ingredients
Freezing medium 1	60 % FBS 40 % X-VIVO 20
Freezing medium 2	75 % FBS 25 % DMSO
MACS buffer	1x PBS 1% FCS 0.5 mM EDTA

Primary cell culture medium	1x RPMI 10 % FCS 100 U/ml Penicillin, 100 µg/ml Streptamycin 1mM Sodium pyruvate 1x Non-essential amino acids 0.5 mM ß-Mercaptoethanol
FACS buffer	1x PBS 2% FBS 0,2 % NaN_3 2mM EDTA
SORT buffer	0.5 M EDTA 1 % FCS 1 M HEPES in 500 ml HBSS

3.1.9 Dextramers

Product	Fluorochom	Allele	Peptide	Company	Cat. No.
MHC dextramer H-2 Kb / SVYDFFVWL / PE	PE	H-2 Kb	SVYDFFVWL	Immudex	JD2199

3.1.10 Routine laboratory material

Product	Company	Catalog No.
Needle (27G)	neolab	194210020
Needle (23G)	BD	300800
Needle (25G)	BD	300400
6.5 mm Transwell® with 3.0 µm Pore Polycarbonate Membrane Insert	Corning	3415
Pipets: 2-20 µL, 20-200 µL, 200-1000 µL	Rainin	L-20XLS+, L-200XLS+, L-1000XLS+
Object carrier Superfrost plus	R. Langenbrinck	03-0060

3.1.11 Laboratory equipment

Equipment	Name	Company
Anesthesia machine	IsoFlo Vaporiser	Eickemeyer
Cell culture incubator	Hera Cell	Heraeus
Centriguges	Laborfuge 400R Laborfuge 40R Biofuge primo R Varifuge K	Heraeus
Microplate Reader	Tecan infinite M200	Tecan
Flow cytometer	FACS Canto II, 8 colours	BD

Laminar flow hood	Hera safe	Thermo Electron Cooperation
Refrigerator (-20 °C)	Premium	Liebherr
Refrigerator (-80 °C)	HeraFreeze	Heraeus
Fridge		Liebherr
Ice machine		
Magnetic stirrer	RCT basic	IKA Werke
Microscope	DMIL	Leica
N2 tank		
pH meter	766	Calimatic
Vortexer	REAX top	Heidolph
Vortexer	Vortex Genie 2	Scientific Industries
Balance	BP 3100P	Sartorius
Water bath	DC3	HAAKE, GFL

3.1.12 Software for data analysis

Product	Company
Flow Jo (Version 7.6.1)	Tree Star, Inc., Ashland, USA
GraphPad PRISM (Version 5)	GraphPad Software, Inc., San Diego, USA

3.3 Methods

3.3.1 Determination of cell numbers

To distinguish dead from live cells, an aliquot of cell suspension was diluted 1:10 with trypan blue. Cell numbers were determined by using a Neubauer counting chamber and the total number of cells per mL was calculated by the formula:

(Counted cell number / number of counted chambers) x 10^4 x dilution factor.

3.3.2 Organ preparation and single cell suspension from *ret* transgenic mice

Mice were sacrificed by cervical dislocation for organ preparation or by asphyxiation with isoflurane for blood collection.

3.3.2.1 Blood

Peripheral blood was obtained by puncture of the caudal (inferior) vena cava with a heparin-wetted syringe. Per mouse, 0.5-0.8 mL blood was collected. Whole blood was centrifuged at 1400 rpm for 7 min and serum was frozen at -80 °C. Peripheral blood was treated with 1 mL lysis buffer and washed with PBS (1400 rpm, 7 min, 4 °C) to get rid of the erythrocytes. Pellet was resuspended in PBS for FACS analysis.

3.3.2.2 Spleen

Mouse spleen was collected in a 15 mL falcon tube with 5 mL PBS. Single cell suspension was prepared by smashing the spleen with a plunger through a 40 µm cell strainer and washing with PBS at 1400 rpm for 7 min. Erythrocytes were depleted with 2 mL lysis buffer followed by 3 min of incubation at room temperature (RT). To stop the reaction, cells were washed with 10 mL PBS before cells were counted and resuspended in medium or PBS dependent on the following assay.

3.3.2.3 Bone marrow

Femur and tibiae from the same mouse were cut at both ends. BM was flushed out with PBS using a syringe with a 23G needle. Cells were filtered through a 40 µm cell strainer and washed with PBS at 1400 rpm, for 7 min. Red blood cells were lysed with 2 mL lysis buffer for 3 min at RT. PBS was used to stop the reaction and cells were washed at 1400 rpm for 7 min. Pellet was resuspended in appropriate buffer for further analysis.

3.3.2.4 Metastatic lymph nodes

LN from the inguinal, axillary and head region were extracted. LN were smashed between two object slides and filtered through a 40 µm cell strainer. The strainer was then washed with PBS to collect all cells. The cells were washed with PBS at 1400 rpm, 7 min and resuspended in PBS for flow cytometry.

3.3.2.5 Skin tumor

The isolated skin tumors from melanoma bearing mice were weight and smashed through a 40 µm cell strainer by a plunger into a 50 mL falcon tube. After the depletion of the erythrocytes, cells were washed with PBS at 1400 rpm for 7 min and resuspended in an appropriate buffer for further analysis.

3.3.3 Fluorescence activated cell sorting (FACS)

Flow cytometry allows for the simultaneous, multiparametric analysis of single cells based on the emission of electronic light. Cells that pass the laser emit scattered light. The forward scatter (FSC) gives information about the size, the side scatter (SSC) measures the granularity of the cell. With the emitted fluorescence of the bound antibody, it is possible to analyze the frequency of antigen expressing cells, as well as the intensity of the expression.

3.3.4 Surface staining

$1x10^6$ cells were transferred into a 96-well flat-bottom plate and centrifuged at 1000 rpm for 7 min. The supernatant was discarded and the pellet was resuspended in fluorescence-activated cell sorting (FACS) buffer with Fc-blocking reagent for 10 min at 4 °C. Cells were washed with 100 µL FACS buffer and centrifuged (1000 rpm, 7 min). The pellet was stained with fluorochrom-conjugated monoclonal antibodies against surface antigens. After incubation of 30 min at 4 °C, cells were centrifuged (1000 rpm, 7 min), washed twice with 200 µL FACS buffer and measured with FACSCanto II (BD) using the BD Diva Software V.6.1.1. At least 800.000 events were measured for CCR5 analysis and 20.000 events for $CD8^+$ T cell proliferation. FlowJo software 7.6.1 (Tree Star) was used for dot plots or histograms.

3.3.5 Intracellular staining

For intracellular staining, single cell suspension was incubated in 100 µL of fixation/ permeabilization solution (1:4 dilution) (eBioscience) for 45 min at 4 °C and subsequently washed twice with 200 µL permeabilization buffer before fluorescently labeled antibodies against intracellular antigens were added. After 30 min incubation at 4 °C, cells were washed with FACS buffer, resuspended in 100 µL of the same and measured by flow cytometry (FACSCanto II from BD Biosciences). FlowJo software 7.6.1 (Tree Star) was used for data analysis and shown as dot plots and histograms.

3.3.6 Bio-plex assay

For the detection of multiple cytokines and chemokines in the serum and lysates of skin tumors and metastatic LN, bio-plex assay was performed. Bio-plex assay is based on capture of antibodies that are directed against particular soluble factors and conjugated with beads. The reaction is detected by antibodies coupled to horseradish peroxidase.

3.3.6.1 Preparation of skin tumor and metastatic LN lysates

Skin tumors and metastatic LN were isolated and one small piece (3 mm²) of the tumor or LN was snap frozen in liquid nitrogen. To prepare lysates of the tissue, 250 µL lysis buffer for the tumor or 150 µL for the LN were added to the frozen samples. The tissue was mechanically smashed in an Eppendorf tube then frozen at -80 °C for 10 min. Lysates were thawed on ice and the rest of the tissue was broken down in the ultrasonic bath for 20 min at 4 °C. Lysates were again frozen at -80 °C for 20 min and thawed on ice before they were centrifuged at 1300 rpm for 20 min at 4 °C. Supernatant was transferred into a new Eppendorf tube and protein concentration was determined by bicinchoninic acid (BCA) assay. Samples were diluted with bio-plex sample diluent to a concentration of 1 mg/mL total protein. Cytokine and chemokine concentration were finally determined with a bio-plex protein array according to the manufacturer´s instructions.

3.3.6.2 Preparation of serum

Serum was centrifuged at 13000 rpm for 10 min, 4 °C and protein concentration was measured by BCA assay. For the bio-plex protein array, 30 µL serum was used and the final cytokine or chemokine concentration was then recalculated with the total protein concentration measured before by Pierce BCA Protein Assay Kit.

3.3.6.3 Procedure of the assay

Analysis of chronic inflammatory factors (CCL2, CCL3, CCL4, CCL5, IL-1β, IL-1RA, IL-2, IL-4, IL-5, IL-6, IL-7, IL-8, IL-9, IL-10, IL12p70, IL13, IL-15, IL17A, TGF-β, FGF-2, eotaxin, G-CSF, GM-CSF, IFN-γ, interferon-gamma induced protein 10 (IP-10), TNF-α, VEGF, and PDGF-AB/BB) in serum samples and metastasis lysates of the same melanoma patient were performed by the multiplex technology (Bio-Rad) according to the manufacturer´s protocol. Concentration of chronic inflammatory factors in serum and LN lysates of WT and *ret* transgenic mice without visible skin tumors, as well as in skin tumor lysates of *ret* transgenic tumor bearing mice, were measured by multiplex technology according to the manufacturer´s protocol. Bio-plex Manager™ software (Version 6.0) was used for the acquisition and data analysis.

3.3.7 Proliferation Assay

In order to analyze the immunosuppressive activity of CCR5 MDSC subsets on T cell proliferation, $CCR5^+$ MDSC or $CCR5^-$ MDSC were sorted and co-cultured with $CD8^+$ T cells isolated from the spleens of BL/6 mice.

For MDSC isolation, BM from femur and tibiae of tumor bearing mice were collected and prepared as described in 3.2.2.3. After lysis of the erythrocytes, BM cell suspension was stained with anti-mouse CD11b-APC Cy7, anti-mouse Gr-1-PE Cy7 and anti-mouse CCR5-PE

for 30 min at 4 °C. Cell suspension was then washed with PBS at 1400 rpm for 7 min and the pellet was resuspended with SORT-buffer. $CCR5^+$ and $CCR5^-$ subsets of $CD11b^+Gr1^+$ MDSC were sorted using FACSAria cell sorter (BD Biosciences). The purity of sorted cell populations was 99%.

For the isolation of T cells, the spleen of one WT mouse was isolated and single cell suspension was prepared. Pellet was resuspended in PBS and cells were counted by Neubauer counting chamber. The cell suspension was centrifuged at 1400 rpm for 7 min and the pellet was resuspended in MACS buffer according to the provided MACS protocol to isolate $CD8^+$ T cells. For the detection of proliferating T cells, the cell suspension was centrifuged at 1400 rpm for 7 min and the pellet was stained with 1 µM CFSE for 5 min at 37 °C in the water bath. The reaction was stopped by adding 10 mL MDSC complete medium. Cells were centrifuged at 1400 rpm for 7 min and the pellet was resuspended in MDSC complete medium to count the cells by Neubauer counting chamber.

For co-culturing, $2x10^4$ $CD8^+$ T cells and the appropriate amount of $CCR5^+$ or $CCR5^-$ MDSC were cultivated in 96 U-bottom well plates in MDSC complete medium. For T cell activation, Dynabeads® magnetic beads at a bead-to-T cell ratio of 1:1 were prepared according to the Dynabeads® mouse T-activator CD3/CD28 kit protocol and added to the co-culture. MDSC activation and proliferation was ensured by adding 40 ng/mL GM-CSF and 40 ng/mL IL-6 (peproTech) to the culture. After 3 days of co-culture at 37 °C, 5 % CO_2 and 95 % humidity, cells were pelleted. Cells were stained with anti-mouse CD8-eFluor450 antibodies to identify $CD8^+$ T cells by flow cytometry.

3.3.8 MHC dextramer staining of TRP-2 specific $CD8^+$ T cells

Dextramer® Technology is based on the interaction of TCR on T cells and MHC complex on APC. Fluorescent labeled MHC dextramers enables the detection of antigen-specific T cells *ex vivo* by flow cytometry. In this case, the MHC complex contained the TRP-2 derived $peptide_{180\text{-}188}$ (SVYDFFVWL).

Cells were prepared as described in 3.3.2. After Fc-blocking, cells were incubated with 10 µL PE-conjugated MHC dextramer for 10 min at 4 °C. Anti-mouse CD8-APC Cy7 and anti-mouse CCR5-APC were added and incubated another 20 min at 4 °C. Cells were washed four times with 200 µL FACS buffer and then measured with FACSCanto II.

3.3.9 Analysis of MDSC migration capacity

The transwell assay is a commonly used method to analyze the migratory capacity of cells due to chemotaxis. The transwell system consists of inserts with a permeable membrane of 0.3 µm micro pores. This membrane separates the well in an upper and lower chamber. Myeloid cells

from the BM of WT mice were isolated with the MDSC isolation kit (Miltenyi). In the upper chamber, $5x10^5$ MDSC were seeded in medium supplemented with 40 ng/mL GM-CSF and 40 ng/mL IL-6. The lower chambers were loaded with 10 ng/mL CCL3, 15 ng/mL CCL4 or 40 ng/mL CCL5 as described (Sapir et al., 2010). The mCCR5-Ig fusion protein was added to a final concentration of 20 ng/mL. Cells migrated for 3 h at 37 °C, 5 % CO_2. After incubation, the content of the lower chamber was collected and cells were counted three times with the Neubauer counting chamber.

3.3.10 Therapy of *ret* transgenic mice with the mCCR5-Ig fusion protein

mCCR5-Ig was constructed as previously described (Sapir et al., 2010) and provided by InVivo BioTech Services (Berlin). *Ret* transgenic tumor bearing mice were injected intraperitoneally (i.p.) with 10 mg/kg mCCR5-Ig in 200 µL PBS twice per week for three weeks. The control group of mice with tumors of similar size received the corresponding amount of anti-mouse immunoglobulin G (IgG) (Sigma-Aldrich). Both groups were monitored for tumor progression.

3.3.11 Characteristics of melanoma patients at different stages

Peripheral blood and metastases were obtained from 66 melanoma patients of stage I-IV (AJCC 2009) who were seen at the Skin Cancer Center (University Medical Center Mannheim, Germany) from January 2013 to August 2015 (ethics approval: 2010-318N-MA). Exclusion criteria were cardiac disease, autoimmune disease, diabetes mellitus, and immunotherapies within 6 months before the patient's visit. Peripheral blood from 14 age- and gender-matched healthy donors (HD) without indications of immune-related diseases were obtained at the Institute of Transfusion Medicine and Immunology, Medical Faculty Mannheim, Heidelberg University, German Red Cross Blood Service Baden Württemberg-Hessen (Mannheim, Germany) after informed consent and used as controls. Characteristics of patients and HD are listed in Table 15

Table 1: Characteristics of melanoma patients and HD

Baseline characteristic	Melanoma patients	Healthy donors
Subjects (n)	66	14
Melanoma stage, n (%)		
I	16 (24.2%)	
II	20 (30.3%)	
III	19 (28.8%)	
IV	11 (16.6%)	
Sex, n (%)		
Female	19 (28.8%)	6 (42.9%)
Male	47 (71.2%)	8 (57.1%)
Age (years)[a] (range)	62.37 (33-90)	59,82 (51-69)

[a] Age at the blood draw

3.3.12 PBMC isolation from human peripheral blood samples

Peripheral blood from heparinized venous blood and skin metastasis was obtained from untreated melanoma patients of different stages (stage I-IV) in the Department of Dermatology (University Medical Center Mannheim). Peripheral blood mononuclear cells (PBMC) were isolated from the peripheral blood by density gradient centrifugation. Two Leucosep tubes per patient were filled with 15 mL Biocoll and spun down at 1400 rpm for 10 sec. Blood was diluted with 15 mL RPMI before distributing it equally to the prepared Leucosep tubes and centrifuged at 2000 rpm for 20 min (without break). PBMC layers of both Leucosep tubes were carefully removed with a pasteur pipet and washed with RPMI in a final volume of 50 mL at 1400 rpm for 7 min. The pellet was resuspended in an appropriate amount of X-VIVO 20 to count the cells and then washed again. Isolated PBMC were directly stained and measured by flow cytometry or stored in liquid nitrogen until the time of experimentation. $1x10^7$ cells were resuspended in 500 µL freezing medium 1 (see 3.1.8). Afterwards, 500 µL freezing medium 2 (see 3.1.8) was added to the cell suspension and frozen in “Mr. Frosty” overnight. The other day, cells were transferred from -80 °C to liquid nitrogen for long term storage.

Frozen cryotubes were shortly submerged in a 37 °C water bath till the cell suspension was almost thawed. Cells were transferred in 15 mL tubes and washed with 10 mL RPMI at 1400 rpm for 10 min before staining for FACS analysis.

Serum was collected from venous blood samples after centrifugation at 1400 rpm for 10 min and frozen at -20 °C until bio-plex assay was performed.

3.3.13 Preparation of tumor samples from melanoma patients

Fresh melanoma skin metastasis was smashed mechanically with a plunger through a 40 µm cell strainer to get a single cell suspension. Cells were washed with PBS and lysis of the erythrocytes was performed as described for mouse tumors. Single cell suspension was stained on the same day and measured by flow cytometry.

3.3.14 Statistical analysis

Statistical analyses were performed using GraphPad Prism software. Results were assessed with a one-way ANOVA test or an unpaired two-tailed Student's t test. Throughout the analysis, $p < 0.05$ was considered as statistically significant.

4 Results

4.1 The role of CCR5-CCR5 ligand interaction in melanoma-bearing mice

It has been previously demonstrated that MDSC are active and accumulate during tumor progression in *ret* transgenic mice and in melanoma patients (Meyer et al., 2011; Jiang et al., 2015). To address the question whether CCR5 plays a role in the recruitment and activity of immunosuppressive cells, we analyzed the CCR5-CCR5 ligand interaction in *ret* transgenic melanoma bearing mice and in melanoma patients.

4.1.1 CCR5 expression on MDSC in melanoma-bearing mice

To identify mouse CCR5$^+$ MDSC the following monoclonal antibodies (mAb) were used: anti-CD11b, anti-Gr-1, anti-CCR5, anti-Ly6C and anti-CD45.2 (for skin tumors). Upon gating for singlets, live cells and CD11b/Gr1 double positive cells were gated (Fig. 2). Whole MDSC populations were gated for CCR5$^+$ and CCR5$^-$ MDSC. Mouse MDSC were further characterized as monocytic (Ly6C^{high}) and granulocytic (Ly6C$^{low/neg}$) MDSC and then analyzed for their immunosuppressive phenotype by NO and ROS production, as well as PD-L1 and ARG-1 expression, of each CCR5 MDSC subset.

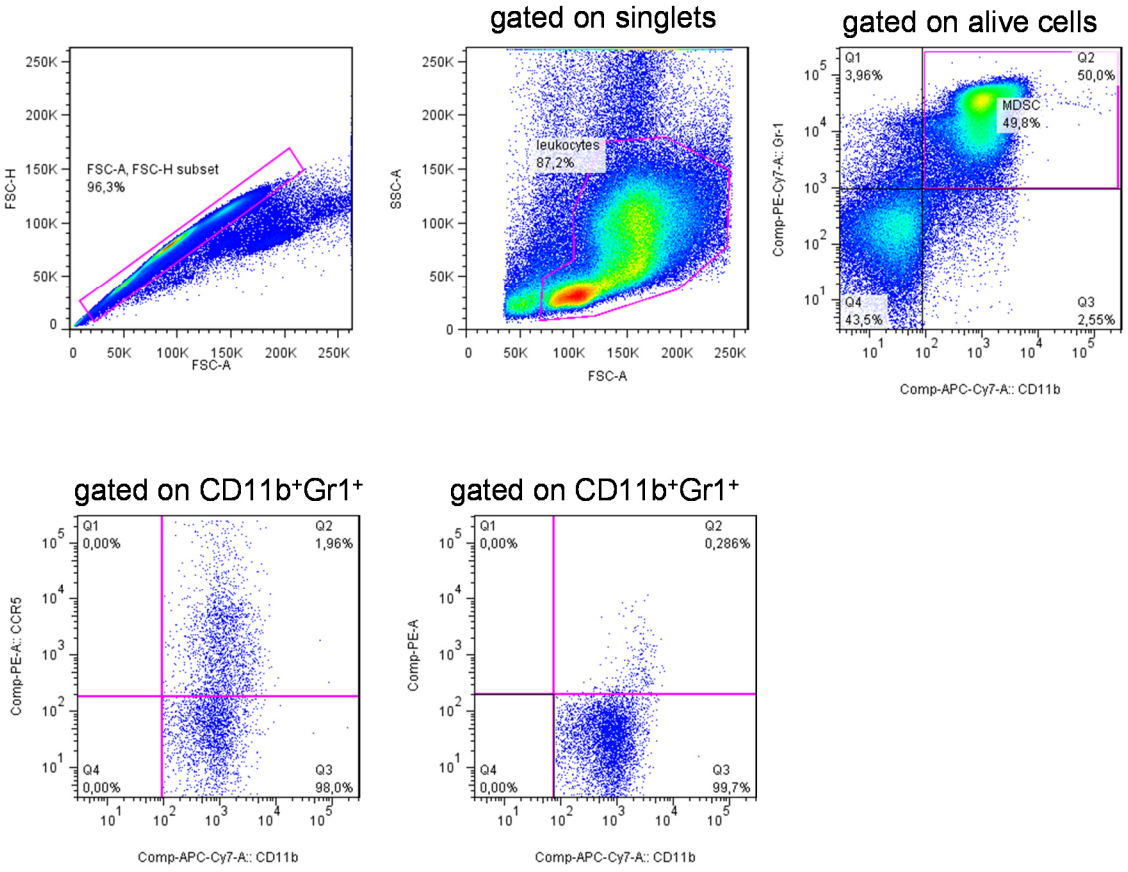

Figure 2: Gating strategy of CCR5 expressing CD11b$^+$Gr1$^+$ cells (MDSC) in the BM of tumor bearing mice. Representative dot plots of the BM are shown.

The expression of CCR5 on mouse MDSC was assessed in the BM, peripheral blood, spleen, metastatic LN and skin tumor samples (Fig. 3). The frequency of CCR5 expressing MDSC in melanoma lesions was elevated as compared to that in the periphery (the BM and peripheral blood) (Fig. 3A). The CCR5 expression intensity on MDSC was higher in skin tumors as compared to the peripheral blood (Fig. 3B). To study the relation between the frequency of invading CCR5 expressing MDSC at the tumor site and metastatic LN during melanoma progression, we performed a linear regression analysis. It was shown that the accumulation of CCR5$^+$ MDSC in skin tumors and metastatic LN correlated with increased tumor weight, which was used as an indicator of tumor progression (Fig. 3C, D). Furthermore, the level of CCR5 expression on MDSC increased in melanoma lesions with tumor weight (Fig. 3E,F). These findings suggest that CCR5 is an important molecule for the migration of MDSC to melanoma lesions.

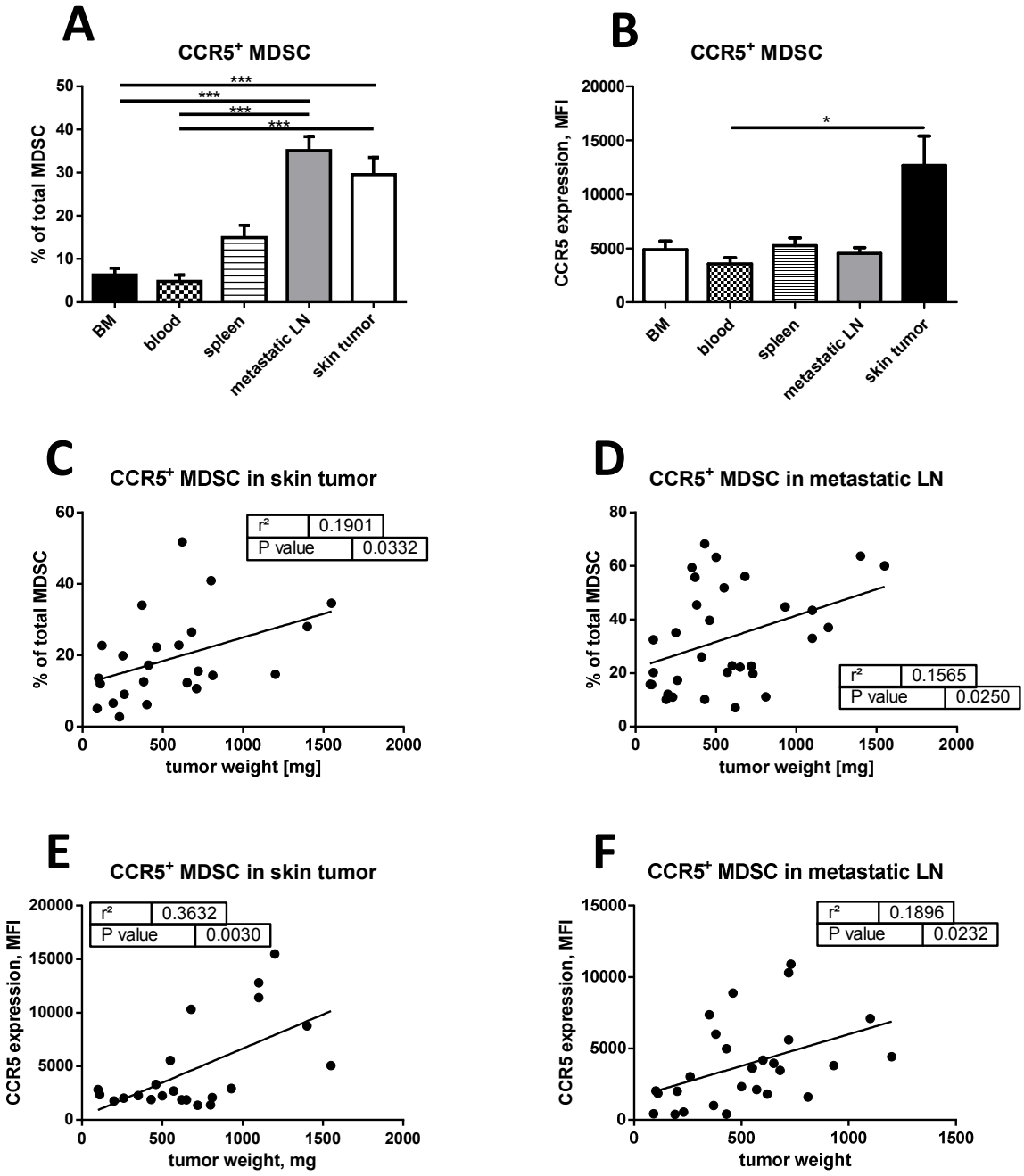

Figure 3: CCR5 expression on MDSC of *ret* transgenic tumor bearing mice. A. CCR5 expressing MDSC in BM, peripheral blood, spleen, metastatic LN and skin tumors were measured by flow cytometry. Results are shown as the percentage of CCR5$^+$ MDSC within total MDSC (mean and SEM). **B.** The intensity of CCR5 expression on MDSC is presented as the mean fluorescence intensity (MFI) ± SEM. The weight of each tumor sample was plotted against the percentage of tumor-infiltrating CCR5 expressing MDSC within total MDSC in skin tumors (**C**, n=24) and metastatic LN (**D**, n=32). The intensity of CCR5 expression on MDSC in skin tumors (**E**, n=22) and metastatic LN (**F**, n=28) was plotted against the tumor weight. The correlation was calculated using a linear regression analysis. 500,000 live cells in BM and peripheral blood, 800,000 live cells in spleen and metastatic LN and 200,000 CD45$^+$ live cells in skin tumor were analyzed. *p < 0.05, ***p < 0.001.

4.1.2 CCR5 expression pattern on MDSC subsets in tumor bearing mice

We next aimed to investigate the expression of CCR5 on MDSC subsets. Fig. 4 shows the frequency of $CCR5^+$ Gr-MDSC and Mo-MDSC in the BM, peripheral blood, spleen, metastatic LN and skin tumors during melanoma development. The frequency of CCR5 expressing Gr-MDSC was raised in skin tumors as compared to the BM, peripheral blood and spleen (Fig. 4A). The frequency of CCR5 expressing Mo-MDSC was also elevated in skin tumors as compared to the BM, peripheral blood and spleen (Fig. 4B). This CCR5 expression pattern is similar to the situation with the total population of MDSC.

Furthermore, we found significantly higher CCR5 expression on Gr-MDSC in metastatic LN and spleen than on the monocytic subpopulation in these organs (Fig. 4C). In accordance with our data on the frequency of $CCR5^+$ Gr-MDSC, the intensity of CCR5 expression in skin tumors was higher than in the BM, peripheral blood and spleen (Fig. 4D). For Mo-MDSC, the level of CCR5 expression in skin tumors and metastatic LN was enhanced as compared to the peripheral blood (Fig. 4E). Analyzing different MDSC subsets, the intensity of CCR5 expression on Gr-MDSC in skin tumors was found to be increased as compared to the monocytic subset (Fig. 4F).

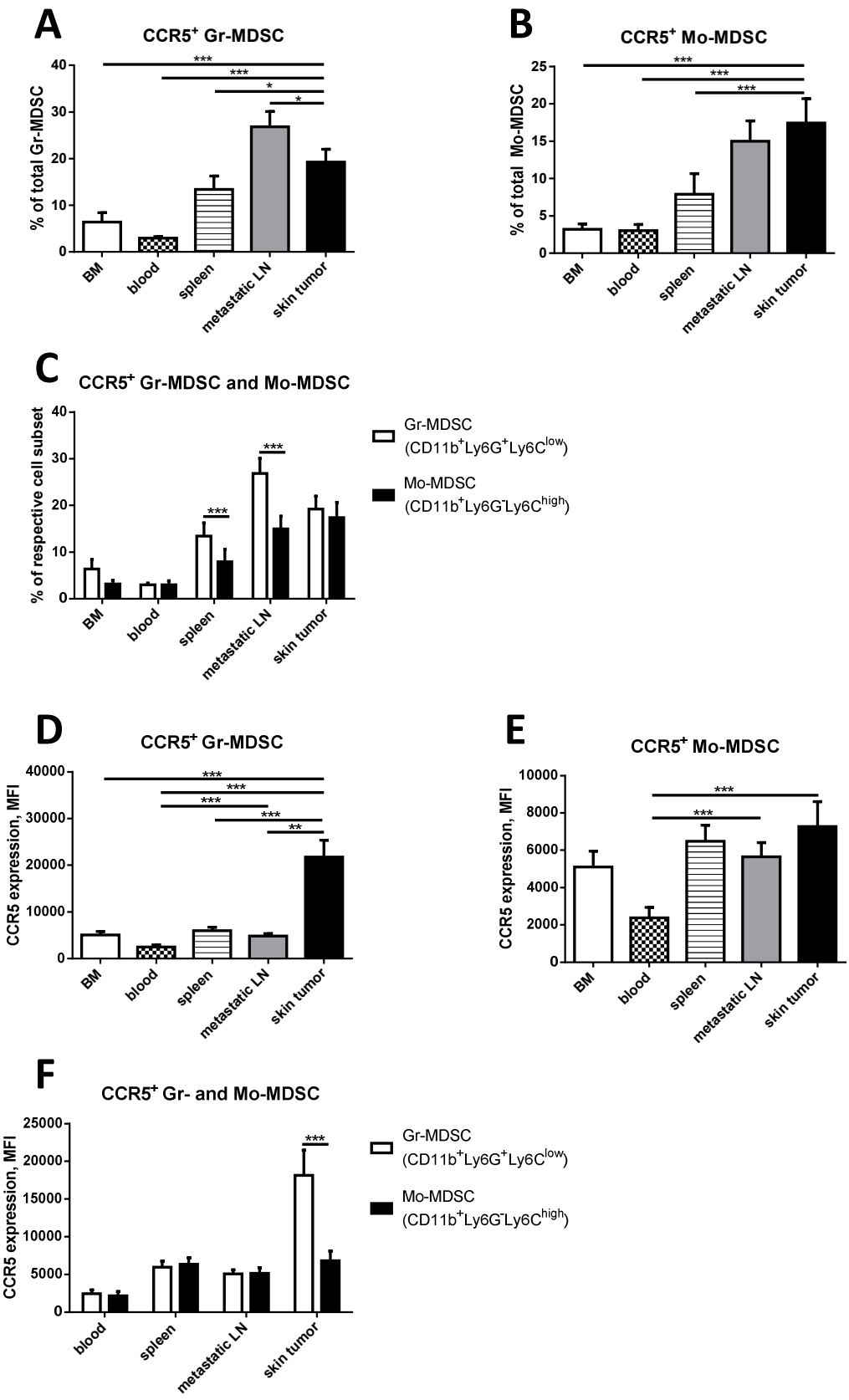
A
CCR5+ Gr-MDSC
% of total Gr-MDSC
BM
blood
spleen
metastatic LN
skin tumor
B
CCR5+ Mo-MDSC
% of total Mo-MDSC
C
CCR5+ Gr-MDSC and Mo-MDSC
% of respective cell subset
Gr-MDSC
(CD11b+Ly6G+Ly6Clow)
Mo-MDSC
(CD11b+Ly6G-Ly6Chigh)
D
CCR5+ Gr-MDSC
CCR5 expression, MFI
E
CCR5+ Mo-MDSC
F
CCR5+ Gr- and Mo-MDSC

Figure 4: Expression of CCR5 on Gr-MDSC and Mo-MDSC in tumor bearing mice. CCR5 expression on Gr- ($CD11b^+Ly6G^+Ly6C^-$) and Mo- ($CD11b^+Ly6G^-Ly6C^+$) MDSC in BM, peripheral blood, spleen, metastatic LN and skin tumor was measured by flow cytometry. The frequency of $CCR5^+$ Gr-MDSC (**A**, n=28) and $CCR5^+$ Mo-MDSC (**B**, n=27) within total $CCR5^+$ MDSC was analyzed in tumor bearing mice (mean and SEM). **C**. A direct comparison between the frequency of $CCR5^+$ Gr-MDSC and $CCR5^+$ Mo-MDSC among total $CCR5^+$ MDSC (n=27-28). **D**. Expression level of CCR5 on Gr-MDSC (n=28) and **E**. Mo-MDSC (n=27) is presented as MFI ± SEM. **F**. The intensity of CCR5 expression on Gr-MDSC was compared to Mo-MDSC and is shown as MFI ± SEM (n=28). *p < 0.05, **p < 0.01, ***p < 0.001.

4.1.3 Increased production of chronic inflammatory mediators in melanoma lesions

To evaluate factors involved in the activation and recruitment of MDSC, serum, metastatic LN and skin tumors were collected. Melanoma lesions were lysed and protein concentration was determined in serum and lysates using a bio-plex assay (Fig. 5). We found that metastatic LN displayed the highest level of CCL3, CCL4, CCL5, CCL2, IP-10, IL-6, VEGF, and TGF-β. Importantly, their concentrations in skin tumors were also significantly higher than in serum. These results suggest that the secretion of chronic inflammatory factors support the activation of $CCR5^+$ MDSC and also the migration of these cells to the melanoma microenvironment.

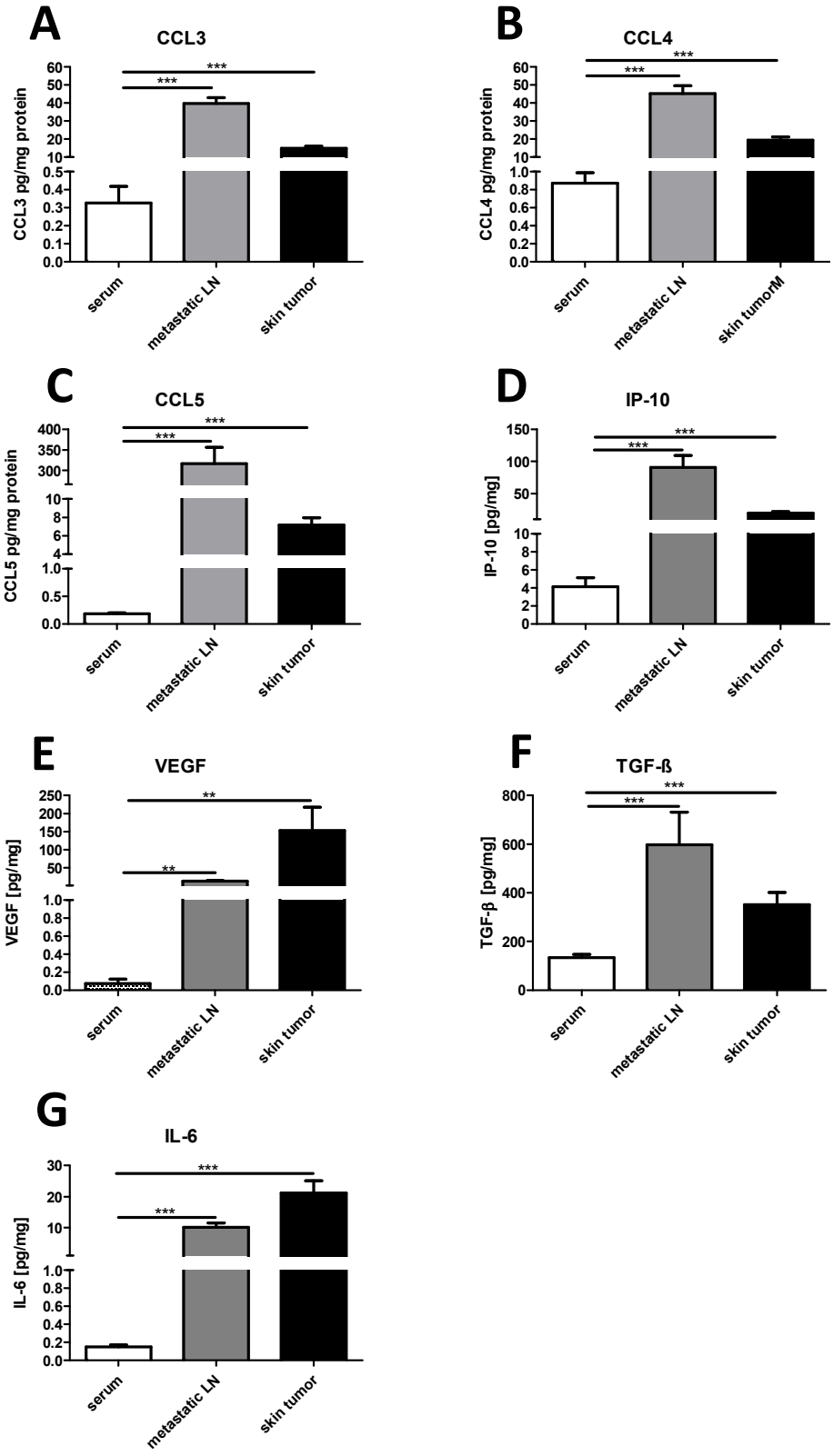

Figure 5: Production of chronic inflammatory mediators in melanoma bearing mice. Concentration of CCL3, CCL4, CCL5 (**A-C**, n=25), CCL2 (**D**, n=16), IP-10, IL-6, VEGF, TGF-β (**E-H**, n=17) was measured in serum and lysates of metastatic LN and skin tumors using bio-plex assay. Results are expressed as pg/mg protein (mean ± SEM). **p < 0.01, ***p < 0.001.

4.1.4 Production of chronic inflammatory mediators in melanoma lesions during tumor development

Chronic inflammatory factors produced in the process of melanoma development play an important role in tumor growth but also in the recruitment of immune cells to the site of the tumor. To get insights into their distribution and concentration during tumor development, we measured their production in tumors with different weights (Fig. 6). The level of CCL3, VEGF and TGF-β was found to be significantly increased, whereas CCL5 production was elevated only slightly in skin tumors. In contrast, the production of CCL3 was decreased during tumor progression in metastatic LN.

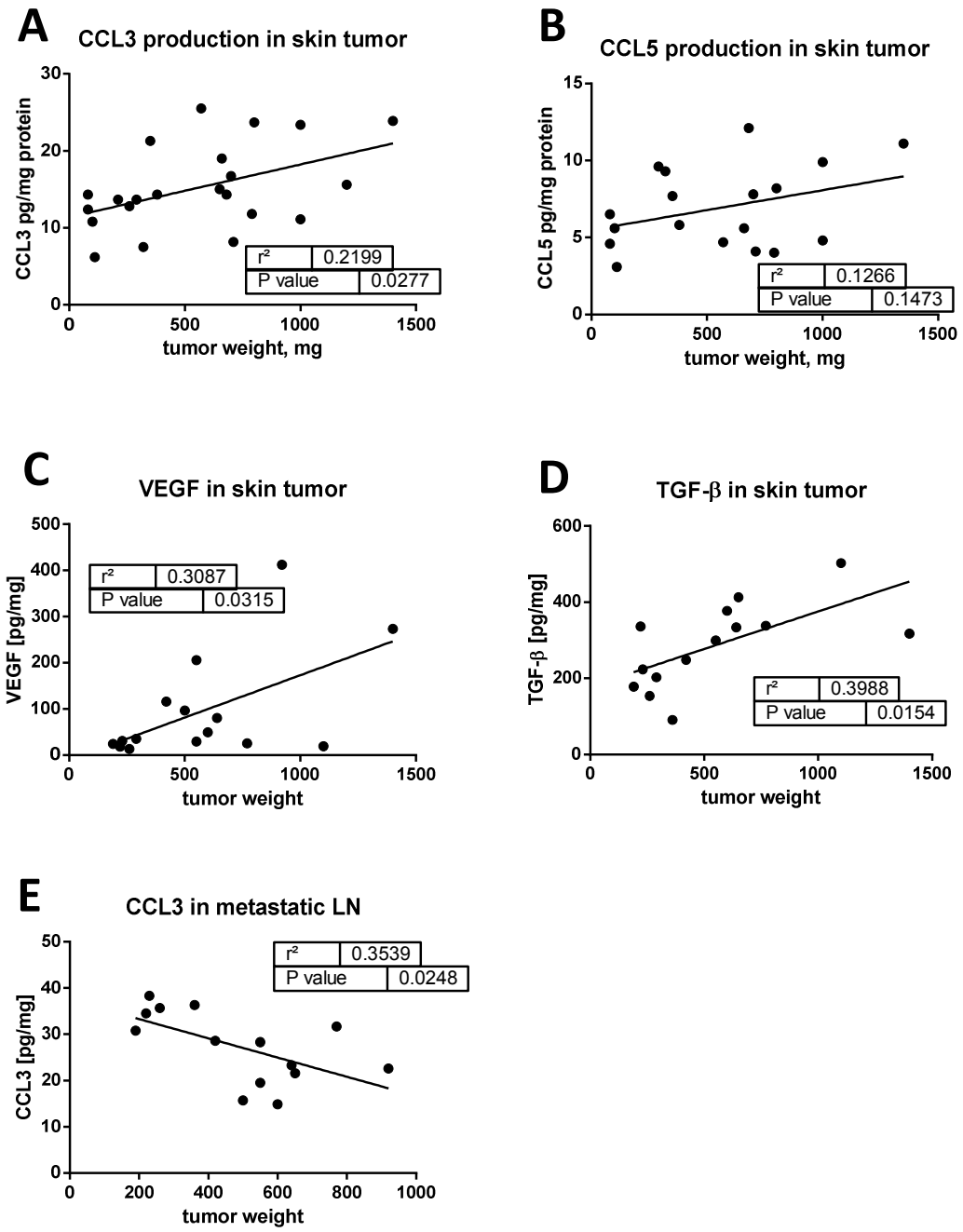

Figure 6: Chronic inflammatory mediators during tumor progression. The level of CCL3 (**A**, n=22), CCL5 (**B**, n=18), VEGF (**C**, n=15), TGF-β (**D**, n=14) production in skin tumors and CCL3 (**E**, n=14) production in metastatic LN was plotted against the tumor weight. The correlation was evaluated by a linear regression analysis. **p < 0.001, ***p < 0.001.

4.1.5 Immunosuppressive activity of CCR5$^+$ MDSC in tumor bearing mice

4.1.5.1 Immunosuppressive phenotype of CCR5$^+$ MDSC

Since NO and ROS production, as well as ARG-1 expression, are considered as key factors of the immunosuppressive phenotype of MDSC (Lu and Gabrilovich, 2012), we measured these molecules in CCR5$^+$ MDSC from the BM, peripheral blood, spleen, and melanoma lesions. We found that CCR5$^+$ MDSC from skin tumors and the peripheral blood produced significantly more NO than their CCR5$^-$ counterparts, indicating an enhanced immunosuppressive capacity of the CCR5$^+$ MDSC subset (Fig. 7A). Interestingly, the level of NO production in CCR5$^+$ MDSC from melanoma lesions was increased as compared to these cells in the peripheral blood.

Next, we analyzed ROS production and observed that in the BM, spleen, metastatic LN and skin tumors, CCR5$^+$ MDSC produced significantly more ROS as compared to the CCR5$^-$ MDSC (Fig. 7B). In addition, ROS production by CCR5$^+$ MDSC in metastatic LN was higher than in the peripheral blood. The frequency of ROS producing CCR5$^+$ MDSC was elevated in metastatic LN and skin tumor as compared to peripheral blood (Fig. 7C).

Furthermore, the level of ARG-1 expression on CCR5$^+$ MDSC in peripheral blood, spleen, metastatic LN and skin tumor was upregulated as compared to the CCR5$^-$ counterpart (Fig. 7D). We also studied PD-L1 expression on CCR5$^+$ MDSC. Interestingly, the frequency of PD-L1 expressing CCR5$^+$ MDSC in all analyzed organs was significantly increased as compared to the CCR5$^-$ MDSC subset (Fig. 7E). The level of PD-L1 expression on CCR5$^+$ MDSC was higher in melanoma lesions as compared to the BM and peripheral blood (Fig. 7F). To conclude, CCR5$^+$ MDSC demonstrated an enhanced immunosuppressive phenotype reflected by increased NO and ROS production, as well as ARG-1 and PD-L1 expression, when compared to their CCR5$^-$ counterpart.

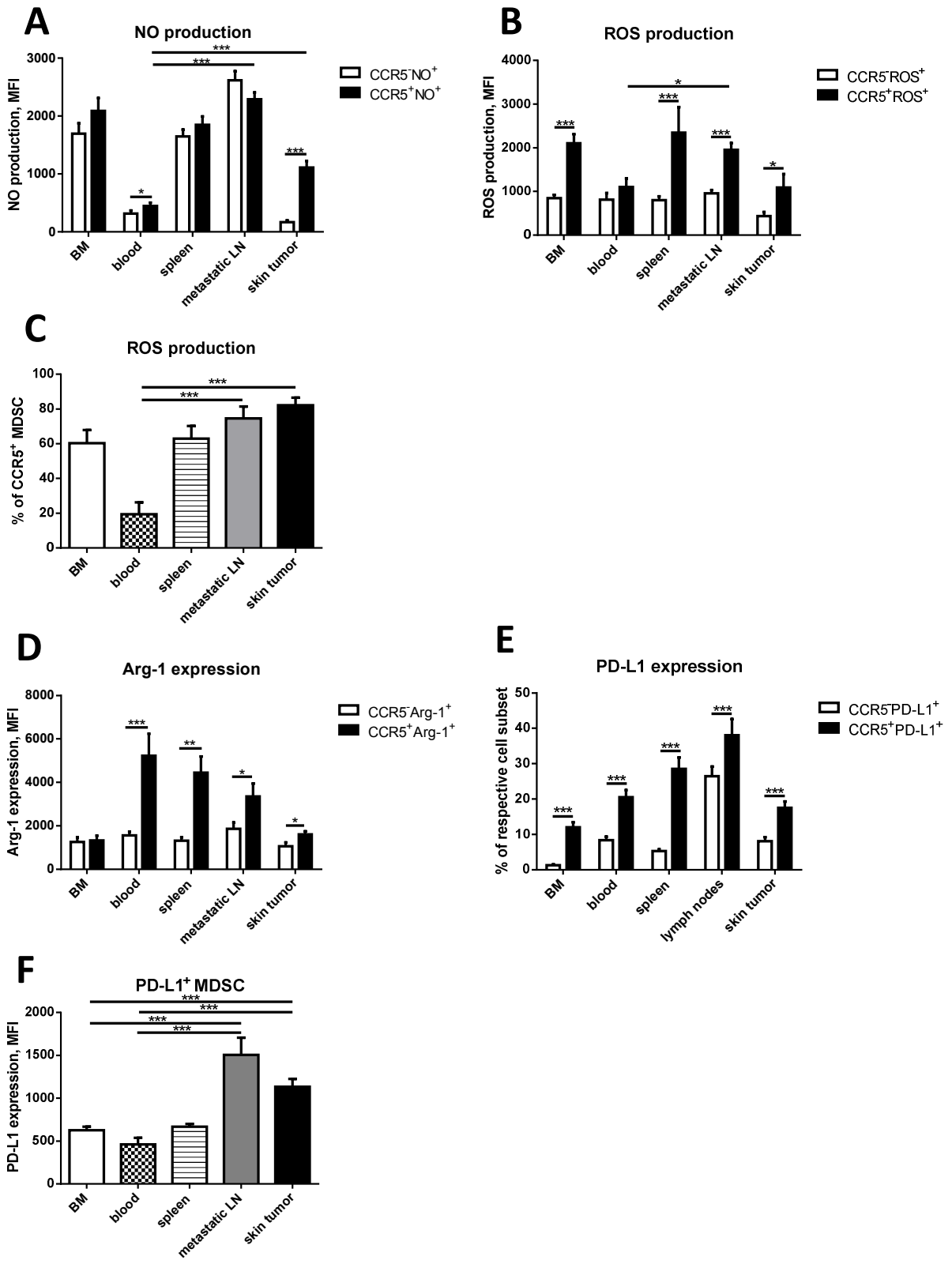

Figure 7: Immunosuppressive phenotype of CCR5⁺ MDSC in *ret* transgenic mice. BM, blood, spleen, metastatic LN and skin tumors were isolated from tumor bearing mice and stained for flow cytometry. Direct comparison between CCR5⁺ MDSC and CCR5⁻ MDSC in the production of NO (**A**.) and ROS (**B**.) is shown and expressed as MFI ± SEM. **C.** The frequency of ROS producing cells by CCR5⁺ MDSC in different organs is presented as the number of ROS producing cells among CCR5⁺ MDSC (mean ± SEM). **D.** The level of ARG-1 expression on CCR5⁺ MDSC and CCR5⁻ MDSC was

assessed and is shown as MFI ± SEM. **E.** The frequency of PD-L1 expressing $CCR5^+$ MDSC and $CCR5^-$ MDSC was analyzed and is presented as the percentage of CCR5 expressing MDSC among the respective cell subset (mean and SEM). **F.** Frequency of PD-L1 expressing $CCR5^+$ MDSC in different organs are presented (BM, n=27; peripheral blood, n=25; spleen, n=27; metastatic LN, n=27; skin tumor, n=25). *p < 0.05, **p < 0.01, ***p < 0.001.

4.1.5.2 Immunosuppressive phenotype of $CCR5^+$ MDSC in melanoma lesions during tumor progression

To determine the immunosuppressive phenotype of $CCR5^+$ MDSC in course of melanoma progression, we analyzed NO and ROS production and the ARG-1 and PD-L1 expression in $CCR5^+$ MDSC at different phases of melanoma progression (Fig. 8). It was found that the frequency of NO producing $CCR5^+$ MDSC increased in skin tumors and metastatic LN (Fig. 8 A,B) during tumor development. Furthermore, we found an increased frequency of ROS producing $CCR5^+$ MDSC in skin tumors and metastatic LN (Fig. 8 C-F), as well as a higher intensity of ROS production in these organs during melanoma progression. Moreover, tumor-infiltrating $CCR5^+$ MDSC that express ARG-1 accumulated in melanoma lesions and the level of ARG-1 expression raised with tumor load (Fig. 8 G-I). Interestingly, the frequency of PD-L1 expressing $CCR5^+$ MDSC and also the intensity of PD-L1 expression of these cells were elevated with increasing tumor weight in skin tumors and metastatic LN (Fig. 8 J-M).

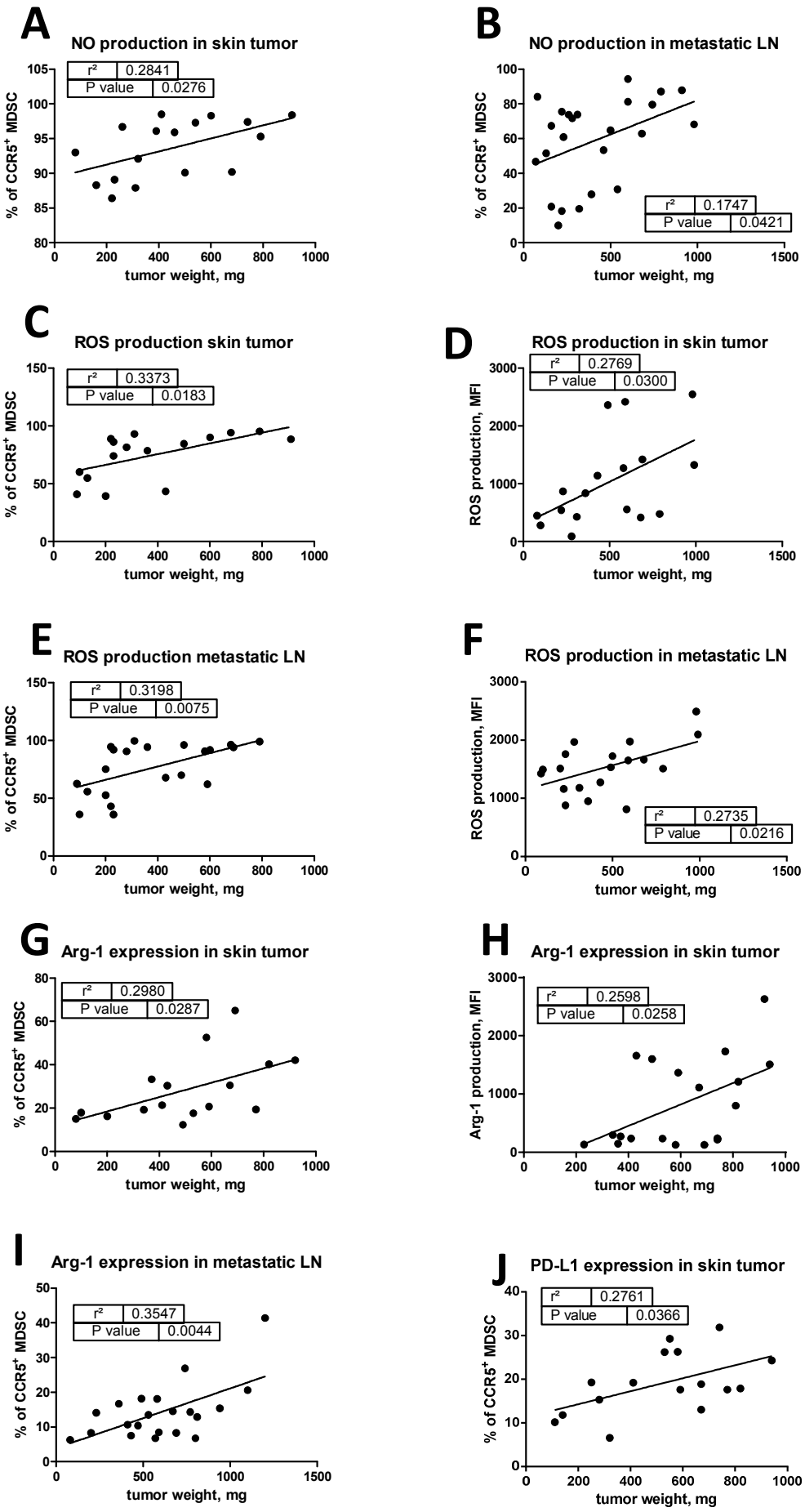
A
NO production in skin tumor
r² 0.2841
P value 0.0276
% of CCR5+ MDSC
tumor weight, mg
B
NO production in metastatic LN
r² 0.1747
P value 0.0421
% of CCR5+ MDSC
tumor weight, mg
C
ROS production skin tumor
r² 0.3373
P value 0.0183
% of CCR5+ MDSC
tumor weight, mg
D
ROS production in skin tumor
r² 0.2769
P value 0.0300
ROS production, MFI
tumor weight, mg
E
ROS production metastatic LN
r² 0.3198
P value 0.0075
% of CCR5+ MDSC
tumor weight, mg
F
ROS production in metastatic LN
r² 0.2735
P value 0.0216
ROS production, MFI
tumor weight, mg
G
Arg-1 expression in skin tumor
r² 0.2980
P value 0.0287
% of CCR5+ MDSC
tumor weight, mg
H
Arg-1 expression in skin tumor
r² 0.2598
P value 0.0258
Arg-1 production, MFI
tumor weight, mg
I
Arg-1 expression in metastatic LN
r² 0.3547
P value 0.0044
% of CCR5+ MDSC
tumor weight, mg
J
PD-L1 expression in skin tumor
r² 0.2761
P value 0.0366
% of CCR5+ MDSC
tumor weight, mg

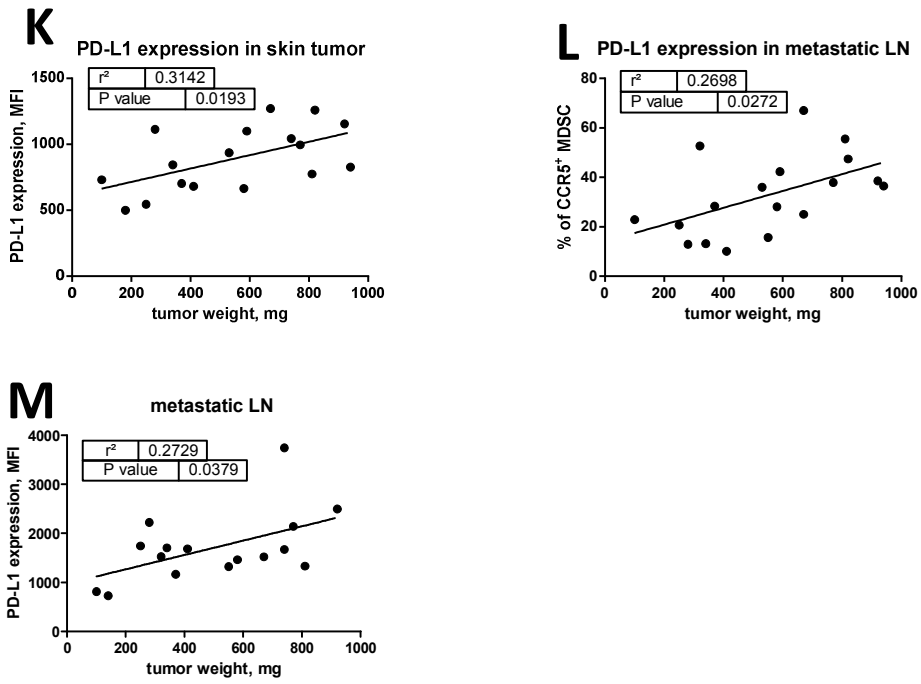

Figure 8: Functional phenotype of CCR5⁺ MDSC in melanoma lesions in course of tumor progression. NO and ROS production, as well as ARG-1 and PD-L1 expression of CCR5⁺ MDSC, was analyzed by flow cytometry and was plotted against the tumor load. Frequency of NO production in skin tumors (**A**, n=17) and intensity of NO production in metastatic LN (**B**, n=24) was measured. The frequency of ROS producing CCR5⁺ MDSC in melanoma lesions (skin tumor **C**. and metastatic LN **E**.) and the intensity of ROS production in skin tumors and metastatic LN is shown in **D**. and **F**. The expression of ARG-1 is presented as the percentage of CCR5⁺ MDSC (**G**). The ARG-1 expression intensity in CCR5⁺ MDSC in skin tumors (**H**) and metastatic LN (**I**) is presented as MFI. The frequency of PD-L1 expressing CCR5⁺ MDSC in skin tumors (**J**) and metastatic LN (**K**) and the level of PD-L1 expression on CCR5⁺ MDSC is shown in melanoma lesions (**L, M**). The correlation was evaluated by a linear regression analysis. *p < 0.05, **p < 0.01, ***p < 0.001.

4.1.6 Immunosuppressive effect of CCR5⁺ MDSC on CD8⁺ T cells

In previous studies, MDSC from *ret* transgenic tumor bearing mice were shown to block the activation and proliferation of T cells (Meyer et al., 2011). Here, we performed a proliferation assay evaluating the ability of CCR5⁺ MDSC to inhibit T cell proliferation. For this experiment, CCR5⁺ and CCR5⁻ MDSC subsets were isolated from the BM of tumor bearing mice by FACS. CD8⁺ T cells were isolated from the spleen of WT mice by magnetic cell sorting, labeled with CFSE and stimulated with anti-CD3/CD28 beads. CCR5⁺ MDSC or CCR5⁻ MDSC were co-cultured with T cells for three days and T cell proliferation was measured via CFSE dilution by FACS analysis (Fig. 9A). We observed that both CCR5⁺ and CCR5⁻ MDSC inhibited proliferation of stimulated T cells as compared to T cells cultured alone (Fig. 9B). Moreover,

we detected a dose-dependent effect of MDSC on T cell proliferation. Comparing effects of BM-derived MDSC subsets, we found that CCR5$^+$ MDSC exerted a tendency for stronger inhibition of T cell proliferation than their CCR5$^-$ counterparts (Fig. 9B).

Taken together, CCR5$^+$ MDSC showed significantly higher NO and ROS production, as well as an elevated ARG-1 and PD-L1 expression as compared to CCR5$^-$ MDSC derived from the same organ. Moreover, they displayed a slightly stronger capacity to suppress T cell proliferation than CCR5$^-$ cells.

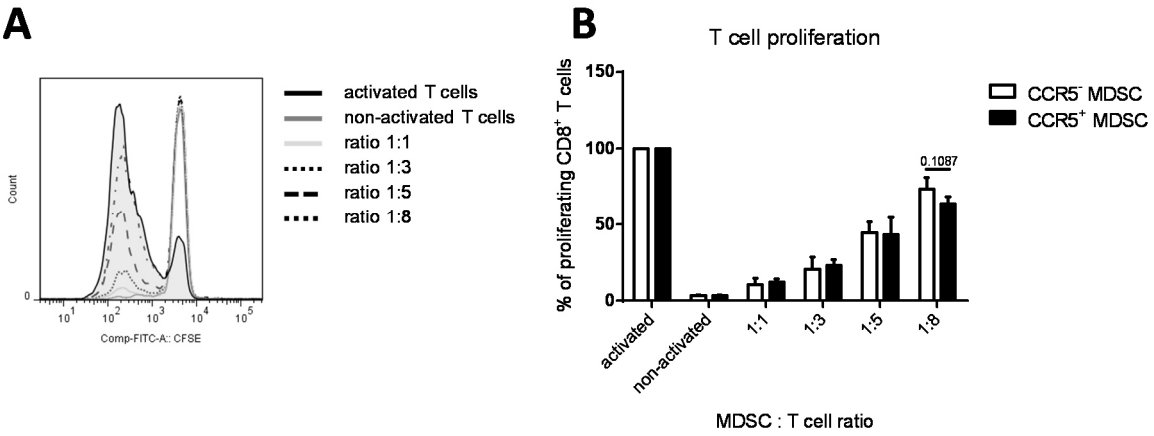

Figure 9: CCR5$^+$ MDSC from *ret* transgenic mice inhibit T cell proliferation. CCR5$^+$ MDSC and CCR5$^-$ MDSC from BM of tumor bearing mice were sorted by FACSAria and co-cultured at different ratios with CFSE-labeled CD8$^+$ T cells isolated from naïve C57BL/6 splenocytes and stimulated with anti-CD3/CD28 beads. Proliferation was assessed by CFSE dilution on day 3 by flow cytometry. **A.** A representative histogram assessing T cell proliferation is shown. **B.** The frequency of proliferating T cells cultured with MDSC at different ratios is presented. Data represents the mean of three experiments (mean ± SEM).

4.1.7 Chemokine-mediated migration capacity of MDSC

Next, we investigated the impact of chemokines on the migration of MDSC. Therefore, we performed a chemotaxis assay in a transwell system (Fig. 10). In this assay, we analyzed the CCR5 ligand-mediated migration of IMC isolated from the BM of WT mice and the neutralization capacity of the fusion protein mCCR5-Ig (Sapir et al., 2010). This fusion protein encodes 30 amino acids of the second extracellular domain of CCR5 and thus binds and neutralizes the biological function of all three CCR5 ligands. As a control for the mCCR5-Ig, we used an anti-mouse IgG antibody. We found that the migration of IMC was significantly induced by each of the CCR5 ligands CCL3, CCL4 and CCL5 as compared to medium without

any supplements. Analyzing the IMC migration with all three CCR5 ligands, we found no stimulation of migration capacity as compared to the single ligand-mediated migration. Importantly, the mCCR5-Ig fusion protein significantly abrogated the ligand-induced migration of IMC. Therefore, we demonstrated that the CCR5-CCR5 ligand axis is crucial for the migration of IMC *ex vitro*.

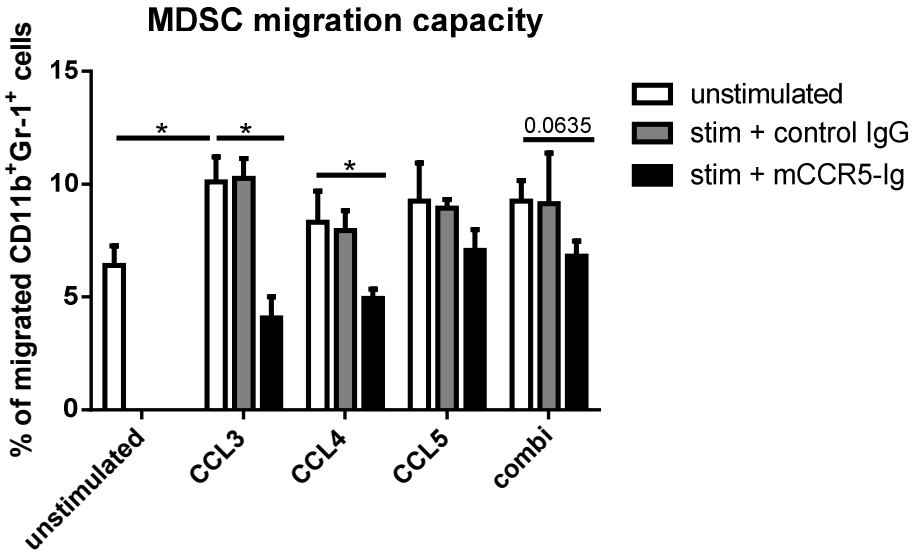

Figure 10: CCR5 ligand-induced migration capacity of CD11b$^+$Gr-1$^+$ cells. IMC were isolated from the BM of healthy C57BL/6 mice using the MDSC Isolation kit. Chemotaxis assay was performed in a transwell system. 2x10^6 cells were incubated for 3 h at 37°C. The lower chamber contained single chemokines (15 ng/mL CCL3, 10 ng/mL CCL4 or 50 ng/mL CCL5) or a combination (CCL3, CCL4,CCL5). mCCR5-Ig (20 ng/mL) or anti-mouse IgG as a control was added. Data of two experiments are presented as the percentage of migrated CD11b$^+$Gr-1$^+$ cells among total cells (mean and SEM). *p < 0.05.

4.1.8 Role of CCR5 on various T cell subsets in melanoma-bearing mice

4.1.8.1 CCR5 expression on various T cell subsets infiltrating melanoma lesions

Next, we studied the expression of CCR5 on T cells from *ret* transgenic tumor bearing mice since it was described its expression on various T cell subsets (Fukada et al., 2002; Ward et al., 2015).

We collected the peripheral blood, spleen, metastatic LN and skin tumors of *ret* transgenic tumor bearing mice, prepared a single cell suspension and stained it with different T cell markers. Fig. 11 shows a representative gating strategy of CCR5 expressing $CD4^+$ Treg, naïve $CD4^+$ T cells, activated $CD4^+$ T cells and $CD8^+$ T cells. We first gated singlets and live cells, followed by the identification of $CD3^+$ T cells. Then T cells were divided on $CD4^+$ and $CD8^+$ T cells. $CD4^+CD25^+FoxP3^+$ T cells were identified as Treg. $CD25^-FoxP3^-$ cells represented $CD4^+$ naïve T cells and $CD25^+FoxP3^-$ were classified as $CD4^+$ activated T cells. All $CD4^+$ and $CD8^+$ T cell subsets were then gated for $CCR5^+$ and $CCR5^-$ expression followed by the analysis of activation markers (CD69, PD-1, TCR ζ-chain) to evaluate their functional status.

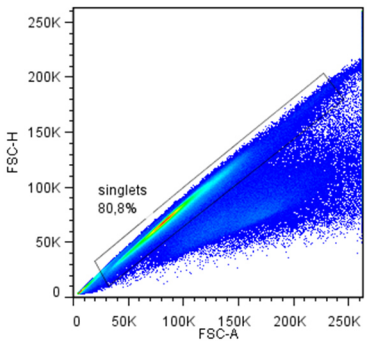

gated on singlets

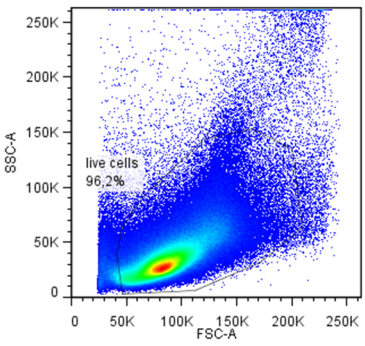

gated on alive cells

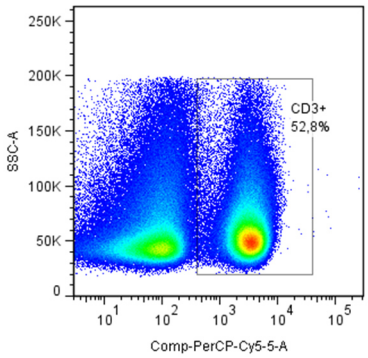

gated on CD3⁺ cells

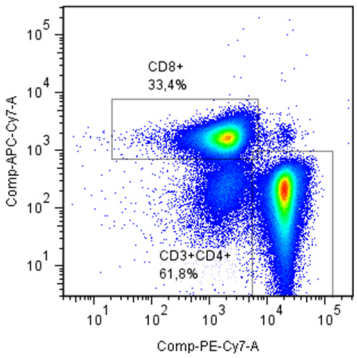

gated on CD3⁺CD4⁺

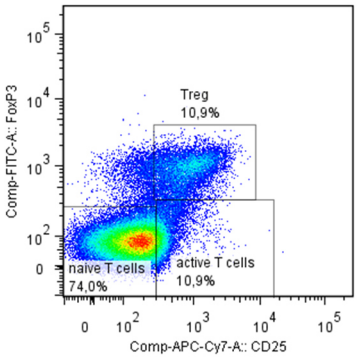

gated on CD25⁺FoxP3⁻

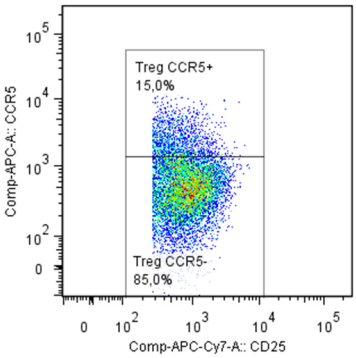

gated on CD25⁺FoxP3⁻

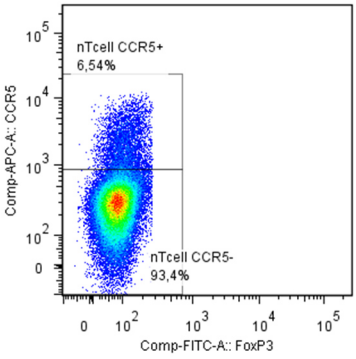

gated on CD25⁺FoxP3⁻

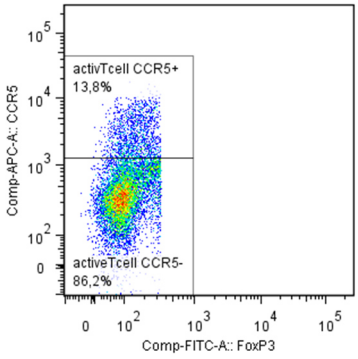

Figure 11: Gating strategy of CCR5 expressing T cell subsets in splenocytes of *ret* transgenic mice. Representative dot plots of the spleen are shown.

We analyzed the CCR5 expression on various T cell subsets of *ret* transgenic tumor bearing mice. In melanoma lesions, the highest frequency of CCR5 expressing cells was detected among Treg (Fig. 12A, B). Interestingly, the frequency of $CCR5^+$ cells among naïve $CD4^+$, activated $CD4^+$ and $CD8^+$ T cells was significantly lower than on $CD4^+$ Treg subset. Therefore, immunosuppressive Treg infiltrating melanoma lesions are characterized by enhanced CCR5 expression as compared to conventional $CD4^+$ and $CD8^+$ T cells.

Studying the frequency of $CCR5^+CD4^+$ Treg in different organs, we observed an increased frequency of $CCR5^+$ Treg in melanoma lesions as compared to the peripheral blood (Fig. 12C). Furthermore, CCR5 expression intensity was higher in metastatic LN than in the peripheral blood (Fig. 12D).

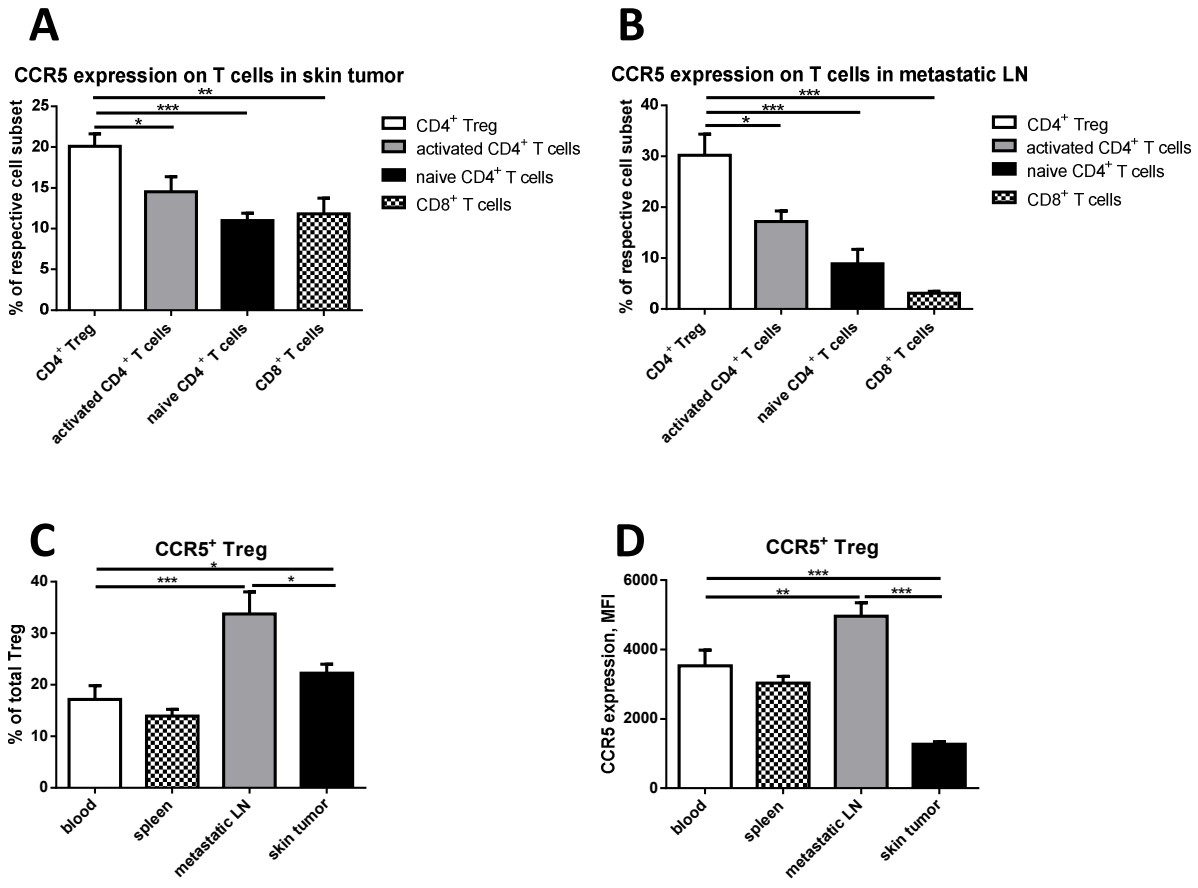

Figure 12: CCR5 expression on various T cell subsets of *ret* transgenic mice. Metastatic LN and skin tumors were isolated from tumor bearing mice and single cell suspension was prepared. Cells were analyzed by flow cytometry. CCR5 expression on naïve and activated $CD4^+$ T cells, $CD4^+$ Treg and $CD8^+$ T cells were analyzed in skin tumors (**A,** n=12-20) and metastatic LN (**B,** n=12-20). Data is presented as the frequency of the respective T cells subset (mean and SEM). The frequency of CCR5 expressing Treg (**C**, n=15-19) and the intensity of CCR5 expression (**D**, n=15-20) were assessed in peripheral blood, spleen, metastatic LN and skin tumors of the same tumor bearing *ret* transgenic mouse (mean and SEM). *p < 0.05, **p < 0.01, ***p < 0.001.

4.1.8.2 Distribution of CCR5 expressing Treg subsets in melanoma lesions

Similar to MDSC, Treg are known to play an immunosuppressive role in the tumor microenvironment as they inhibit T cell proliferation. We examined tumor infiltration by $CCR5^+$ Treg during melanoma development and further measured their frequency among Treg infiltrating tumors of different weights (as an indicator of tumor progression) (Fig. 13). We found that $CCR5^+$ Treg infiltration significantly increased in skin tumors and metastatic LN during the course of melanoma progression (Fig. 13A, B). Analyzing the activation of $CCR5^+$ Treg, we found an augmented frequency of CD69 expressing $CCR5^+$ Treg in peripheral blood, spleen, and melanoma lesions as compared to their $CCR5^-$ Treg counterpart (Fig. 13C). Moreover, the intensity of CD69 expression on $CCR5^+$ Treg in peripheral blood, and melanoma lesions was shown to be higher than on $CCR5^-$ Treg (Fig. 13D). A statistically significant accumulation of $CD69^+CCR5^+$ Treg was displayed in skin tumors as compared to the peripheral blood, spleen, and metastatic LN (Fig. 13E).

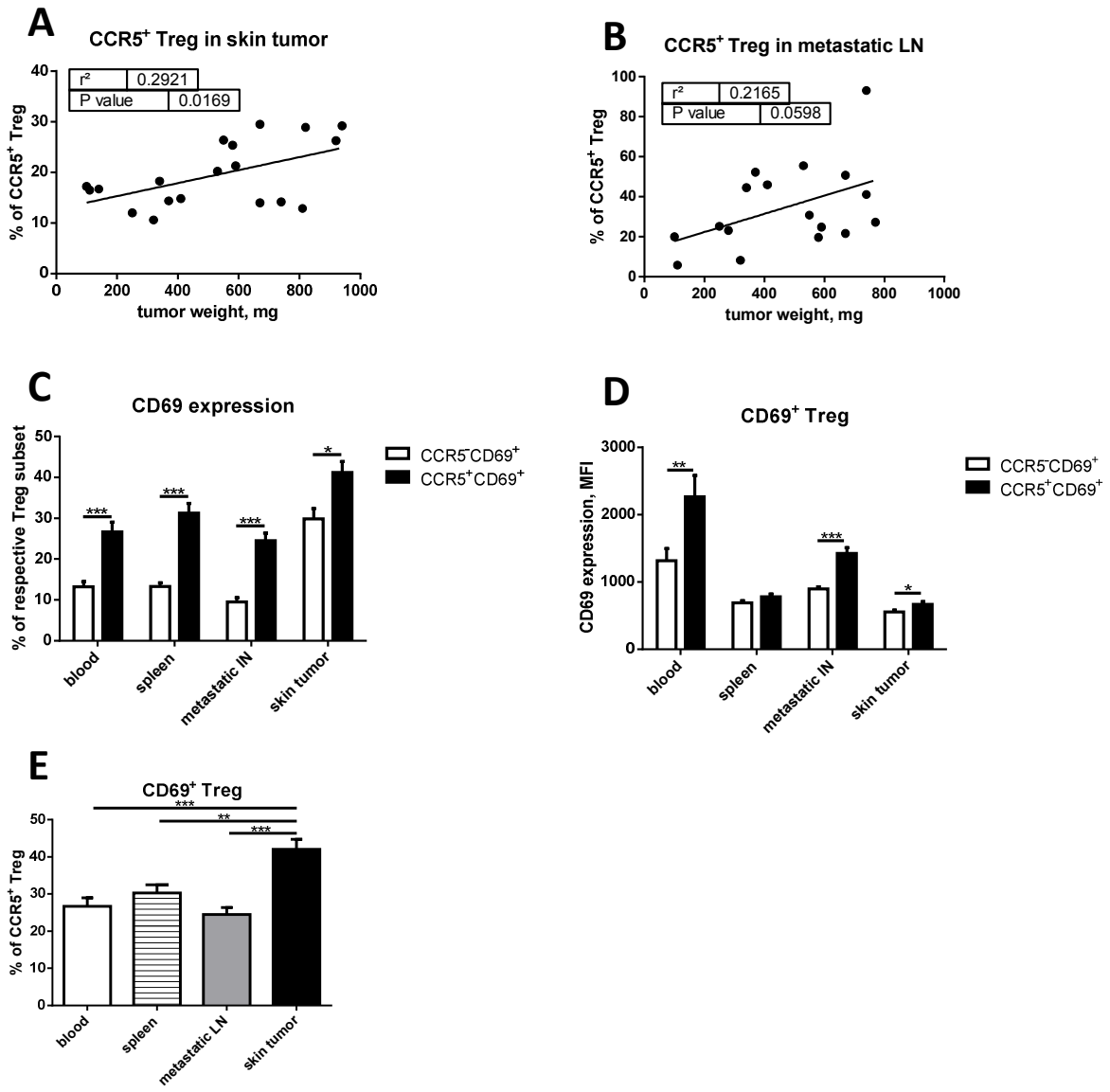

Figure 13: CCR5⁺ Treg in tumor bearing mice. Cells from the peripheral blood, spleen and melanoma lesions were measured by flow cytometry. The frequency of CCR5 expressing Treg in skin tumors (**A**, n=19) and metastatic LN (**B**, n=17) were plotted against the tumor weight. The activity of CCR5⁺ Treg was analyzed by CD69 expression. The frequency of CD69 expressing CCR5⁺ and CCR5⁻ Treg in peripheral blood, spleen, metastatic LN and skin tumor was analyzed (mean and SEM) (**C**, n=17). The intensity of CD69 expression on CCR5⁺ and CCR5⁻ Treg in the periphery and melanoma lesions is shown as MFI (**D**, n=17). The frequency of CD69 expression on CCR5⁺ Treg in tumor bearing mice is presented in **E** (mean and SEM, n=17). *p < 0.05, **p < 0.01, ***p < 0.001.

4.1.8.3 TRP-2 specific CCR5⁺CD8⁺ T cells in the *ret* transgenic mouse melanoma model

To elucidate the tumor-specific immunity in the *ret* transgenic mouse melanoma model, we used MHC dextramers specific for the tumor associated antigen TRP-2. TRP-2 is expressed by melanoma cells and recognized by cytotoxic CD8⁺ T cells (Wang et al., 1996). We found that the frequency of TRP-2 specific CCR5⁺CD8⁺ T cells is significantly increased in the periphery, as well as in metastatic LN and skin tumors as compared to their CCR5⁻ counterparts (Fig. 14A). Furthermore, we detected that the frequency of melanoma specific CCR5 expressing CD8⁺ T cells was elevated in melanoma lesions (Fig. 14B). However, these tumor-specific CCR5⁺CD8⁺ T cells were reduced in course of tumor progression in skin tumors and metastatic LN (Fig. 14C, D). These data indicate that the greatest part of TRP2-specific CD8⁺ T cells was CCR5⁺, which decreased during melanoma development. This result was in contrast to the CCR5⁺ MDSC that increased with tumor progression.

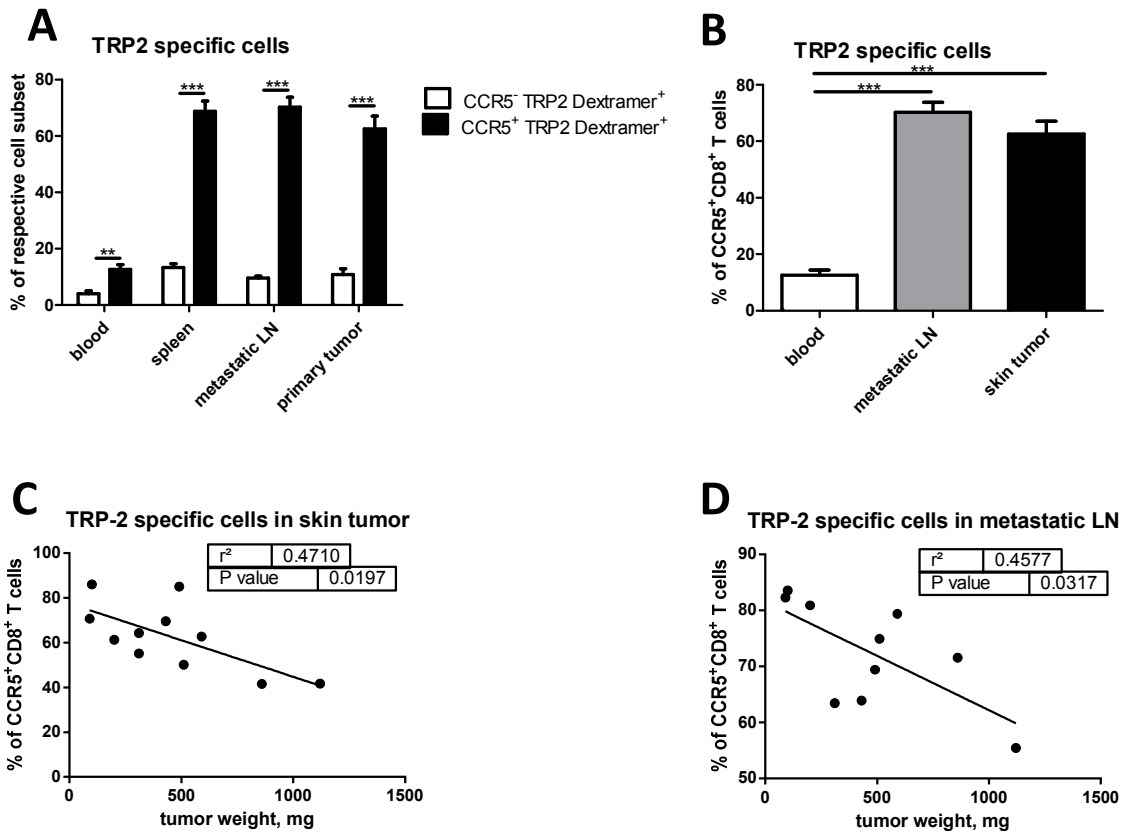

Figure 14: TRP-2 specificity of CCR5 expressing, CD8⁺ T cells in melanoma bearing mice. Direct comparison between CCR5⁺ and CCR5⁻ melanoma specific, CD8⁺ T cells in peripheral blood, spleen, metastatic LN and skin tumor was performed by flow cytometry (**A**, n=11). Results are presented as the frequency of TRP2-specific CCR5⁺CD8⁺ T cells (mean ± SEM). The frequency of TRP-2 specific CCR5⁺CD8⁺ T cells in blood and melanoma lesions is presented (mean and SEM) (**B**, n=11). A correlation between the TRP-2 specific CCR5⁺CD8⁺ T cells and the tumor weight in skin tumors (**C**,

n=11) and metastatic LN (**D**, n=10) was evaluated by a linear regression analysis. *p < 0.05, **p < 0.01, ***p < 0.001.

4.2 Treatment of *ret* transgenic tumor bearing mice with mCCR5-Ig

4.2.1 Effect of soluble CCR5-Ig on survival of *ret* transgenic mice

Tumor bearing *ret* transgenic mice were injected i.p. with mCCR5-Ig twice per week for 3 weeks. The control group was treated with anti-mouse IgG. We found that treated mice displayed a significantly increased survival as compared to the control group (Fig. 15). Thus, in the therapy group, 3 out of 7 mice were living 53 days after the treatment onset, whereas all mice in the control group died after 49 days.

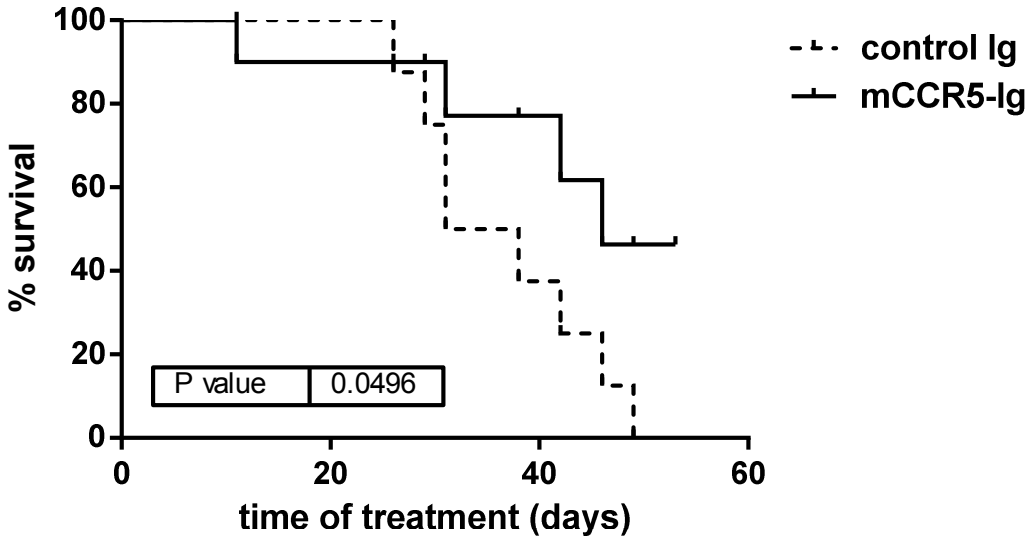

Figure 15: Survival of tumor bearing mice after mCCR5-Ig treatment. Mice were injected i.p. with mCCR5-Ig (10 mg/kg in 200 µl) twice per week for 3 weeks. Mice in the control group received the same concentration of anti-mouse IgG. Survival of mice (n=7-8 mice) is shown as a Kaplan-Meier curve.

4.2.2 Analysis of immune cells in mCCR5-Ig treated tumor bearing mice

Next, we aimed to analyze the effect of mCCR5-Ig therapy on different immune cell populations in the BM, peripheral blood, metastatic LN and skin tumors. Mice were treated for three weeks followed by the study of MDSC, Treg, conventional $CD4^+$ and $CD8^+$ T cells one day after the last injection.

As shown in Fig. 16A, the frequency of MDSC decreased in skin tumors of *ret* transgenic mice after mCCR5-Ig therapy as compared to the mice from control group. Moreover, we demonstrated that NO production by MDSC was significantly lower in skin tumors and the peripheral blood of mCCR5-Ig treated mice as compared to the control mice (Fig. 16B). Importantly, the frequency of $CCR5^+$ MDSC was significantly reduced in skin tumors as compared to the control mice (Fig. 16C). Furthermore, the frequency of these cells was decreased during tumor development (Fig. 16D) indicating a blocking effect of the fusion protein mCCR5-Ig.

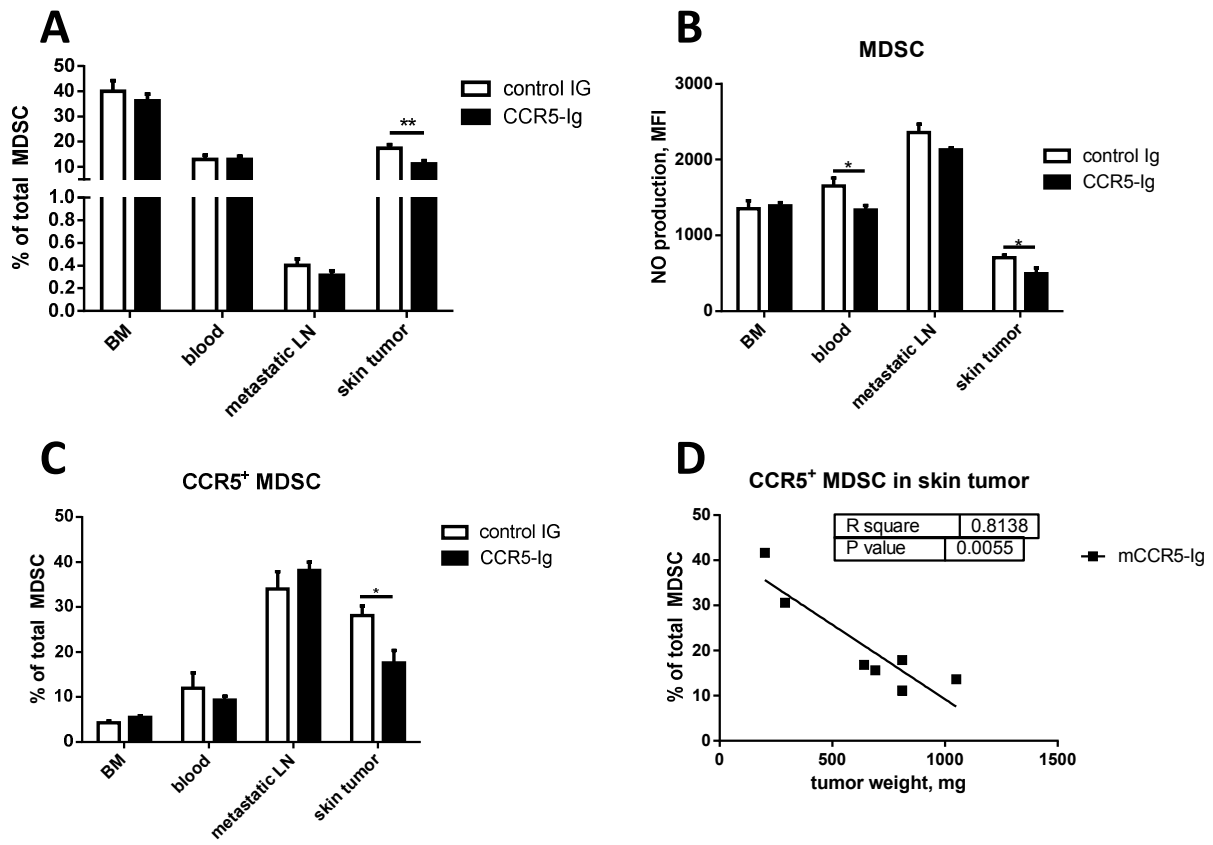

Figure 16: mCCR5-Ig reduced the frequency of tumor-infiltrating MDSC in *ret* transgenic mice. MDSC in BM, peripheral blood, metastatic LN and skin tumors in mCCR5-Ig treated (n=7) and control mice (n=8) were measured by flow cytometry. **A.** Frequency of MDSC in treated and control mice was assessed and results are presented as the percentage of total MDSC within alive cells (mean ± SEM). **B.** NO production of MDSC in the treated and untreated groups was determined and are presented as the MFI ± SEM. **C.** The frequency of $CCR5^+$ MDSC in mCCR5-Ig treated mice and control mice is demonstrated and presented as percentage of $CCR5^+$ MDSC within total MDSC (mean and SEM). **D.** The weight of each tumor sample was plotted against the percentage of tumor-infiltrating CCR5 expressing MDSC within total MDSC in skin tumors (n=7). The correlation was calculated using linear regression analysis. 500,000 live cells in BM and peripheral blood, 800,000 live cells in metastatic LN and 200,000 $CD45^+$ live cells in tumors were analyzed. $p^* < 0.05$, $p^{***} < 0,001$.

Analyzing different T cell populations, we found a decreased frequency of total Treg in skin tumors from treated mice as compared to the control group (Fig. 17A-B). In addition, the activation of Treg measured by CD69 expression was reduced in metastatic LN of treated mice as compared to the control (Fig. 17C). Importantly, the frequency of CCR5 expressing Treg was reduced in skin tumors after treatment (Fig. 17D). Moreover, we observed that the frequency of $CCR5^+$ Treg was diminished with tumor progression (Fig. 17E).

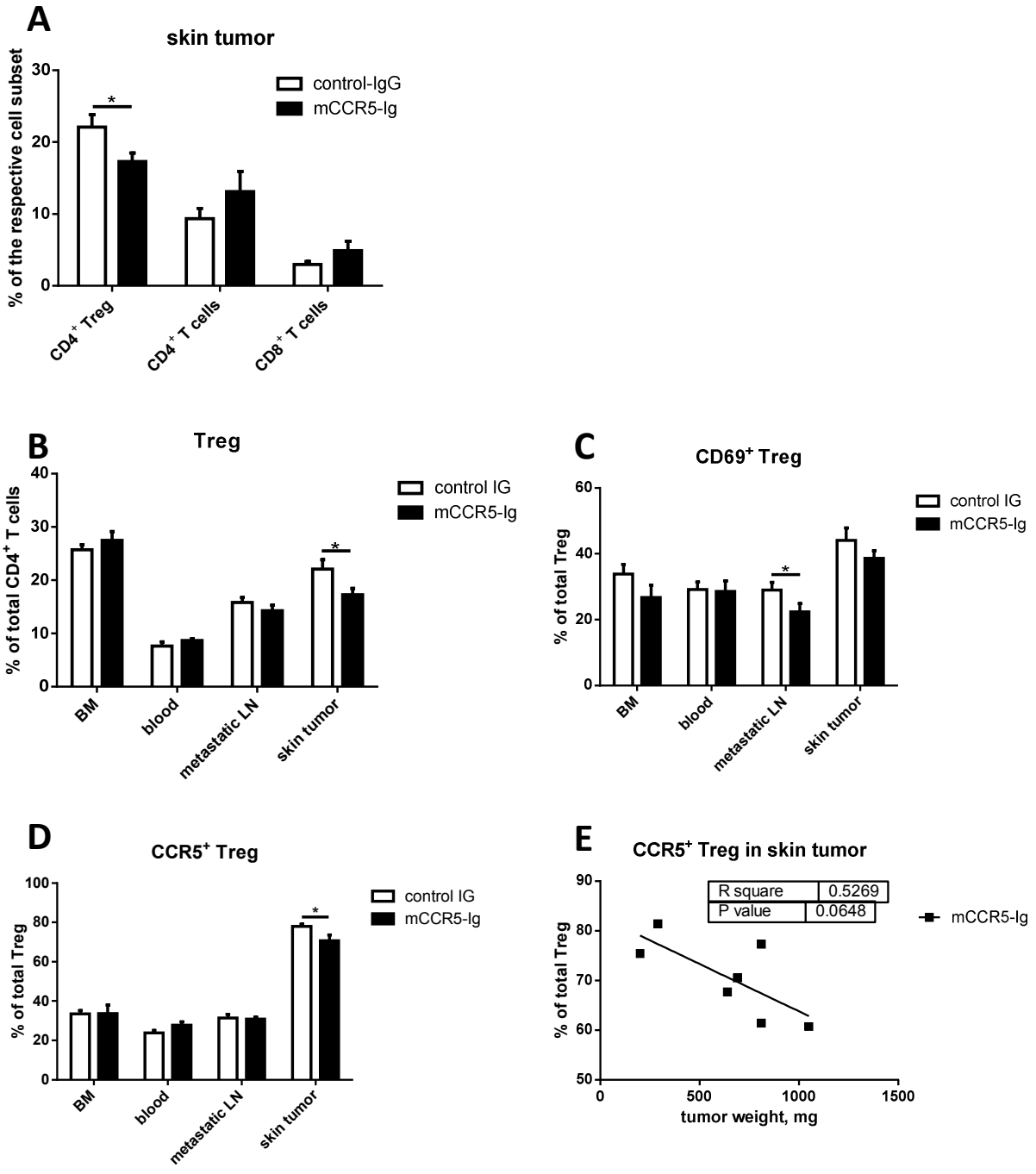

Figure 17: Reduced frequency of Treg in mCCR5-Ig treated *ret* transgenic mice. A. The frequency of Treg, $CD4^+$ and $CD8^+$ T cells in BM, peripheral blood, metastatic LN and skin tumors was measured in treated (n=7) and control (n=8) mice groups by flow cytometry. Results are shown as the percentage of the respective T cell subset (mean and SEM). **B.** The frequency of Treg in various organs was assessed and is presented as the percentage of Treg within $CD4^+$ T cells (mean and SEM). **C.** CD69 expression on Treg was measured and is shown as the percentage of $CD69^+$ Treg within Treg (mean and SEM). **D.** The frequency of CCR5 expressing Treg in various organs was analyzed and is presented as the percentage of $CCR5^+$ Treg within total Treg (mean and SEM). **E.** The weight of each tumor sample was plotted against the percentage of tumor-infiltrating CCR5 expressing Treg within total $CD4^+$ T cells in the skin tumors (n=7). The correlation was calculated using linear regression analysis. 500,000 live cells in BM and peripheral blood, 800,000 live cells in metastatic LN and 200,000 $CD45^+$ live cells in tumors were analyzed. *p < 0.05, ***p < 0.001.

The data demonstrates that mCCR5-Ig can block the migration of immunosuppressive cells such as MDSC and Treg to the tumor microenvironment, indicating that the CCR5-CCR5 ligand axis plays a major role in the recruitment of MDSC and Treg to the tumor site. Moreover, this was associated with the accumulation of non-regulatory $CD4^+$ and $CD8^+$ T cells in the tumor microenvironment.

4.3 CCR5 expression on MDSC in melanoma patients

4.3.1 Elevated CCR5 expression on Mo-MDSC and Gr-MDSC in melanoma patients during tumor progression

Next, we studied the role of CCR5 expression in human MDSC. PBMC from the peripheral blood, as well as single cell suspension of metastasis from melanoma patients, were isolated and stained for the following markers: anti-human CD45.2, anti-human HLA-DR, anti-human CD11b, anti-human CD14, anti-human CD15, anti-human CCR5, anti-human PD-L1 and anti-human ARG-1. In addition, we detected NO and ROS. Unstained cells, as well as FMO, were used as negative controls. Human $CCR5^+$ MDSC were identified by gating on singlets (Fig. 18). Human MDSC were gated for HLA-$DR^{low/neg}$ and $CD11b^+$ cells. Monocytic and granulocytic MDSC were identified by the expression of CD14 or CD15 respectively. Analysis of the immunosuppressive phenotype was performed by measuring NO and ROS production, as well as PD-L1 and ARG-1 expression on the different CCR5 cell subsets.

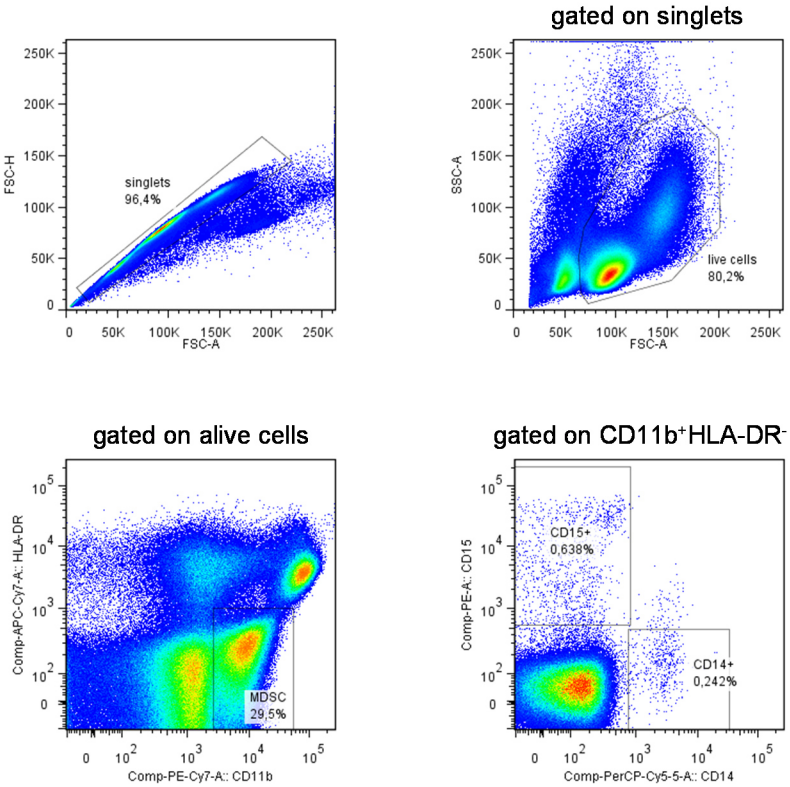

Figure 18: Gating strategy for CCR5$^+$ MDSC from melanoma patients. MDSC from the peripheral blood of human melanoma patients. PBMC were isolated by density gradient centrifugation and frozen in liquid nitrogen. Cells were then thawed and stained for FACS analysis

CCR5$^+$ MDSC were studied in skin metastasis and peripheral blood of melanoma patients with different stages by flow cytometry. Interestingly, we found no expression of CCR5 on CD45.2$^-$ tumor cells (data not shown). Melanoma patients showed a significantly higher frequency of Mo-MDSC as compared to their counterparts in HD (Fig. 19A). For the granulocytic subset, we could not detect any differences in the frequency as compared to HD or in melanoma patients at different stages (Fig. 19B). Next, we investigated the CCR5 expression on Mo-MDSC and Gr-MDSC in patients with melanoma in different stages. The frequency of CCR5$^+$ Mo-MDSC, as well as CCR5$^+$ Gr-MDSC, was significantly increased in melanoma patients as compared to HD (Fig. 19C, D). Moreover, we could show a significant increase in the intensity of CCR5 expression on Mo-MDSC in patients of different stages as compared to IMC in HD (Fig. 19E,F).

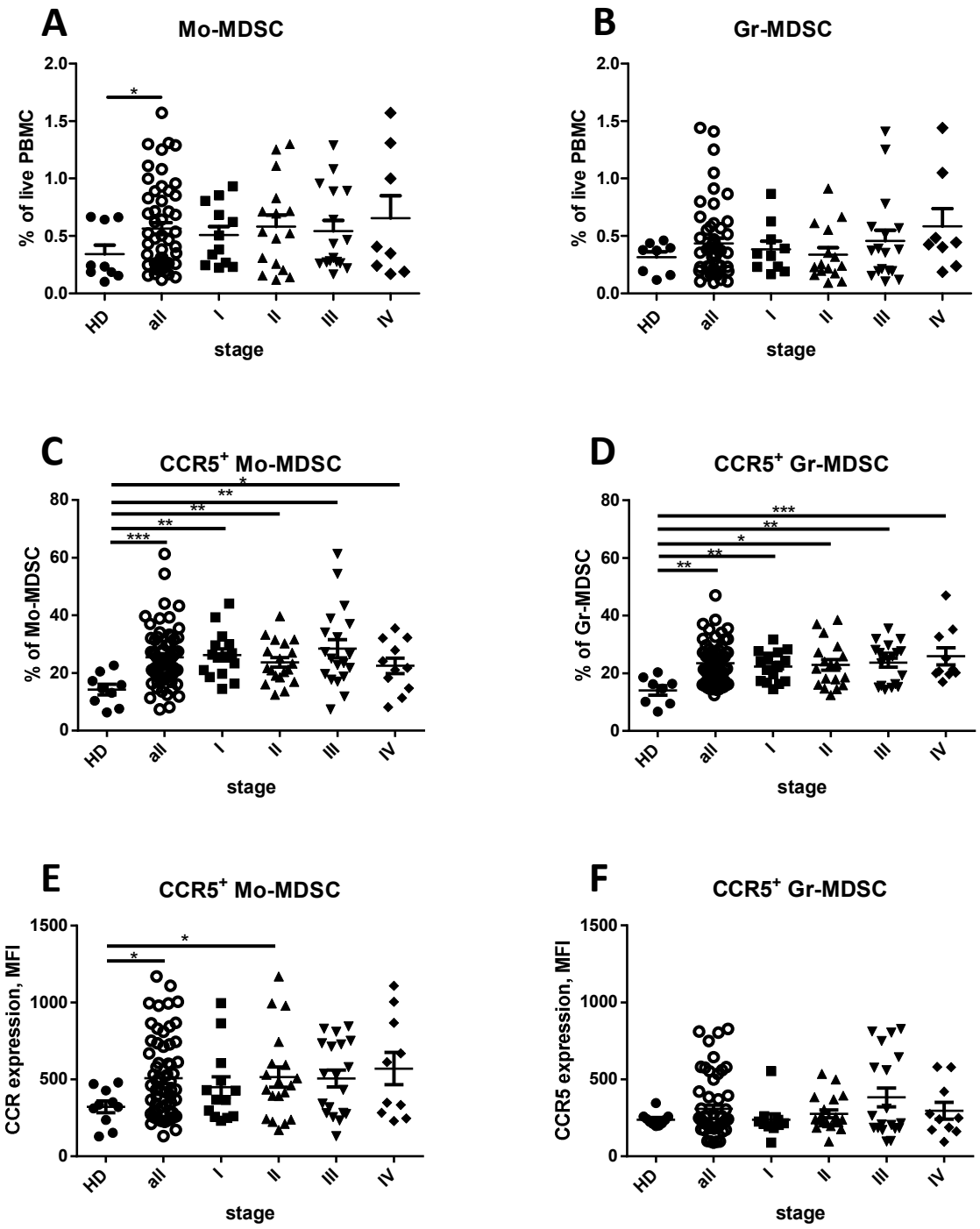

Figure 19: Analysis of CCR5⁺ MDSC of melanoma patients during course of tumor progression. PBMC from the peripheral blood of melanoma patients and HD were assessed by flow cytometry. The frequency of Mo-MDSC (**A**) and Gr-MDSC (**B**) in melanoma patients and HD is presented as the percentage of these cells within live PBMC. The frequency of CCR5⁺ Mo-MDSC (**C**) and CCR5⁺ Gr-MDSC (**D**) is shown as the percentage of the respective MDSC subset. CCR5 expression level of Mo-MDSC (**E**) and Gr-MDSC (**F**) is shown as the mean fluorescence intensity (MFI). *p < 0.05, **p < 0.01, ***p < 0.001.

4.3.2 Immunosuppressive phenotype of CCR5$^+$ Mo-MDSC and CCR5$^+$ Gr-MDSC in melanoma patients

To evaluate the immunosuppressive phenotype of circulating CCR5$^+$ Mo-MDSC and CCR5$^+$ Gr-MDSC in melanoma patients at different stages, we analyzed the NO and ROS production as well as the ARG-1 and PD-L1 expression (Fig. 20).

The level of NO production by CCR5$^+$ Mo-MDSC in stage III melanoma patients was significantly elevated as compared to stage I patients (Fig. 20A). The intensity of NO production by CCR5$^+$ Gr-MDSC was higher in patients of stage II and III than in stage I patients (Fig. 20B). Furthermore, in patients with advanced melanoma (stage III and stage IV), CCR5$^+$ Mo-MDSC showed higher NO production than their CCR5$^-$ Mo-MDSC counterpart (Fig. 20C). CCR5$^+$ Gr-MDSC from patients stage III and stage IV also produced more NO as compared to their CCR5$^-$ counterpart (Fig. 20D).

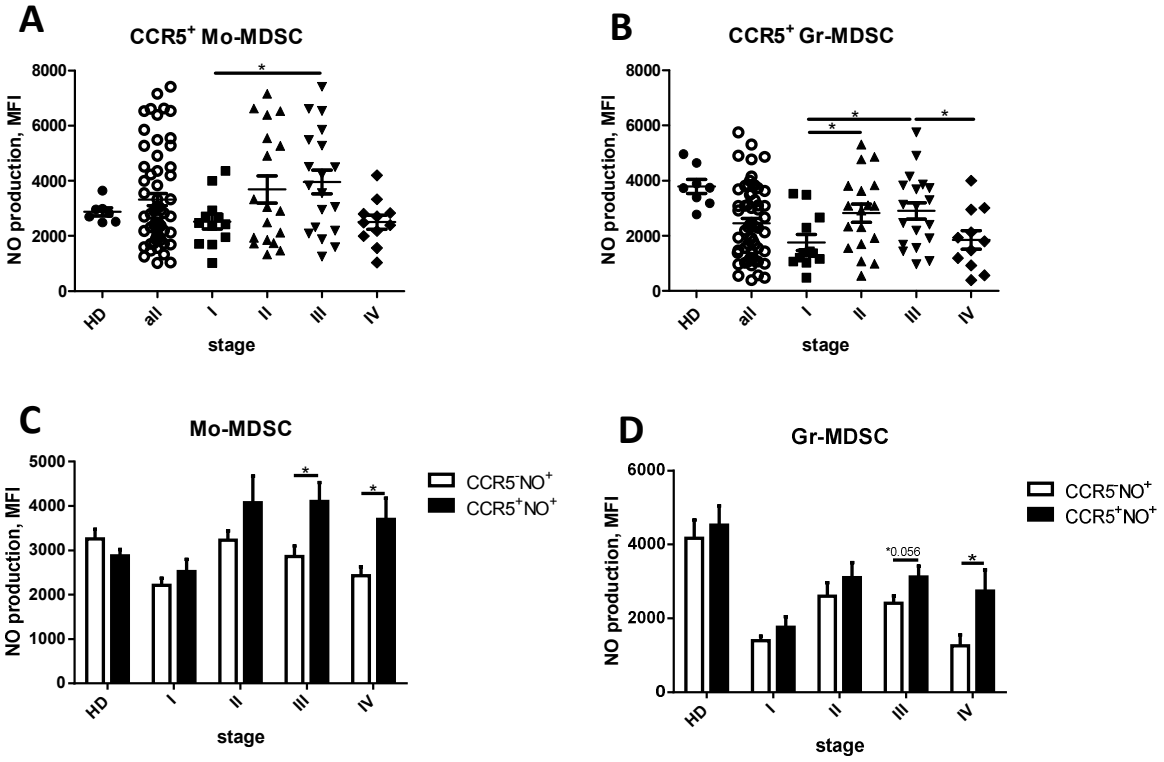

Figure 20: NO production of CCR5$^+$ MDSC in melanoma patients. PBMC were isolated from the peripheral blood from melanoma patients and HD and analyzed by flow cytometry. The NO production by CCR5$^+$ Mo-MDSC (**A**) and CCR5$^+$ Gr-MDSC (**B**) was plotted against melanoma patients at different stages and HD. Data is presented as the MFI of NO in CCR5$^+$ MDSC subsets. **C.** and **D.** show the NO production in CCR5$^+$ and CCR5$^-$ MDSC subsets in melanoma patients and HD (mean and SEM). *p < 0.05.

The analysis of patients at various stages of melanoma revealed that CCR5$^+$ Mo-MDSC from stage IV patients produced significantly more ROS than stage III and stage I patients and their myeloid counterparts in HD (Fig. 21A). The analysis of ROS producing CCR5$^+$ Gr-MDSC showed that the ROS intensity was increased in melanoma patients with stage II as compared to stage I patients (Fig. 21B). The frequency of ROS producing CCR5$^+$ Mo-MDSC in stage II and III melanoma was elevated as compared to their CCR5$^-$ counterparts (Fig. 21C). Furthermore, the level of ROS production in CCR5$^+$ Gr-MDSC was higher in patients of stage II and III as compared to their CCR5$^-$ counterparts (Fig. 21D).

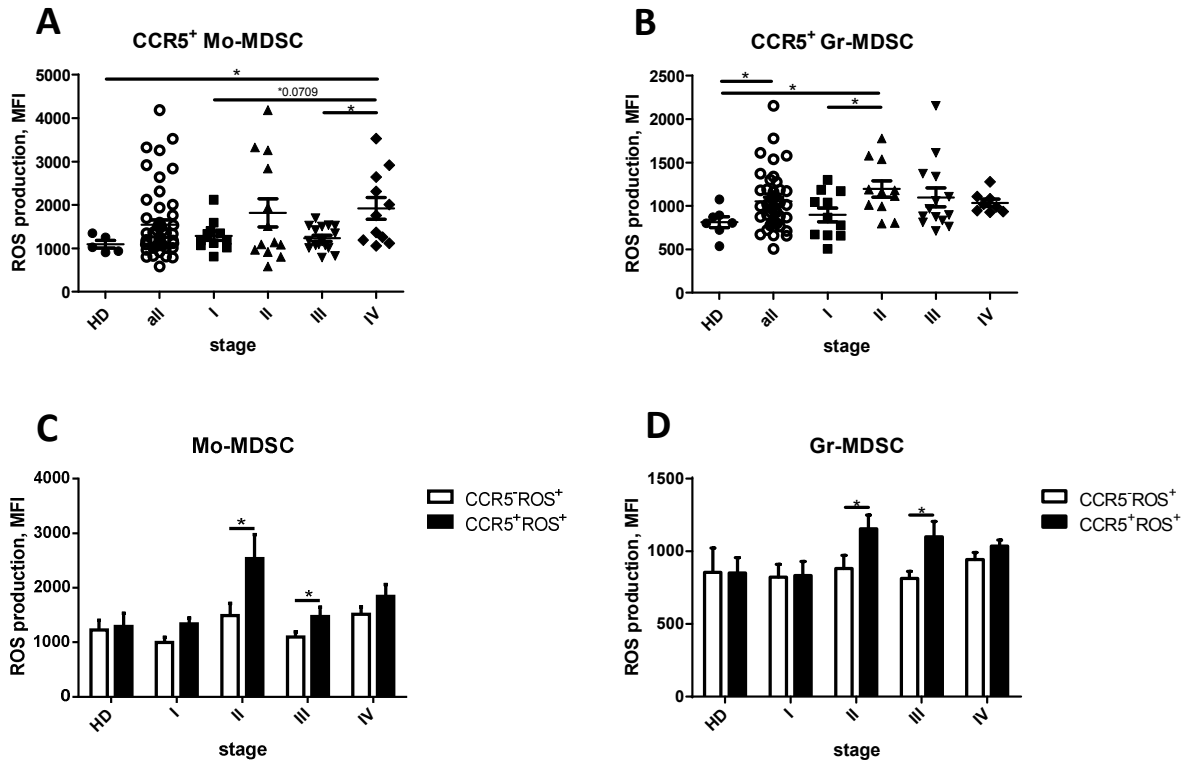

Figure 21: ROS production of CCR5$^+$ MDSC in melanoma patients. PBMC were isolated from the peripheral blood from melanoma patients and HD and analyzed by flow cytometry. The ROS production of CCR5$^+$ Mo-MDSC (**A**) and CCR5$^+$ Gr-MDSC (**B**) was plotted against melanoma patients at different stages and HD. Data is presented as the MFI of ROS in CCR5$^+$ MDSC subsets. **C**. and **D**. show the ROS production in CCR5$^+$ and CCR5$^-$ MDSC subsets in melanoma patients and HD (mean and SEM). *p < 0.05.

The frequency of ARG-1 expressing CCR5$^+$ Mo-MDSC was found to be increased in the group containing all melanoma patients as compared to HD (Fig. 22A). In addition, the frequency of ARG-1 expressing CCR5$^+$ Mo-MDSC was elevated in patients of stage III and II as compared to stage I melanoma patients. For the granulocytic subset, we detected that stage IV melanoma patients had an increased frequency of ARG-1 expressing CCR5$^+$ cells as compared to those in stage I melanoma patients and their healthy counterparts (Fig. 22B). Also the frequency of ARG-1 expressing CCR5$^+$ Gr-MDSC from melanoma patients of all groups was raised as compared to the MDSC counterpart in HD. Stage II, III, and IV melanoma patients showed a higher frequency of ARG-1 expressing CCR5$^+$ Mo-MDSC than ARG-1 expressing CCR5$^-$ Mo-MDSC (Fig. 22C). When comparing circulating ARG-1 expressing Gr-MDSC in patients of different stages, we found a higher frequency of ARG-1 expressing CCR5$^+$ Gr-MDSC than CCR5$^-$ Gr-MDSC in melanoma patients of stage II, III and IV (Fig. 22D). Furthermore, the level of ARG-1 expression measured as MFI was higher in CCR5$^+$ Mo-MDSC from stage II, III, and IV patients as compared to their CCR5$^-$ counterpart (Fig. 22E).

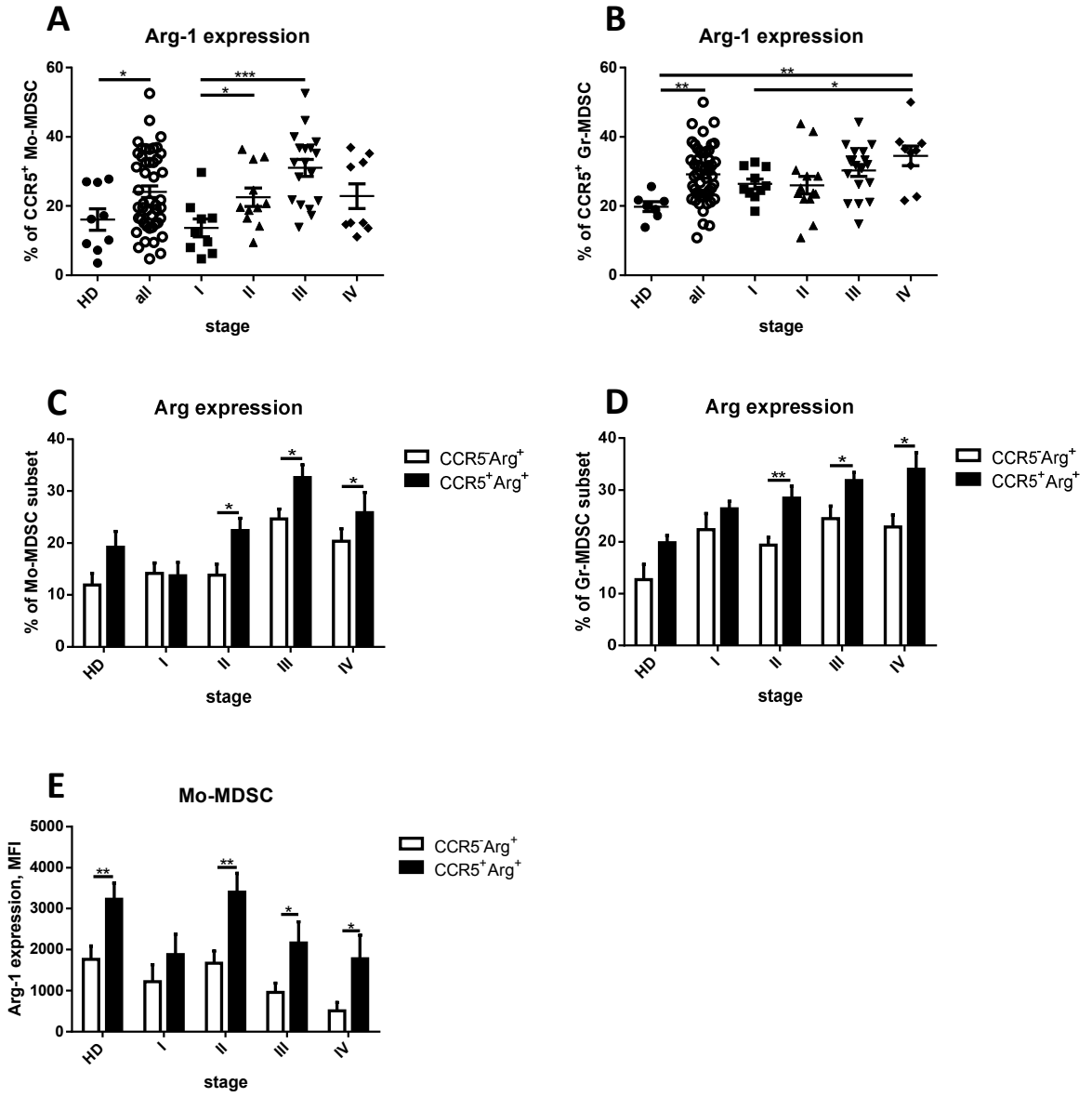

Figure 22: ARG-1 expression on CCR5$^+$ MDSC in melanoma patients. PBMC were isolated from the peripheral blood from melanoma patients and HD and analyzed by flow cytometry. The frequency of ARG-1 expression on CCR5$^+$ Mo-MDSC (**A**) and CCR5$^+$ Gr-MDSC (**B**) was plotted against melanoma patients at different stages and HD. Data is presented as the percentage of ARG-1 expressing CCR5$^+$ MDSC subsets. **C**. and **D**. show the ARG-1 expression in CCR5$^+$ and CCR5$^-$ MDSC subsets in melanoma patients and HD (mean and SEM). The intensity of ARG-1 expression on CCR5$^+$ and CCR5$^-$ MDSC of melanoma patients and HD is presented as MFI (**E**). *p < 0.05, **p < 0.01, ***p < 0.001.

Next, we analyzed the PD-L1 expression on CCR5$^+$ MDSC subsets in melanoma patients. The frequency of CCR5$^+$ Mo-MDSC (Fig. 23A) and CCR5$^+$ Gr-MDSC (Fig. 23B) was increased in stage III melanoma patients as compared to stage I and II patients and to HD. However, we could not detect any significant differences in the PD-L1 expression between CCR5$^+$ and CCR5$^-$ MDSC subsets (Fig. 23C, D).

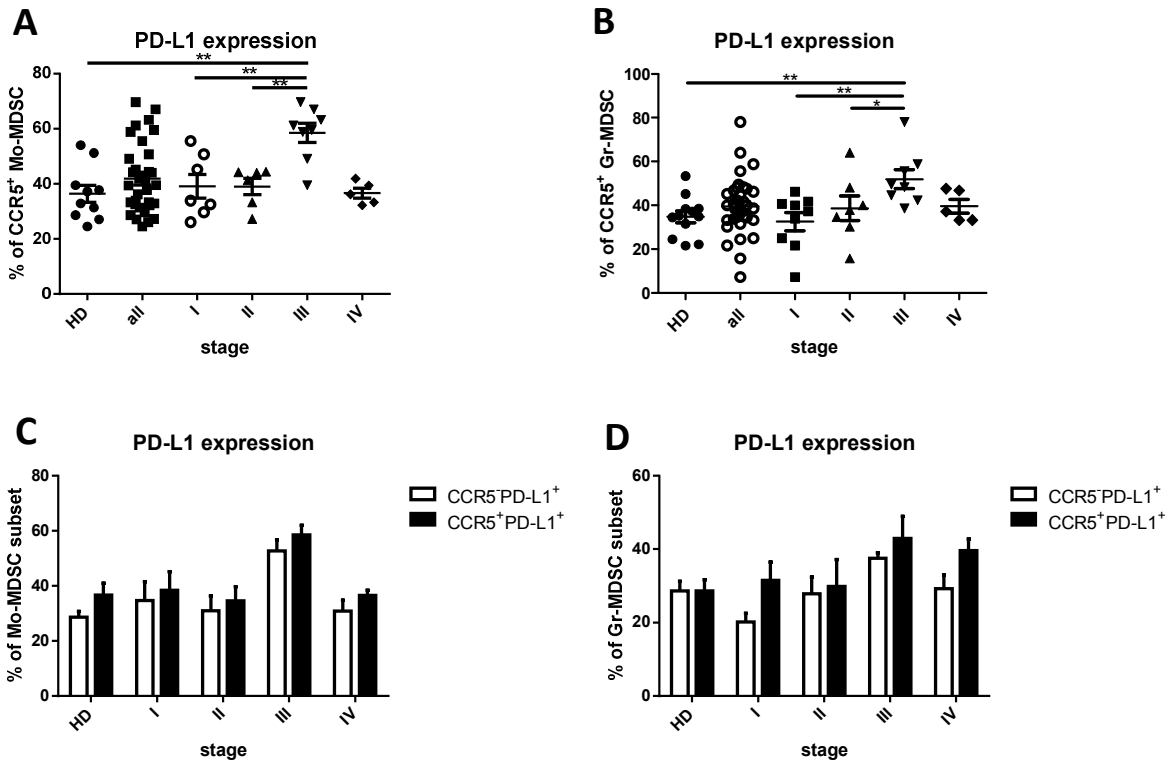

Figure 23: PD-L1 expression on CCR5⁺ MDSC in melanoma patients. PBMC were isolated from the peripheral blood from melanoma patients and HD and analyzed by flow cytometry. The frequency of PD-L1 expression on CCR5⁺ Mo-MDSC (**A**) and CCR5⁺ Gr-MDSC (**B**) was plotted against melanoma patients at different stages and HD. Data is presented as the percentage of PD-L1 expressing CCR5⁺ MDSC subsets. **C.** and **D.** show the PD-L1 expression in CCR5⁺ and CCR5⁻ MDSC subsets in melanoma patients and HD (mean and SEM). **p < 0.01, ***p < 0.001.

4.3.3 Accumulation of CCR5⁺ Mo-MDSC in skin tumors of melanoma patients

To elucidate the role of CCR5 in the recruitment of MDSC and Treg to the tumor microenvironment in melanoma patients, we studied peripheral blood and tumor tissue samples from the same patient. We found a significantly increased frequency of CCR5⁺ Mo-MDSC in tumor tissue as compared to the peripheral blood (Fig. 24A). In contrast, the frequency of CCR5⁺ Gr-MDSC in the tumor tissue was only slightly increased (Fig. 24B).

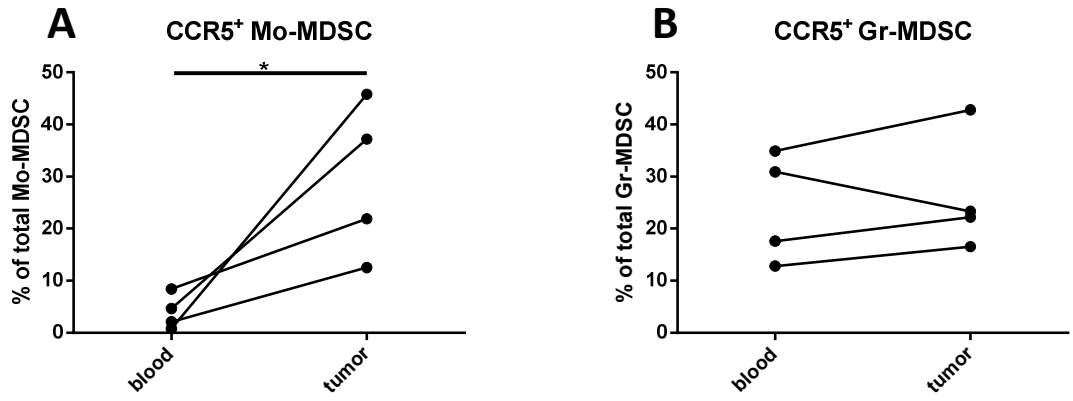

Figure 24: CCR5 expression on immunosuppressive cells in melanoma patients. PBMC and skin metastasis cells from stage III and IV melanoma patients were analyzed by flow cytometry. The frequency of CCR5 expression on Mo-MDSC (**A**), Gr-MDSC (**B**) is shown. Data is presented as the percentage of CCR5 expressing MDSC subsets or Treg within live PBMC. *p < 0.05.

4.3.4 Increased concentration of chronic inflammatory mediators in tumors

Chronic inflammatory factors are involved in the activation, stimulation and recruitment of MDSC to the tumor microenvironment (Umansky and Sevko, 2013; Ugel et al., 2015; Arvelo et al., 2016). Therefore, we investigated such factors in the serum and tumor lysates of melanoma patients using bio-plex technique (Fig. 25). In all studied samples, CCL3, CCL4, CCL5, GM-CSF, VEGF, TNF-α, and IFN-γ displayed significantly higher concentrations in the tumor as compared to the serum.

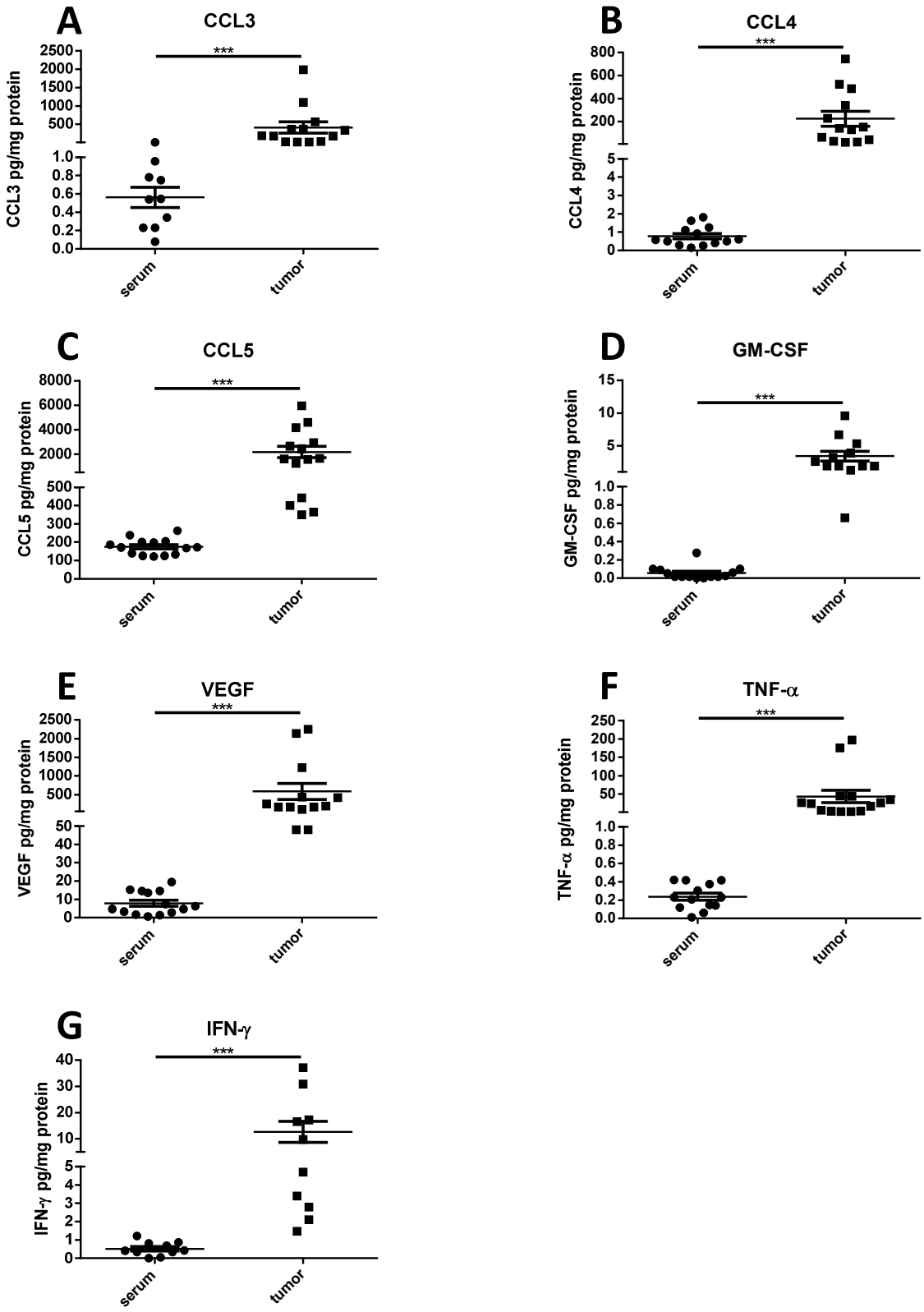

Figure 25: Increased concentrations of chronic inflammatory factors for MDSC migration in skin tumors of melanoma patients of different stages. Inflammatory factors were measured in serum and skin metastasis lysates of 14 patients at different stages by bio-plex assay. Levels of CCL3, CCL4, CCL5, GM-CSF, VEGF, TNF-α and IFN-γ are expressed as pg/mg protein (**A-G**). *$p < 0.05$, **$p < 0.01$, ***$p < 0.001$.

4.3.5 CCR5 is highly expressed on Treg

Since we demonstrated that CCR5 is an important molecule on Treg in mice, we aimed to study its expression on Treg from the peripheral blood of melanoma patients with different stages. Fig. 26 shows a representative gating strategy of $CCR5^+$ Treg from isolated PBMC of a melanoma patient at stage IV.

First, singlets and live cells were gated. CD3 and CD4 double positive cells were identified. Out of these cells, CD127 negative cells were analyzed. To identify Treg, CD25 and FoxP3 double positive cells were gated. Treg were characterized as $CCR5^+$ or $CCR5^-$, and the CD45RA and CD69 expression of the respective cell subset was analyzed.

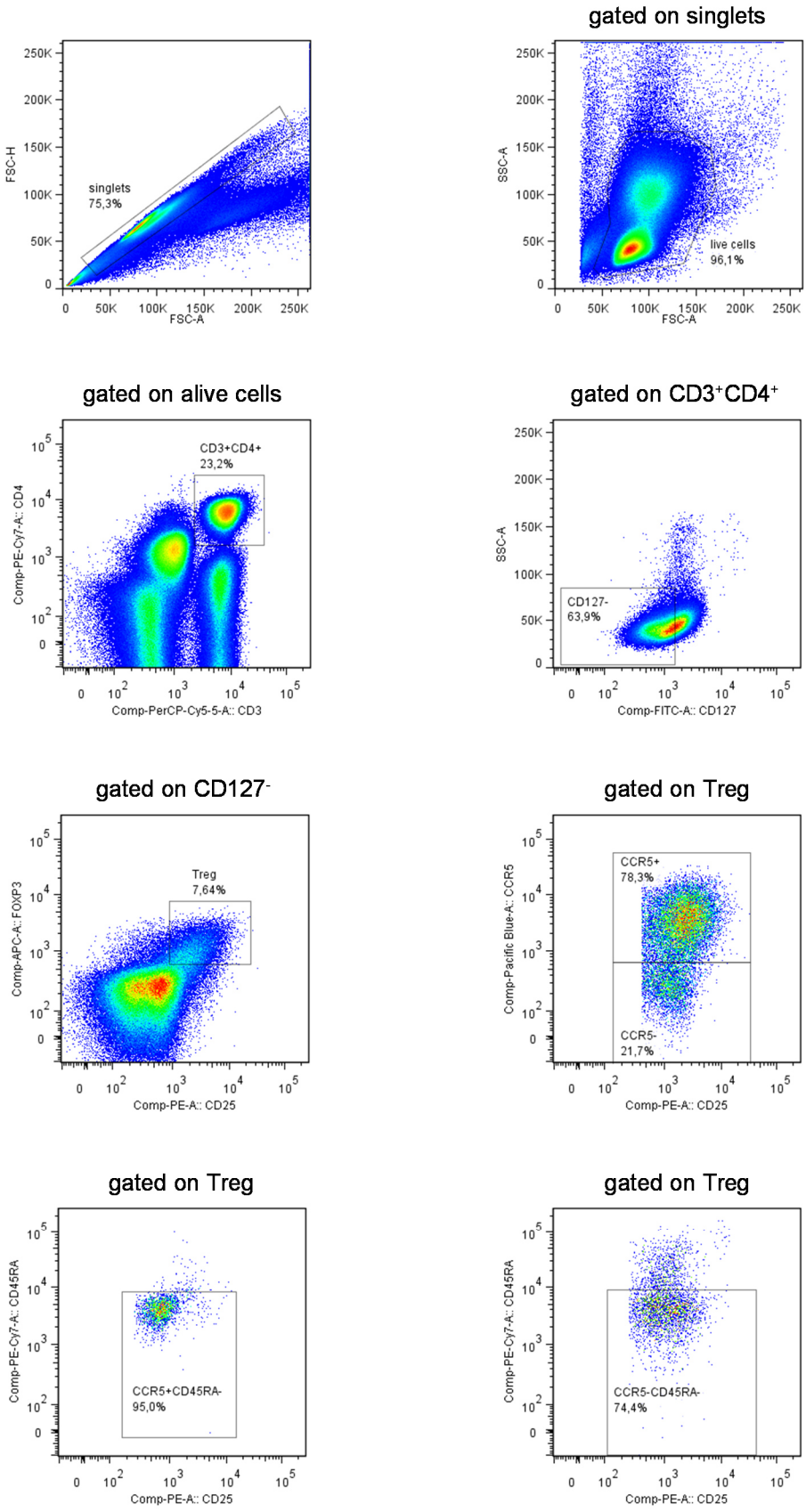

Figure 26: Gating strategy of CD45RA$^-$CCR5$^+$CD4$^+$Treg.

The frequency of Treg was assessed as the percentage of $CD4^+CD127^-CD25^+FoxP3^-$ cells among total $CD4^+$ T cells. We detected an increased frequency of circulating Treg in stage IV melanoma patients as compared to all other analyzed groups (Fig. 27A). Moreover, we assessed an increased frequency of CCR5 expressing Treg in melanoma patients as compared to HD (Fig. 27B). Furthermore, $CCR5^+$ Treg were significantly increased in patients with advanced melanoma (stage IV) as compared to stage II patients and HD. In addition, we observed a significantly higher level of CCR5 expression on Treg in the group with all melanoma patients and in the group with melanoma patients stage I as compared to HD (Fig. 27C). Interestingly, the frequency of antigen-experienced $CD45RA^-CCR5^+$ Treg in stage III was found to be increased as compared to stage I melanoma patients and HD (Fig. 27D). Furthermore, we demonstrated a slightly higher CCR5 expression on Treg in tumor tissue as compared to the peripheral blood (Fig. 27 E).

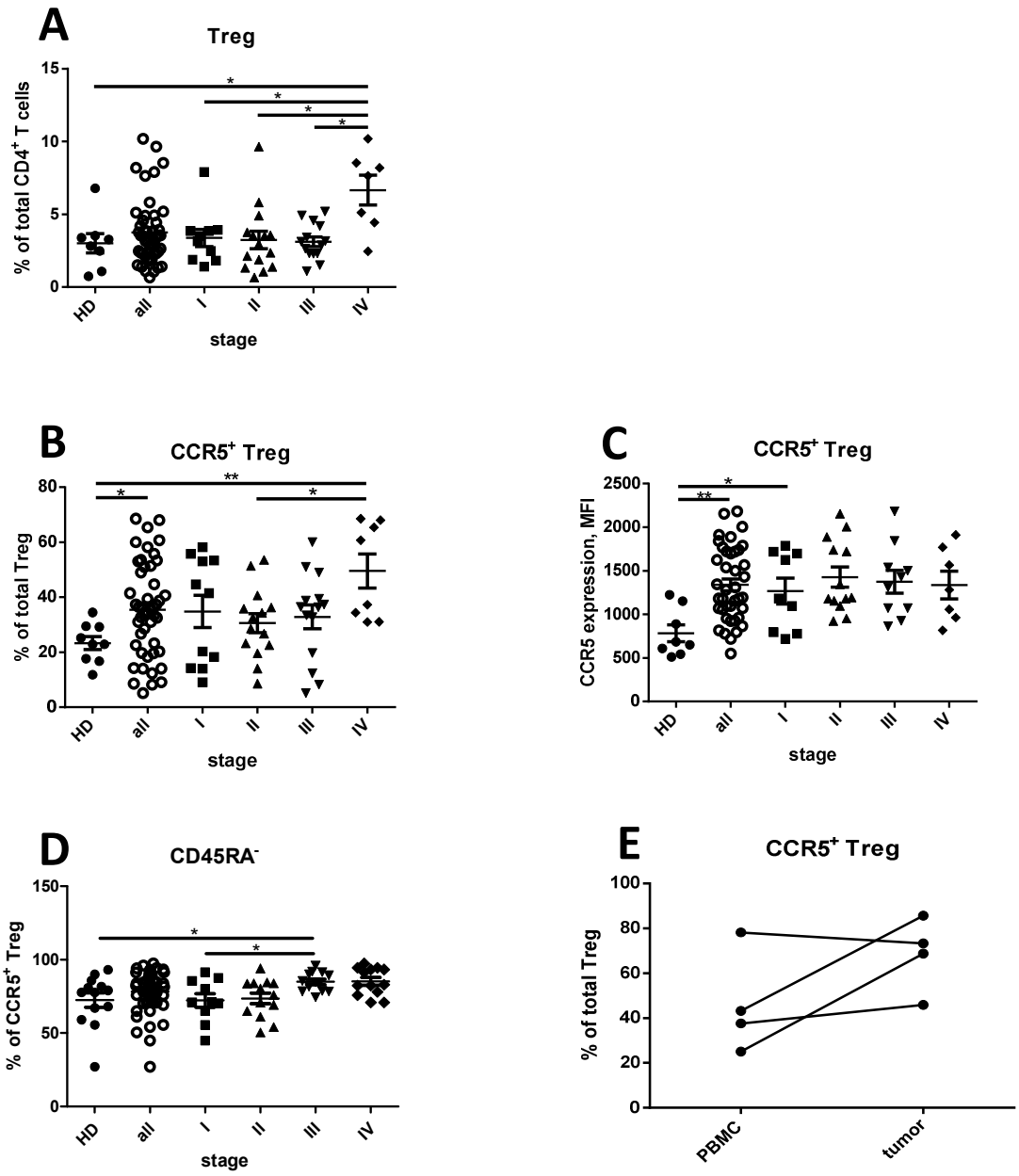

Figure 27: Evaluation of Treg in melanoma patients during tumor progression. PBMC from the peripheral blood of melanoma patients and HD were analyzed by flow cytometry. The frequency of $CD4^+$ Treg in 66 melanoma patients of different stages and HD were assessed and the percentage of these cells within total $CD4^+$ T cells is shown (**A**). CCR5 expression on $CD4^+$ Treg was analyzed and the results of expression are presented as a frequency (**B**) and MFI (**C**). The frequency of $CD45RA^-CCR5^+$ Treg was assessed by flow cytometry and is shown as the percentage of $CCR5^+$ Treg (**D**). PBMC and skin metastasis cells from stage III and IV melanoma patients were analyzed by flow cytometry. The frequency of CCR5 expression on Treg is shown (**E**). *$p < 0.05$, **$p < 0.01$.

5 Discussion

Malignant melanoma is the most aggressive form of human skin cancer with the highest morbidity (Nikolaou and Stratigos, 2014). Several standardized therapies to eliminate tumor cells are already in use like radiotherapy and chemotherapy. However, they are characterized by tumor relapse and therapeutic failure. In the last decades, a great attention was focused on tumor-infiltrating immune cells that have different roles in cancer. On one hand, they suppress tumor growth by eliminating tumor cells and on the other hand, they promote tumor progression and metastasis by inhibiting anti-tumor immune response (Bindea et al., 2014).

5.1 Expression of CCR5 on murine MDSC

During tumor development, a common mechanism to build up an immunosuppressive microenvironment is the dysregulation of myelopoiesis, which leads to the induction of MDSC (Ugel et al., 2015). The heterogeneous population of MDSC uses several mechanisms to suppress anti-tumor immunity. Each of these mechanisms suppresses the activation, proliferation, migration and effector function of T cells (Kumar et al., 2016). It was found that MDSC accumulate in the BM and spleen of tumor bearing mice (Gabrilovich and Nagaraj, 2009; De Veirman et al., 2014). Previous results from our group revealed that MDSC accumulate during melanoma progression in *ret* transgenic mice (Meyer et al., 2011).

Chemokines are responsible for accumulation of MDSC, in particular CCR5, so we focused on upregulation of CCR5 expression on MDSC. We hypothesize that CCR5 on MDSC might serve two distinct roles: 1) to induce MDSC migration from the BM to the site of the tumor; 2) to provide a strong immunosuppressive activity once pro-inflammatory factors are strongly secreted by the tumor. This would suggest a new therapeutic target for CCR5-CCR5 ligand axis in tumor therapy to regulate the anti-tumor immune response thus resulting in tumor regression.

Accordingly, we found an increased frequency of CCR5 expressing MDSC in melanoma lesions of *ret* transgenic mice as compared to the periphery (the BM and peripheral blood) (Fig.3). The level of CCR5 expression was higher in skin tumors as compared to blood. $CCR5^+$ MDSC accumulated during the course of melanoma progression in skin tumors and metastatic LN. Moreover, the CCR5 expression level increased during tumor development. Our data showed that $CCR5^+$ Mo-MDSC and $CCR5^+$ Gr-MDSC accumulated in melanoma lesions of *ret* transgenic mice and the level of CCR5 expression was higher in metastatic LN and skin tumors as compared to BM and peripheral blood (Fig. 4). In *ret* transgenic mice, the frequency of $CCR5^+$ cells was higher among Gr-MDSC than among Mo-MDSC. The data suggests for the

first time, that CCR5 is important for the migration of MDSC to the site of the tumor and that tumors might secret factors leading to an upregulation of CCR5 expression in tumor-infiltrating MDSC and thus to the recruitment of these cells into the tumor microenvironment.

To prove the second hypothesis, we analyzed the immunosuppressive phenotype of MDSC. We found that $CCR5^+$ MDSC represented a higher production of NO and ROS, as well as an elevated expression of ARG-1 and PD-L1, than their $CCR5^-$ counterpart in melanoma lesions (Fig. 7). This was in agreement with a previous report, showing an increased NO production and ARG-1 expression on total MDSC (Meyer et al., 2011). Notably, we observed that the frequency of $CCR5^+$ MDSC producing NO and ROS and expressing ARG-1 and PD-L1 accumulated during tumor progression in *ret* transgenic mice (Fig. 8), reflecting their increased immunosuppressive function.

We next analyzed the impact of CCR5 expression on the activation of MDSC. To this end, we stimulated $CD8^+$ T cells isolated from the spleen of WT mice through the engagement of CD3 and CD28 and co-cultured them with CCR5 MDSC subsets isolated from the BM of tumor bearing mice. Similar to the previous results (Meyer et al., 2011) that total MDSC from tumors of *ret* transgenic mice show inhibitory effects on T cell proliferation, we observed that both $CCR5^+$ and $CCR5^-$ MDSC inhibited proliferation of stimulated T cells as compared to T cells cultured alone (Fig. 9B). Moreover, we detected a dose-dependent effect of MDSC on T cell proliferation. Comparing effects of BM-derived MDSC subsets, we found that $CCR5^+$ MDSC exerted a tendency for stronger inhibition of T cell proliferation than their $CCR5^-$ counterparts (Fig. 9B).

Taken together, we suggest that the upregulation of CCR5 expression on MDSC could regulate not only the migration of MDSC from the BM to the tumor but also their immunosuppressive phenotype during tumor progression. Our *ex vivo* data showed that $CCR5^+$ MDSC displayed a stronger immunosuppressive phenotype than $CCR5^-$ cells indicated by increased NO and ROS production, as well as an elevated ARG-1 and PD-L1 expression. Moreover, we demonstrated that $CCR5^+$ MDSC displayed only a slightly stronger capacity to suppress T cell proliferation than $CCR5^-$ cells.

This apparent discrepancy between our data indicating a more immunosuppressive phenotype for $CCR5^+$ MDSC and the results demonstrating only slightly increased immunosuppressive activity of $CCR5^+$ MDSC might be due to the fact that we isolated $CCR5^+$ MDSC from the BM and not from melanoma lesions, where they should have displayed stronger immunosuppressive activity than in the BM. This was due to the insufficient amounts of $CCR5^+$ and $CCR5^-$ MDSC that could be isolated from skin tumors or metastatic LN.

5.2 Inflammatory factors in migration, accumulation and activity of MDSC

We observed that the frequency of CCR5 expressing MDSC was increased and that the level of CCR5 expression was elevated with tumor load (indicator for tumor progression). This led to the suggestion that microenvironmental factors might induce CCR5 expression. We previously showed in *ret* transgenic mice that melanoma lesions contained increasingly high amounts of the inflammatory factors VEGF, IL-1β, IL-6 and TGF-β (Zhao et al., 2009). Furthermore, it was demonstrated that the concentration of pro-inflammatory cytokines like IFN-γ, IL-1β and GM-CSF was more elevated in quickly growing tumors than in slowly growing tumors (Meyer et al., 2011). In concordance with this data, we found an increased level of VEGF, TGF-β, CXCL10 and IL-6 in melanoma lesions of *ret* transgenic, tumor bearing mice as compared to serum (Fig. 5). Several recent studies reported that these factors might be a major inducer of MDSC (Umansky and Sevko, 2013; Stromnes et al., 2014; Ugel et al., 2015). It was shown that the reduction in the level of pro-inflammatory cytokines in the tumor microenvironment is associated with decreased frequency and activity of MDSC to suppress T cell proliferation *in vitro* (Sade-Feldman et al., 2013). It has been recently reported that an increased concentration of TNF-α induced CCL5 secretion is correlated with the aggressiveness of tumors in various mouse transplantable models (Katanov et al., 2015). In our study, we could not find an increased TNF-α level in melanoma lesions as compared to the serum, but found that the concentration of all three CCR5 ligands (CCL3, CCL4 and CCL5) were elevated in skin tumors (Fig. 5). The increased concentration of CCR5 ligands and the elevated frequency of $CCR5^+$ cells in melanoma lesions led us to suggest that CCR5 ligands might be inducers for CCR5 expression on MDSC and that different chemokine signals might be important for the chemotaxis of MDSC from the BM to the tumor (Kitamura et al., 2015a). Consistent with this suggestion, *in vitro* studies showed that the migration, adhesion and differentiation of human monocytes are induced by CCL2, CXCL18 and CXCL12 respectively (Qian et al., 2011; Kitamura et al., 2015b). Therefore, we analyzed the CCR5 ligand-induced migration capacity of MDSC *in vitro*. The CCR5 ligands increased the percentage of migrated cells as compared to unstimulated MDSC. Furthermore, we found that the inhibition of CCR5 ligands by mCCR5-Ig resulted in the reduced migration capacity of MDSC (Fig. 10). Thus, the inhibition of CCR5 ligands by mCCR5-Ig might be a novel target for immunotherapy to neutralize the tumor microenvironment.

5.3 Pattern of CCR5 expression on Treg and non-regulatory T cells in mice

Murine models demonstrated that the frequency of Treg increases during tumor progression and the depletion or inhibition of Treg enhances anti-tumor immune response (Facciabene et al., 2012). The treatment of melanoma bearing mice with anti-CD25 monoclonal antibody depletes Treg and facilitates $CD4^+$ T cell-mediated, anti-tumor immunity which results in a suppressed tumor growth (Jones et al., 2002). It was shown that the depletion of Treg leads to the complete regression of tumors (Li et al., 2010). Furthermore, the elimination of Treg results in the activation of $CD8^+$ T cells and in an elevated level of these cells in the tumor.

In our study, we found that CCR5 expression is not restricted to the immunosuppressive compartment of myeloid cells but also lymphocytes express CCR5. CCR5 expressing Treg were enriched in melanoma lesions of *ret* transgenic mice as compared to the peripheral blood, whereas only very few conventional $CD4^+$ and $CD8^+$ T cells from the metastatic LN and skin tumors expressed CCR5 (Fig. 12). Furthermore, the frequency of CCR5 expressing Treg was increased during course of melanoma development (Fig. 13). It was shown that Treg are recruited to the site of a tumor by CCL4 and CCL5 whereas CCR5 deficient mice show a reduced amount of Treg (Schlecker et al., 2012). Similar to our data, it was shown that Treg infiltrate into the tumor and that this infiltration is mediated by CCR5-CCR5 ligand interaction (Tan et al., 2009). They suggested that the blockage of this axis demonstrates a novel immunomodulatory strategy for the treatment of pancreatic adenocarcinoma. Interestingly, the disruption of the axis slows down the tumor growth although the migration of $CD4^+$ T cells dropped only down of 20 %, mostly affecting Teff (Tan et al., 2009). Moreover, it was found that the CCR5-CCR5 ligand axis is important for Treg migration to the inflamed tissue (de Oliveira et al., 2014). We next analyzed Treg for their CD69 expression. CD69 is an activation marker, which is expressed on the surface of memory T cells and Treg (Radulovic and Niess, 2015). We found an increased amount of CD69 expressing $CCR5^+$ Treg in peripheral blood, spleen, metastatic LN and skin tumors as compared to $CCR5^-$ Treg (Fig. 13). Furthermore, the CD69 expression level was elevated in $CCR5^+$ Treg.

CCR5 might not only play a role in chemoattraction of leukocytes but also in T cell activation (Gonzalez-Martin et al., 2012). In $CD4^+$ lymphocytes, CCR5 acts as a costimulatory receptor that does not play a role in the migration of these cells (Molon et al., 2005). It was found that CCR5 expression on $CD8^+$ T cells is necessary for the tumor killing and for their migration to the site of tumor in a spontaneous breast cancer mouse model (Gonzalez-Martin et al., 2011). In our study, we found a low proportion of $CD4^+$ and $CD8^+$ T cells expressing CCR5 in melanoma lesions as compared to the spleen and peripheral blood (Fig. 14) leading to the

suggestion that $CD4^+$ and $CD8^+$ T cells may have other mechanisms involved in the migration of conventional T cell into the tumor microenvironment. One mechanism was proposed that CCR2-CCL2 interactions could be the major axis for the migration of CTL in colorectal carcinoma patients (Berencsi et al., 2011). Another study reported that CXCR3 ligands together with CCL5 favor T cell infiltration in cutaneous metastasis (Hong et al., 2011).

We further assessed the frequency of melanoma-specific $CCR5^+CD8^+$ T cells by analyzing TRP-2 specific cells and found that these cells were elevated in the peripheral blood, spleen, metastatic LN and skin tumors as compared to their $CCR5^-$ counterpart. It was shown that the frequency of antigen-specific T cells was reduced in the peripheral blood of patients with advanced melanoma (Weide et al., 2014). Consistent with this information, we demonstrated in melanoma bearing mice that the frequency of TRP-2 specific $CCR5^+CD8^+$ T cells diminished during tumor development.

Collectively, these observations suggest a crucial role for CCR5 expression on Treg in the migration to the site of tumors and in the immunosuppressive activity at the tumor microenvironment. Furthermore, the data imply that other pathways have to be involved in non-regulatory T cell recruitment.

5.4 The role of CCR5 on MDSC in melanoma patients

In 1996, the CCR5Δ32 mutation was discovered (Dean et al., 1996; Liu et al., 1996; Samson et al., 1996). The mutated CCR5 prevents cells of HIV envelope fusion (Barmania and Pepper, 2013). It was found that high levels of CCR5 correlate with non-metastatic colorectal cancer, whereas low or deficient CCR5 expression correlate with an advanced form of disease (Zimmermann et al., 2010). Patients suffering from breast cancer with CCR5-Δ32 had longer metastasis-free survival (Span et al., 2015).

We assessed the distribution of MDSC subsets in the peripheral blood of melanoma patients of different stages and their counterparts in HD. Several studies demonstrated that the frequency of MDSC increases in the periphery of malignant melanoma patients and that this correlates with tumor burden (Filipazzi et al., 2012; Schilling et al., 2013). It was detected that the frequency of MDSC and Treg is elevated in the peripheral blood of melanoma patients as compared to HD (Jiang et al., 2015). Moreover, the increased frequency of MDSC is associated with a negative impact on survival. Monocytic MDSC expressing $CD11b^+CD33^+CD14^+HLA\text{-}DR^{low}$ were shown to be upregulated in stage I-IV melanoma patients (Rudolph et al., 2014). Similar to this data, we found an accumulation of monocytic MDSC ($CD11b^+HLD\text{-}DR^{-/low}CD14^+CD15^-$) in melanoma patients as compared to IMC in HD.

We observed for the first time the CCR5 expression on human MDSC and found that the frequency of CCR5 expressing MDSC was higher in melanoma patients as compared to melanoma bearing mice indicating a more important role for CCR5 in a clinical situation. In a cohort of four patients, we found a significantly increased frequency of $CCR5^+$ Mo-MDSC in metastatic melanoma as compared to the serum. We could not observe any significance for $CCR5^+$ Gr-MDSC since the number of samples was low (Fig. 25). The proportion of MDSC in colorectal carcinoma was found to be correlated with modal metastasis, distant metastases and tumor stage (Sun et al., 2012). However, it has been reported that melanoma-infiltrating MDSC show an impaired ability to suppress T cell proliferation *in vitro* as compared to circulating MDSC (Gros et al., 2012). Analyzing the peripheral blood of melanoma patients, we demonstrated that the frequency of $CCR5^+$ Mo-MDSC and $CCR5^+$ Gr-MDSC was increased as compared to IMC in HD (Fig. 20). Furthermore, the level of CCR5 expression was higher in Mo-MDSC of melanoma patients as in IMC of HD. Thus it may lead to an enhanced MDSC accumulation and contribute to tumor-associated immune suppression.

Analysis of the immunosuppressive phenotype of CCR5 expressing MDSC subsets revealed that circulating $CCR5^+$ Mo-MDSC and $CCR5^+$ Gr-MDSC from melanoma patients produce NO and ROS and express ARG-1 and PD-L1 during tumor development. The CCR5 expressing MDSC subsets are characterized by substantially elevated NO and ROS production, as well as ARG-1 and PD-L1 expression, as compared to $CCR5^-$ cells.

Taken together, the results demonstrate that $CCR5^+$ MDSC in melanoma patients show a similar immunosuppressive phenotype to that of mice, indicating that CCR5 not only plays a key role in the recruitment of human MDSC to the tumor microenvironment but also show that $CCR5^+$ MDSC possess a stronger immunosuppressive phenotype as their $CCR5^-$ counterparts.

5.5 Modulation of MDSC by chronic inflammatory factors in cancer patients

It has been proposed that cytokine secretion by tumor cells increases the infiltrating immune cells in various cancer types to promote or suppress cancer progression according to the type of infiltrating cells (Koizumi et al., 2007). Since we already showed that $CCR5^+$ Mo-MDSC accumulated in skin cancer as compared to serum, next we analyzed pro-inflammatory cytokines and chemokines in tumor samples and serum of melanoma patients. An increased concentration of IL-1β and IFN-γ in the serum of advanced melanoma patients as compared to HD has been described (Jiang et al., 2015). In our study, the levels of GM-CSF, VEGF,

TNF-α and IFN-γ were elevated in tumor samples of melanoma patients as compared to serum (Fig. 28). These observations create the conditions for MDSC accumulation and activity at the site of tumor. Similar to our results obtained in mice, we demonstrated an elevated concentration of CCR5 ligands CCL3, CCL4 and CCL5 in the tumor tissue as compared to the serum. Our observations are in agreement with a previous study showing that CCL5 is elevated in the serum of breast cancer patients and that CCL5 is overexpressed in colon cancer and metastasis as compared to healthy tissues (Cambien et al., 2011). Interestingly, hypoxia was found to promote an increased production of CCR5 and CCL5 in breast cancer cells (Lin et al., 2012).

Therefore, pro-inflammatory cytokines and CCR5 ligands might play a role in the recruitment of human MDSC from the peripheral blood to the tumor microenvironment and contribute to the tumor associated immune suppression.

5.6 CCR5 expression on Treg in cancer patients

It was demonstrated that Treg are present in the peripheral blood of cancer patients and that these cells are able to inhibit functions of other immune cells (Bergmann et al., 2008). Advanced stage melanoma patients are correlated with increased frequency of Treg indicating that melanoma promotes immunosuppressive Treg (McCarter et al., 2007; Jiang et al., 2015). The accumulation of Treg in the peripheral blood of melanoma patients is linked to poor prognosis. We demonstrated that the frequency of Treg increased in advanced stage melanoma patients (stage IV) as compared to early stage patients (stage I-III) and HD (Fig. 27), which was also showed by other authors (Woo et al., 2001; Strauss et al., 2007).

We further observed an accumulation of $CCR5^+$ Treg in patients stage IV as compared to early stage patients and HD. Moreover, the level of CCR5 expression on Treg was higher in melanoma patients as compared to HD. Furthermore, the frequency of antigen-experienced $CCR5^+$ Treg, measured by $CD45RA^-$ expression, was elevated in advanced stage melanoma patients as compared to early stage patients and HD. In agreement with our data, it was found that the blockage of CCR5, CXCR3 and CXCR6 reduce Treg recruitment in the tumor microenvironment (Oldham et al., 2012).

5.7 The role of CCR5 in anti-cancer therapy

We next asked if the inhibition of CCR5 ligands by mCCR5-Ig is relevant to the *in vivo* situation and if this might be a novel target for immunotherapy. It is known that the distribution of immune cells in cancer is controlled by soluble chemoattractants like chemokines that can modify myelopoiesis (Ugel et al., 2015). The blockage of CCL3 secretion from metastasis-associated macrophages was found to be a potential target for the treatment of metastatic breast cancer (Kitamura et al., 2015b). Furthermore, it has been shown that CCL2 induces macrophage recruitment in human breast cancer, suggesting that blocking CCL2 could help to inhibit macrophage migration (Ugel et al., 2015). However, a humanized monoclonal CCL2-neutralizing antibody (CNTO888) was ineffective to suppress serum CCL2 level since the feedback mechanisms promote CCL2 production (Sandhu et al., 2013).

To this end, we studied the effect of mCCR5-Ig in *ret* transgenic, tumor bearing mice that binds and neutralizes all three CCR5 ligands (CCL3, CCL4 and CCL5) simultaneously. The fusion protein was previously described (Sapir et al., 2010). In a colon tumor model, the knockdown of CCL5 resulted in a reduce tumor growth in mice and decreased apoptosis of tumor-infiltrated $CD8^+$ T cells. This indicates that CCL5 not only induced the migration of immunosuppressive cells to the tumor microenvironment, but also enhances their suppressive activity (Chang et al., 2012). In agreement with this observation, we found after mCCR5-Ig treatment 3 out of 7 mice were still alive in the therapy group while all mice were dead in the control group (Fig. 15). Furthermore, the frequency of MDSC were found to be decreased in the skin tumors after the treatment, suggesting that CCR5 have the capacity to induce the migration of these cells to melanoma lesions in *ret* transgenic mice (Fig. 16-17). We detected reduced production of NO by MDSC in the tumor of the mCCR5-Ig group as compared to the control group and to the BM. Interestingly, we found that not only $CCR5^+$ MDSC but also $CCR5^+$ Treg were reduced in the skin tumors of treated mice as compared to mice treated with anti-mouse IgG (control mice). Moreover, the frequency of these tumor-infiltrating cells was shown to be decreased during melanoma progression (Fig. 16-17). The activity of Treg, indicated by the expression of CD69, was reduced in the metastatic LN of the therapy group as compared to the control group. Moreover, the frequency of effector $CD4^+$ and $CD8^+$ T cells showed a tendency for increase in the tumors of mCCR5-Ig injected mice as compared to the control group (Fig. 17).

A recent study indicated that CCR5 is expressed mostly on metastatic colorectal cancer cells and to some extent on lymphocytes and myeloid cells (Halama et al., 2016). They found that T cells in colorectal cancer invasive margins promote the growth and invasiveness of tumor cells by the secretion of CCL5. It was demonstrated that the blockage of CCR5 by maraviroc leads to an inhibition of tumor cells migration and induces tumor cell death in colon cancer

patients. CCL5/CCR3 axis was found to induce metastasis formation also in breast cancer (Velasco-Velazquez et al., 2014; Palucka and Coussens, 2016).

Moreover, in a basal breast cancer model, CCR5 induced tumor cell invasiveness and metastasis (Velasco-Velazquez and Pestell, 2013), whereas the blockage of CCR5 by maraviroc or vicriviroc reduced metastasis (Velasco-Velazquez et al., 2012). Furthermore, maraviroc hampers the development of hepatocellular carcinoma (Ochoa-Callejero et al., 2013) in mice and reduces pulmonary metastasis in mouse models of breast cancer (Velasco-Velazquez et al., 2012) indicating that CCR5 antagonists can be used as a therapy to reduce the risk of metastasis in basal breast cancer patients.

5.8 Conclusion

Immunosuppressive cells like MDSC play a crucial role in the network that regulates anti-tumor immune response. Therefore, the exact mechanism for their migration and activation need to be elucidated.

In this study, we discovered a new role for CCR5-CCR5 ligand interactions in the recruitment of immunosuppressive cells to the site of tumor. We found high levels of CCR5 ligands and pro-inflammatory mediators in melanoma lesions of *ret* transgenic mice and in skin metastasis of patients that were able to attract $CCR5^+$ cells to the site of tumor. We demonstrated for the first time that CCR5 expression is elevated on MDSC, which was correlated with an increased immunosuppressive phenotype and an elevated activity of MDSC to inhibit anti-tumor immunity in a mouse melanoma model and melanoma patients. Moreover, the blockage of CCR5 ligands by mCCR5-Ig inhibited MDSC tumor-infiltration and restored $CD4^+$ and $CD8^+$ T cell accumulation in the tumor microenvironment. These results create a basis for the development of novel combinatory immunotherapeutic strategies for melanoma patients.

6 References

Abschuetz, O., Osen, W., Frank, K., Kato, M., Schadendorf, D., and Umansky, V. (2012). T-Cell Mediated Immune Responses Induced in ret Transgenic Mouse Model of Malignant Melanoma. Cancers (Basel) *4*, 490-503.

Alberts, B., Johnson, A., Lewis, J., Raff, M., Roberts, K., and Peter, W. (2015). Molecular Biology of the Cell. 6th edition. New York: Garland Science.

Aldinucci, D., and Colombatti, A. (2014). The inflammatory chemokine CCL5 and cancer progression. Mediators Inflamm *2014*, 292376.

Arvelo, F., Sojo, F., and Cotte, C. (2016). Tumour progression and metastasis. Ecancermedicalscience *10*, 617.

Balistreri, C.R., Carruba, G., Calabro, M., Campisi, I., Di Carlo, D., Lio, D., Colonna-Romano, G., Candore, G., and Caruso, C. (2009). CCR5 proinflammatory allele in prostate cancer risk: a pilot study in patients and centenarians from Sicily. Ann N Y Acad Sci *1155*, 289-292.

Baniyash, M. (2004). TCR zeta-chain downregulation: curtailing an excessive inflammatory immune response. Nat Rev Immunol *4*, 675-687.

Barmania, F., and Pepper, M.S. (2013). C-C chemokine receptor type five (CCR5): An emerging target for the control of HIV infection. Applied & Translational Genomics *2*, 3-16.

Berencsi, K., Rani, P., Zhang, T., Gross, L., Mastrangelo, M., Meropol, N.J., Herlyn, D., and Somasundaram, R. (2011). In vitro migration of cytotoxic T lymphocyte derived from a colon carcinoma patient is dependent on CCL2 and CCR2. J Transl Med *9*, 33.

Bergmann, C., Strauss, L., Wang, Y., Szczepanski, M.J., Lang, S., Johnson, J.T., and Whiteside, T.L. (2008). T regulatory type 1 cells in squamous cell carcinoma of the head and neck: mechanisms of suppression and expansion in advanced disease. Clin Cancer Res *14*, 3706-3715.

Bertolotto, C. (2013). Melanoma: From Melanocyte to Genetic Alterations and Clinical Options. Scientifica (Cairo) *2013*, 635203.

Bhatia, S., Tykodi, S.S., and Thompson, J.A. (2009). Treatment of metastatic melanoma: an overview. Oncology (Williston Park) *23*, 488-496.

Bindea, G., Mlecnik, B., Angell, H.K., and Galon, J. (2014). The immune landscape of human tumors: Implications for cancer immunotherapy. Oncoimmunology *3*, e27456.

Bonomo, A., Kehn, P.J., and Shevach, E.M. (1995). Post-thymectomy autoimmunity: abnormal T-cell homeostasis. Immunol Today *16*, 61-67.

Bronte, V., Serafini, P., De Santo, C., Marigo, I., Tosello, V., Mazzoni, A., Segal, D.M., Staib, C., Lowel, M., Sutter, G., Colombo, M.P., and Zanovello, P. (2003). IL-4-induced arginase 1 suppresses alloreactive T cells in tumor-bearing mice. J Immunol *170*, 270-278.

Bryant, V.L., and Slade, C.A. (2015). Chemokines, their receptors and human disease: the good, the bad and the itchy. Immunol Cell Biol *93*, 364-371.

Cambien, B., Richard-Fiardo, P., Karimdjee, B.F., Martini, V., Ferrua, B., Pitard, B., Schmid-Antomarchi, H., and Schmid-Alliana, A. (2011). CCL5 neutralization restricts cancer growth and potentiates the targeting of PDGFRbeta in colorectal carcinoma. PLoS One *6*, e28842.

Chang, L.Y., Lin, Y.C., Mahalingam, J., Huang, C.T., Chen, T.W., Kang, C.W., Peng, H.M., Chu, Y.Y., Chiang, J.M., Dutta, A., Day, Y.J., Chen, T.C., Yeh, C.T., and Lin, C.Y. (2012). Tumor-derived chemokine CCL5 enhances TGF-beta-mediated killing of CD8(+) T cells in colon cancer by T-regulatory cells. Cancer Res *72*, 1092-1102.

Chapman, P.B., Hauschild, A., Robert, C., Haanen, J.B., Ascierto, P., Larkin, J., Dummer, R., Garbe, C., Testori, A., Maio, M., Hogg, D., Lorigan, P., Lebbe, C., Jouary, T., Schadendorf, D., Ribas, A., O'Day, S.J., Sosman, J.A., Kirkwood, J.M., Eggermont, A.M., Dreno, B., Nolop, K., Li, J., Nelson, B., Hou, J., Lee, R.J., Flaherty, K.T., and McArthur, G.A. (2011). Improved survival with vemurafenib in melanoma with BRAF V600E mutation. N Engl J Med *364*, 2507-2516.

Cheng, P., Corzo, C.A., Luetteke, N., Yu, B., Nagaraj, S., Bui, M.M., Ortiz, M., Nacken, W., Sorg, C., Vogl, T., Roth, J., and Gabrilovich, D.I. (2008). Inhibition of dendritic cell differentiation and accumulation of myeloid-derived suppressor cells in cancer is regulated by S100A9 protein. J Exp Med *205*, 2235-2249.

Condamine, T., and Gabrilovich, D.I. (2011). Molecular mechanisms regulating myeloid-derived suppressor cell differentiation and function. Trends Immunol *32*, 19-25.

Davar, D., and Kirkwood, J.M. (2016). Adjuvant Therapy of Melanoma. Cancer Treat Res *167*, 181-208.

de Oliveira, C.E., Oda, J.M., Losi Guembarovski, R., de Oliveira, K.B., Ariza, C.B., Neto, J.S., Banin Hirata, B.K., and Watanabe, M.A. (2014). CC chemokine receptor 5: the interface of host immunity and cancer. Dis Markers *2014*, 126954.

De Veirman, K., Van Valckenborgh, E., Lahmar, Q., Geeraerts, X., De Bruyne, E., Menu, E., Van Riet, I., Vanderkerken, K., and Van Ginderachter, J.A. (2014). Myeloid-derived suppressor cells as therapeutic target in hematological malignancies. Front Oncol *4*, 349.

Dean, M., Carrington, M., Winkler, C., Huttley, G.A., Smith, M.W., Allikmets, R., Goedert, J.J., Buchbinder, S.P., Vittinghoff, E., Gomperts, E., Donfield, S., Vlahov, D., Kaslow, R., Saah, A., Rinaldo, C., Detels, R., and O'Brien, S.J. (1996). Genetic restriction of HIV-1 infection and progression to AIDS by a deletion allele of the CKR5 structural gene. Hemophilia Growth and Development Study, Multicenter AIDS Cohort Study, Multicenter Hemophilia Cohort Study, San Francisco City Cohort, ALIVE Study. Science *273*, 1856-1862.

Dunn, G.P., Bruce, A.T., Ikeda, H., Old, L.J., and Schreiber, R.D. (2002). Cancer immunoediting: from immunosurveillance to tumor escape. Nat Immunol *3*, 991-998.

Facciabene, A., Motz, G.T., and Coukos, G. (2012). T-regulatory cells: key players in tumor immune escape and angiogenesis. Cancer Res *72*, 2162-2171.

Filipazzi, P., Huber, V., and Rivoltini, L. (2012). Phenotype, function and clinical implications of myeloid-derived suppressor cells in cancer patients. Cancer Immunol Immunother *61*, 255-263.

Fontenot, J.D., Gavin, M.A., and Rudensky, A.Y. (2003). Foxp3 programs the development and function of CD4+CD25+ regulatory T cells. Nat Immunol *4*, 330-336.

Fujimura, T., Ring, S., Umansky, V., Mahnke, K., and Enk, A.H. (2012). Regulatory T cells stimulate B7-H1 expression in myeloid-derived suppressor cells in ret melanomas. J Invest Dermatol *132*, 1239-1246.

Fukada, K., Sobao, Y., Tomiyama, H., Oka, S., and Takiguchi, M. (2002). Functional expression of the chemokine receptor CCR5 on virus epitope-specific memory and effector CD8+ T cells. J Immunol *168*, 2225-2232.

Gabrilovich, D.I., and Nagaraj, S. (2009). Myeloid-derived suppressor cells as regulators of the immune system. Nat Rev Immunol *9*, 162-174.

Gabrilovich, D.I., Ostrand-Rosenberg, S., and Bronte, V. (2012). Coordinated regulation of myeloid cells by tumours. Nat Rev Immunol *12*, 253-268.

Garbe, C., Peris, K., Hauschild, A., Saiag, P., Middleton, M., Spatz, A., Grob, J.J., Malvehy, J., Newton-Bishop, J., Stratigos, A., Pehamberger, H., and Eggermont, A. (2010). Diagnosis and treatment of melanoma: European consensus-based interdisciplinary guideline. Eur J Cancer *46*, 270-283.

Gonzalez-Martin, A., Gomez, L., Lustgarten, J., Mira, E., and Manes, S. (2011). Maximal T cell-mediated antitumor responses rely upon CCR5 expression in both CD4(+) and CD8(+) T cells. Cancer Res *71*, 5455-5466.

Gonzalez-Martin, A., Mira, E., and Manes, S. (2012). CCR5 in cancer immunotherapy: More than an "attractive" receptor for T cells. Oncoimmunology *1*, 106-108.

Gros, A., Turcotte, S., Wunderlich, J.R., Ahmadzadeh, M., Dudley, M.E., and Rosenberg, S.A. (2012). Myeloid cells obtained from the blood but not from the tumor can suppress T-cell proliferation in patients with melanoma. Clin Cancer Res *18*, 5212-5223.

Gwak, J.M., Jang, M.H., Kim, D.I., Seo, A.N., and Park, S.Y. (2015). Prognostic value of tumor-associated macrophages according to histologic locations and hormone receptor status in breast cancer. PLoS One *10*, e0125728.

Halama, N., Zoernig, I., Berthel, A., Kahlert, C., Klupp, F., Suarez-Carmona, M., Suetterlin, T., Brand, K., Krauss, J., Lasitschka, F., Lerchl, T., Luckner-Minden, C., Ulrich, A., Koch, M., Weitz, J., Schneider, M., Buechler, M.W., Zitvogel, L., Herrmann, T., Benner, A., Kunz, C., Luecke, S., Springfeld, C., Grabe, N., Falk, C.S., and Jaeger, D. (2016). Tumoral Immune Cell Exploitation in Colorectal Cancer Metastases Can Be Targeted Effectively by Anti-CCR5 Therapy in Cancer Patients. Cancer Cell *29*, 587-601.

Hanahan, D., and Weinberg, R.A. (2011). Hallmarks of cancer: the next generation. Cell *144*, 646-674.

Harper, A.R., Nayee, S., and Topol, E.J. (2015). Protective alleles and modifier variants in human health and disease. Nat Rev Genet *16*, 689-701.

He, J., Hu, Y., Hu, M., and Li, B. (2015). Development of PD-1/PD-L1 Pathway in Tumor Immune Microenvironment and Treatment for Non-Small Cell Lung Cancer. Sci Rep *5*, 13110.

Hong, M., Puaux, A.L., Huang, C., Loumagne, L., Tow, C., Mackay, C., Kato, M., Prevost-Blondel, A., Avril, M.F., Nardin, A., and Abastado, J.P. (2011). Chemotherapy induces intratumoral expression of chemokines in cutaneous melanoma, favoring T-cell infiltration and tumor control. Cancer Res *71*, 6997-7009.

Houghton, A.N., and Polsky, D. (2002). Focus on melanoma. Cancer Cell *2*, 275-278.

Hu-Lieskovan, S., Mok, S., Homet Moreno, B., Tsoi, J., Robert, L., Goedert, L., Pinheiro, E.M., Koya, R.C., Graeber, T.G., Comin-Anduix, B., and Ribas, A. (2015). Improved antitumor activity of immunotherapy with BRAF and MEK inhibitors in BRAF(V600E) melanoma. Sci Transl Med *7*, 279ra241.

Jayaraman, P., Parikh, F., Lopez-Rivera, E., Hailemichael, Y., Clark, A., Ma, G., Cannan, D., Ramacher, M., Kato, M., Overwijk, W.W., Chen, S.H., Umansky, V.Y., and Sikora, A.G. (2012). Tumor-expressed inducible nitric oxide synthase controls induction of functional myeloid-derived suppressor cells through modulation of vascular endothelial growth factor release. J Immunol *188*, 5365-5376.

Jiang, H., Gebhardt, C., Umansky, L., Beckhove, P., Schulze, T.J., Utikal, J., and Umansky, V. (2015). Elevated chronic inflammatory factors and myeloid-derived suppressor cells indicate poor prognosis in advanced melanoma patients. Int J Cancer *136*, 2352-2360.

Jo, M., and Jung, S.T. (2016). Engineering therapeutic antibodies targeting G-protein-coupled receptors. Exp Mol Med *48*, e207.

Jones, E., Dahm-Vicker, M., Simon, A.K., Green, A., Powrie, F., Cerundolo, V., and Gallimore, A. (2002). Depletion of CD25+ regulatory cells results in suppression of melanoma growth and induction of autoreactivity in mice. Cancer Immun *2*, 1.

Josefowicz, S.Z., Lu, L.F., and Rudensky, A.Y. (2012). Regulatory T cells: mechanisms of differentiation and function. Annu Rev Immunol *30*, 531-564.

Katanov, C., Lerrer, S., Liubomirski, Y., Leider-Trejo, L., Meshel, T., Bar, J., Feniger-Barish, R., Kamer, I., Soria-Artzi, G., Kahani, H., Banerjee, D., and Ben-Baruch, A. (2015). Regulation of the inflammatory profile of stromal cells in human breast cancer: prominent roles for TNF-alpha and the NF-kappaB pathway. Stem Cell Res Ther *6*, 87.

Kato, M., Takahashi, M., Akhand, A.A., Liu, W., Dai, Y., Shimizu, S., Iwamoto, T., Suzuki, H., and Nakashima, I. (1998). Transgenic mouse model for skin malignant melanoma. Oncogene *17*, 1885-1888.

Kawai, T., and Akira, S. (2010). The role of pattern-recognition receptors in innate immunity: update on Toll-like receptors. Nat Immunol *11*, 373-384.

Kimpfler, S., Sevko, A., Ring, S., Falk, C., Osen, W., Frank, K., Kato, M., Mahnke, K., Schadendorf, D., and Umansky, V. (2009). Skin melanoma development in ret transgenic mice despite the depletion of CD25+Foxp3+ regulatory T cells in lymphoid organs. J Immunol *183*, 6330-6337.

Kitamura, T., Qian, B.Z., and Pollard, J.W. (2015a). Immune cell promotion of metastasis. Nat Rev Immunol *15*, 73-86.

Kitamura, T., Qian, B.Z., Soong, D., Cassetta, L., Noy, R., Sugano, G., Kato, Y., Li, J., and Pollard, J.W. (2015b). CCL2-induced chemokine cascade promotes breast cancer metastasis by enhancing retention of metastasis-associated macrophages. J Exp Med *212*, 1043-1059.

Koizumi, K., Hojo, S., Akashi, T., Yasumoto, K., and Saiki, I. (2007). Chemokine receptors in cancer metastasis and cancer cell-derived chemokines in host immune response. Cancer Sci *98*, 1652-1658.

Koshenkov, V.P., Broucek, J., and Kaufman, H.L. (2016). Surgical Management of Melanoma. Cancer Treat Res *167*, 149-179.

Kumar, V., Patel, S., Tcyganov, E., and Gabrilovich, D.I. (2016). The Nature of Myeloid-Derived Suppressor Cells in the Tumor Microenvironment. Trends Immunol *37*, 208-220.

Kusmartsev, S., and Gabrilovich, D.I. (2003). Inhibition of myeloid cell differentiation in cancer: the role of reactive oxygen species. J Leukoc Biol *74*, 186-196.

Kusmartsev, S., Nefedova, Y., Yoder, D., and Gabrilovich, D.I. (2004). Antigen-specific inhibition of CD8+ T cell response by immature myeloid cells in cancer is mediated by reactive oxygen species. J Immunol *172*, 989-999.

Kusmartsev, S., and Gabrilovich, D.I. (2005). STAT1 signaling regulates tumor-associated macrophage-mediated T cell deletion. J Immunol *174*, 4880-4891.

Laidlaw, B.J., Craft, J.E., and Kaech, S.M. (2016). The multifaceted role of CD4(+) T cells in CD8(+) T cell memory. Nat Rev Immunol *16*, 102-111.

Li, X., Kostareli, E., Suffner, J., Garbi, N., and Hammerling, G.J. (2010). Efficient Treg depletion induces T-cell infiltration and rejection of large tumors. Eur J Immunol *40*, 3325-3335.

Lin, S., Wan, S., Sun, L., Hu, J., Fang, D., Zhao, R., Yuan, S., and Zhang, L. (2012). Chemokine C-C motif receptor 5 and C-C motif ligand 5 promote cancer cell migration under hypoxia. Cancer Sci *103*, 904-912.

Lindau, D., Gielen, P., Kroesen, M., Wesseling, P., and Adema, G.J. (2013). The immunosuppressive tumour network: myeloid-derived suppressor cells, regulatory T cells and natural killer T cells. Immunology *138*, 105-115.

Liu, R., Paxton, W.A., Choe, S., Ceradini, D., Martin, S.R., Horuk, R., MacDonald, M.E., Stuhlmann, H., Koup, R.A., and Landau, N.R. (1996). Homozygous defect in HIV-1 coreceptor accounts for resistance of some multiply-exposed individuals to HIV-1 infection. Cell *86*, 367-377.

Lu, T., and Gabrilovich, D.I. (2012). Molecular pathways: tumor-infiltrating myeloid cells and reactive oxygen species in regulation of tumor microenvironment. Clin Cancer Res *18*, 4877-4882.

MacKie, R.M., Hauschild, A., and Eggermont, A.M. (2009). Epidemiology of invasive cutaneous melanoma. Ann Oncol *20 Suppl 6*, vi1-7.

Marvel, D., and Gabrilovich, D.I. (2015). Myeloid-derived suppressor cells in the tumor microenvironment: expect the unexpected. J Clin Invest *125*, 3356-3364.

McCarter, M.D., Baumgartner, J., Escobar, G.A., Richter, D., Lewis, K., Robinson, W., Wilson, C., Palmer, B.E., and Gonzalez, R. (2007). Immunosuppressive dendritic and

regulatory T cells are upregulated in melanoma patients. Ann Surg Oncol *14*, 2854-2860.

Meirow, Y., Kanterman, J., and Baniyash, M. (2015). Paving the Road to Tumor Development and Spreading: Myeloid-Derived Suppressor Cells are Ruling the Fate. Front Immunol *6*, 523.

Meyer, C., Sevko, A., Ramacher, M., Bazhin, A.V., Falk, C.S., Osen, W., Borrello, I., Kato, M., Schadendorf, D., Baniyash, M., and Umansky, V. (2011). Chronic inflammation promotes myeloid-derived suppressor cell activation blocking antitumor immunity in transgenic mouse melanoma model. Proc Natl Acad Sci U S A *108*, 17111-17116.

Mogensen, T.H. (2009). Pathogen recognition and inflammatory signaling in innate immune defenses. Clin Microbiol Rev *22*, 240-273.

Molon, B., Gri, G., Bettella, M., Gomez-Mouton, C., Lanzavecchia, A., Martinez, A.C., Manes, S., and Viola, A. (2005). T cell costimulation by chemokine receptors. Nat Immunol *6*, 465-471.

Monu, N.R., and Frey, A.B. (2012). Myeloid-derived suppressor cells and anti-tumor T cells: a complex relationship. Immunol Invest *41*, 595-613.

Mosmann, T.R., Cherwinski, H., Bond, M.W., Giedlin, M.A., and Coffman, R.L. (1986). Two types of murine helper T cell clone. I. Definition according to profiles of lymphokine activities and secreted proteins. J Immunol *136*, 2348-2357.

Murphy, K.M., Travers, P., Walport, M., and Ehrenstein, M. (2009). Janeway - Immunologie, 7. Aufl. edn Heidelberg: Spektrum, Akad. Verl.

Nagaraj, S., and Gabrilovich, D.I. (2010). Myeloid-derived suppressor cells in human cancer. Cancer J *16*, 348-353.

Ng-Cashin, J., Kuhns, J.J., Burkett, S.E., Powderly, J.D., Craven, R.R., van Deventer, H.W., Kirby, S.L., and Serody, J.S. (2003). Host absence of CCR5 potentiates dendritic cell vaccination. J Immunol *170*, 4201-4208.

Nikolaou, V., and Stratigos, A.J. (2014). Emerging trends in the epidemiology of melanoma. Br J Dermatol *170*, 11-19.

Nishikawa, H., and Sakaguchi, S. (2010). Regulatory T cells in tumor immunity. Int J Cancer *127*, 759-767.

Noman, M.Z., Desantis, G., Janji, B., Hasmim, M., Karray, S., Dessen, P., Bronte, V., and Chouaib, S. (2014). PD-L1 is a novel direct target of HIF-1alpha, and its blockade under hypoxia enhanced MDSC-mediated T cell activation. J Exp Med *211*, 781-790.

Ochoa-Callejero, L., Perez-Martinez, L., Rubio-Mediavilla, S., Oteo, J.A., Martinez, A., and Blanco, J.R. (2013). Maraviroc, a CCR5 antagonist, prevents development of hepatocellular carcinoma in a mouse model. PLoS One *8*, e53992.

Ochoa, A.C., Zea, A.H., Hernandez, C., and Rodriguez, P.C. (2007). Arginase, prostaglandins, and myeloid-derived suppressor cells in renal cell carcinoma. Clin Cancer Res *13*, 721s-726s.

Oldham, K.A., Parsonage, G., Bhatt, R.I., Wallace, D.M., Deshmukh, N., Chaudhri, S., Adams, D.H., and Lee, S.P. (2012). T lymphocyte recruitment into renal cell carcinoma tissue:

a role for chemokine receptors CXCR3, CXCR6, CCR5, and CCR6. Eur Urol *61*, 385-394.

Ostrand-Rosenberg, S., and Sinha, P. (2009). Myeloid-derived suppressor cells: linking inflammation and cancer. J Immunol *182*, 4499-4506.

Ott, P.A. (2015). Combined BRAF and MEK inhibition in BRAF(V600E) mutant melanoma: a synergistic and potentially safe combination partner with immunotherapy. Ann Transl Med *3*, 313.

Palmieri, G., Ombra, M., Colombino, M., Casula, M., Sini, M., Manca, A., Paliogiannis, P., Ascierto, P.A., and Cossu, A. (2015). Multiple Molecular Pathways in Melanomagenesis: Characterization of Therapeutic Targets. Front Oncol *5*, 183.

Palomino, D.C., and Marti, L.C. (2015). Chemokines and immunity. Einstein (Sao Paulo) *13*, 469-473.

Palucka, A.K., and Coussens, L.M. (2016). The Basis of Oncoimmunology. Cell *164*, 1233-1247.

Pan, P.Y., Ma, G., Weber, K.J., Ozao-Choy, J., Wang, G., Yin, B., Divino, C.M., and Chen, S.H. (2010). Immune stimulatory receptor CD40 is required for T-cell suppression and T regulatory cell activation mediated by myeloid-derived suppressor cells in cancer. Cancer Res *70*, 99-108.

Pletinckx, K., Dohler, A., Pavlovic, V., and Lutz, M.B. (2011). Role of dendritic cell maturity/costimulation for generation, homeostasis, and suppressive activity of regulatory T cells. Front Immunol *2*, 39.

Qian, B.Z., Li, J., Zhang, H., Kitamura, T., Zhang, J., Campion, L.R., Kaiser, E.A., Snyder, L.A., and Pollard, J.W. (2011). CCL2 recruits inflammatory monocytes to facilitate breast-tumour metastasis. Nature *475*, 222-225.

Quail, D.F., and Joyce, J.A. (2013). Microenvironmental regulation of tumor progression and metastasis. Nat Med *19*, 1423-1437.

Quatromoni, J.G., and Eruslanov, E. (2012). Tumor-associated macrophages: function, phenotype, and link to prognosis in human lung cancer. Am J Transl Res *4*, 376-389.

Radulovic, K., and Niess, J.H. (2015). CD69 is the crucial regulator of intestinal inflammation: a new target molecule for IBD treatment? J Immunol Res *2015*, 497056.

Raedler, L.A. (2015). Keytruda (Pembrolizumab): First PD-1 Inhibitor Approved for Previously Treated Unresectable or Metastatic Melanoma. Am Health Drug Benefits *8*, 96-100.

Redman, J.M., Gibney, G.T., and Atkins, M.B. (2016). Advances in immunotherapy for melanoma. BMC Med *14*, 20.

Robert, C., Karaszewska, B., Schachter, J., Rutkowski, P., Mackiewicz, A., Stroiakovski, D., Lichinitser, M., Dummer, R., Grange, F., Mortier, L., Chiarion-Sileni, V., Drucis, K., Krajsova, I., Hauschild, A., Lorigan, P., Wolter, P., Long, G.V., Flaherty, K., Nathan, P., Ribas, A., Martin, A.M., Sun, P., Crist, W., Legos, J., Rubin, S.D., Little, S.M., and Schadendorf, D. (2015). Improved overall survival in melanoma with combined dabrafenib and trametinib. N Engl J Med *372*, 30-39.

Robinson, S.C., Scott, K.A., Wilson, J.L., Thompson, R.G., Proudfoot, A.E., and Balkwill, F.R. (2003). A chemokine receptor antagonist inhibits experimental breast tumor growth. Cancer Res *63*, 8360-8365.

Rudolph, B.M., Loquai, C., Gerwe, A., Bacher, N., Steinbrink, K., Grabbe, S., and Tuettenberg, A. (2014). Increased frequencies of CD11b(+) CD33(+) CD14(+) HLA-DR(low) myeloid-derived suppressor cells are an early event in melanoma patients. Exp Dermatol *23*, 202-204.

Sade-Feldman, M., Kanterman, J., Ish-Shalom, E., Elnekave, M., Horwitz, E., and Baniyash, M. (2013). Tumor necrosis factor-alpha blocks differentiation and enhances suppressive activity of immature myeloid cells during chronic inflammation. Immunity *38*, 541-554.

Sakaguchi, S., Sakaguchi, N., Asano, M., Itoh, M., and Toda, M. (1995). Immunologic self-tolerance maintained by activated T cells expressing IL-2 receptor alpha-chains (CD25). Breakdown of a single mechanism of self-tolerance causes various autoimmune diseases. J Immunol *155*, 1151-1164.

Samson, M., Libert, F., Doranz, B.J., Rucker, J., Liesnard, C., Farber, C.M., Saragosti, S., Lapoumeroulie, C., Cognaux, J., Forceille, C., Muyldermans, G., Verhofstede, C., Burtonboy, G., Georges, M., Imai, T., Rana, S., Yi, Y., Smyth, R.J., Collman, R.G., Doms, R.W., Vassart, G., and Parmentier, M. (1996). Resistance to HIV-1 infection in caucasian individuals bearing mutant alleles of the CCR-5 chemokine receptor gene. Nature *382*, 722-725.

Sandhu, S.K., Papadopoulos, K., Fong, P.C., Patnaik, A., Messiou, C., Olmos, D., Wang, G., Tromp, B.J., Puchalski, T.A., Balkwill, F., Berns, B., Seetharam, S., de Bono, J.S., and Tolcher, A.W. (2013). A first-in-human, first-in-class, phase I study of carlumab (CNTO 888), a human monoclonal antibody against CC-chemokine ligand 2 in patients with solid tumors. Cancer Chemother Pharmacol *71*, 1041-1050.

Sapir, Y., Vitenshtein, A., Barsheshet, Y., Zohar, Y., Wildbaum, G., and Karin, N. (2010). A fusion protein encoding the second extracellular domain of CCR5 arrests chemokine-induced cosignaling and effectively suppresses ongoing experimental autoimmune encephalomyelitis. J Immunol *185*, 2589-2599.

Schilling, B., Sucker, A., Griewank, K., Zhao, F., Weide, B., Gorgens, A., Giebel, B., Schadendorf, D., and Paschen, A. (2013). Vemurafenib reverses immunosuppression by myeloid derived suppressor cells. Int J Cancer *133*, 1653-1663.

Schlecker, E., Stojanovic, A., Eisen, C., Quack, C., Falk, C.S., Umansky, V., and Cerwenka, A. (2012). Tumor-infiltrating monocytic myeloid-derived suppressor cells mediate CCR5-dependent recruitment of regulatory T cells favoring tumor growth. J Immunol *189*, 5602-5611.

Schmidt, A., Oberle, N., and Krammer, P.H. (2012). Molecular mechanisms of treg-mediated T cell suppression. Front Immunol *3*, 51.

Schouppe, E., De Baetselier, P., Van Ginderachter, J.A., and Sarukhan, A. (2012). Instruction of myeloid cells by the tumor microenvironment: Open questions on the dynamics and plasticity of different tumor-associated myeloid cell populations. Oncoimmunology *1*, 1135-1145.

Sevko, A., Michels, T., Vrohlings, M., Umansky, L., Beckhove, P., Kato, M., Shurin, G.V., Shurin, M.R., and Umansky, V. (2013). Antitumor effect of paclitaxel is mediated by inhibition of myeloid-derived suppressor cells and chronic inflammation in the spontaneous melanoma model. J Immunol *190*, 2464-2471.

Siegel, R.L., Miller, K.D., and Jemal, A. (2016). Cancer statistics, 2016. CA Cancer J Clin *66*, 7-30.

Sinha, P., Clements, V.K., Bunt, S.K., Albelda, S.M., and Ostrand-Rosenberg, S. (2007). Cross-talk between myeloid-derived suppressor cells and macrophages subverts tumor immunity toward a type 2 response. J Immunol *179*, 977-983.

Solito, S., Falisi, E., Diaz-Montero, C.M., Doni, A., Pinton, L., Rosato, A., Francescato, S., Basso, G., Zanovello, P., Onicescu, G., Garrett-Mayer, E., Montero, A.J., Bronte, V., and Mandruzzato, S. (2011). A human promyelocytic-like population is responsible for the immune suppression mediated by myeloid-derived suppressor cells. Blood *118*, 2254-2265.

Solito, S., Marigo, I., Pinton, L., Damuzzo, V., Mandruzzato, S., and Bronte, V. (2014). Myeloid-derived suppressor cell heterogeneity in human cancers. Ann N Y Acad Sci *1319*, 47-65.

Span, P.N., Pollakis, G., Paxton, W.A., Sweep, F.C., Foekens, J.A., Martens, J.W., Sieuwerts, A.M., and van Laarhoven, H.W. (2015). Improved metastasis-free survival in nonadjuvantly treated postmenopausal breast cancer patients with chemokine receptor 5 del32 frameshift mutations. Int J Cancer *136*, 91-97.

Srivastava, M.K., Sinha, P., Clements, V.K., Rodriguez, P., and Ostrand-Rosenberg, S. (2010). Myeloid-derived suppressor cells inhibit T-cell activation by depleting cystine and cysteine. Cancer Res *70*, 68-77.

Strauss, L., Bergmann, C., Szczepanski, M., Gooding, W., Johnson, J.T., and Whiteside, T.L. (2007). A unique subset of CD4+CD25highFoxp3+ T cells secreting interleukin-10 and transforming growth factor-beta1 mediates suppression in the tumor microenvironment. Clin Cancer Res *13*, 4345-4354.

Stritesky, G.L., Jameson, S.C., and Hogquist, K.A. (2012). Selection of self-reactive T cells in the thymus. Annu Rev Immunol *30*, 95-114.

Stromnes, I.M., Greenberg, P.D., and Hingorani, S.R. (2014). Molecular pathways: myeloid complicity in cancer. Clin Cancer Res *20*, 5157-5170.

Sullivan, R.J., and Flaherty, K. (2013). MAP kinase signaling and inhibition in melanoma. Oncogene *32*, 2373-2379.

Sun, H.L., Zhou, X., Xue, Y.F., Wang, K., Shen, Y.F., Mao, J.J., Guo, H.F., and Miao, Z.N. (2012). Increased frequency and clinical significance of myeloid-derived suppressor cells in human colorectal carcinoma. World J Gastroenterol *18*, 3303-3309.

Talmadge, J.E., and Gabrilovich, D.I. (2013). History of myeloid-derived suppressor cells. Nat Rev Cancer *13*, 739-752.

Tan, M.C., Goedegebuure, P.S., Belt, B.A., Flaherty, B., Sankpal, N., Gillanders, W.E., Eberlein, T.J., Hsieh, C.S., and Linehan, D.C. (2009). Disruption of CCR5-dependent

homing of regulatory T cells inhibits tumor growth in a murine model of pancreatic cancer. J Immunol *182*, 1746-1755.

Toda, A., and Piccirillo, C.A. (2006). Development and function of naturally occurring CD4+CD25+ regulatory T cells. J Leukoc Biol *80*, 458-470.

Ugel, S., De Sanctis, F., Mandruzzato, S., and Bronte, V. (2015). Tumor-induced myeloid deviation: when myeloid-derived suppressor cells meet tumor-associated macrophages. J Clin Invest *125*, 3365-3376.

Ugurel, S., Schrama, D., Keller, G., Schadendorf, D., Brocker, E.B., Houben, R., Zapatka, M., Fink, W., Kaufman, H.L., and Becker, J.C. (2008). Impact of the CCR5 gene polymorphism on the survival of metastatic melanoma patients receiving immunotherapy. Cancer Immunol Immunother *57*, 685-691.

Umansky, V., Abschuetz, O., Osen, W., Ramacher, M., Zhao, F., Kato, M., and Schadendorf, D. (2008). Melanoma-specific memory T cells are functionally active in Ret transgenic mice without macroscopic tumors. Cancer Res *68*, 9451-9458.

Umansky, V., and Sevko, A. (2012). Melanoma-induced immunosuppression and its neutralization. Semin Cancer Biol *22*, 319-326.

Umansky, V., and Sevko, A. (2013). Tumor microenvironment and myeloid-derived suppressor cells. Cancer Microenviron *6*, 169-177.

Vaday, G.G., Peehl, D.M., Kadam, P.A., and Lawrence, D.M. (2006). Expression of CCL5 (RANTES) and CCR5 in prostate cancer. Prostate *66*, 124-134.

van Deventer, H.W., O'Connor, W., Jr., Brickey, W.J., Aris, R.M., Ting, J.P., and Serody, J.S. (2005). C-C chemokine receptor 5 on stromal cells promotes pulmonary metastasis. Cancer Res *65*, 3374-3379.

Velasco-Velazquez, M., Jiao, X., De La Fuente, M., Pestell, T.G., Ertel, A., Lisanti, M.P., and Pestell, R.G. (2012). CCR5 antagonist blocks metastasis of basal breast cancer cells. Cancer Res *72*, 3839-3850.

Velasco-Velazquez, M., and Pestell, R.G. (2013). The CCL5/CCR5 axis promotes metastasis in basal breast cancer. Oncoimmunology *2*, e23660.

Velasco-Velazquez, M., Xolalpa, W., and Pestell, R.G. (2014). The potential to target CCL5/CCR5 in breast cancer. Expert Opin Ther Targets *18*, 1265-1275.

Vignali, D.A., Collison, L.W., and Workman, C.J. (2008). How regulatory T cells work. Nat Rev Immunol *8*, 523-532.

Vinay, D.S., Ryan, E.P., Pawelec, G., Talib, W.H., Stagg, J., Elkord, E., Lichtor, T., Decker, W.K., Whelan, R.L., Kumara, H.M., Signori, E., Honoki, K., Georgakilas, A.G., Amin, A., Helferich, W.G., Boosani, C.S., Guha, G., Ciriolo, M.R., Chen, S., Mohammed, S.I., Azmi, A.S., Keith, W.N., Bilsland, A., Bhakta, D., Halicka, D., Fujii, H., Aquilano, K., Ashraf, S.S., Nowsheen, S., Yang, X., Choi, B.K., and Kwon, B.S. (2015). Immune evasion in cancer: Mechanistic basis and therapeutic strategies. Semin Cancer Biol *35 Suppl*, S185-198.

Vincent, J., Mignot, G., Chalmin, F., Ladoire, S., Bruchard, M., Chevriaux, A., Martin, F., Apetoh, L., Rebe, C., and Ghiringhelli, F. (2010). 5-Fluorouracil selectively kills tumor-

associated myeloid-derived suppressor cells resulting in enhanced T cell-dependent antitumor immunity. Cancer Res *70*, 3052-3061.

Wang, H., Li, P., Wang, L., Xia, Z., Huang, H., Lu, Y., and Li, Z. (2015). High numbers of CD68+ tumor-associated macrophages correlate with poor prognosis in extranodal NK/T-cell lymphoma, nasal type. Ann Hematol *94*, 1535-1544.

Wang, R.F., Appella, E., Kawakami, Y., Kang, X., and Rosenberg, S.A. (1996). Identification of TRP-2 as a human tumor antigen recognized by cytotoxic T lymphocytes. J Exp Med *184*, 2207-2216.

Ward, S.T., Li, K.K., Hepburn, E., Weston, C.J., Curbishley, S.M., Reynolds, G.M., Hejmadi, R.K., Bicknell, R., Eksteen, B., Ismail, T., Rot, A., and Adams, D.H. (2015). The effects of CCR5 inhibition on regulatory T-cell recruitment to colorectal cancer. Br J Cancer *112*, 319-328.

Weide, B., Martens, A., Zelba, H., Stutz, C., Derhovanessian, E., Di Giacomo, A.M., Maio, M., Sucker, A., Schilling, B., Schadendorf, D., Buttner, P., Garbe, C., and Pawelec, G. (2014). Myeloid-derived suppressor cells predict survival of patients with advanced melanoma: comparison with regulatory T cells and NY-ESO-1- or melan-A-specific T cells. Clin Cancer Res *20*, 1601-1609.

Wesolowski, R., Markowitz, J., and Carson, W.E., 3rd (2013). Myeloid derived suppressor cells - a new therapeutic target in the treatment of cancer. J Immunother Cancer *1*, 10.

Woo, E.Y., Chu, C.S., Goletz, T.J., Schlienger, K., Yeh, H., Coukos, G., Rubin, S.C., Kaiser, L.R., and June, C.H. (2001). Regulatory CD4(+)CD25(+) T cells in tumors from patients with early-stage non-small cell lung cancer and late-stage ovarian cancer. Cancer Res *61*, 4766-4772.

Youn, J.I., Nagaraj, S., Collazo, M., and Gabrilovich, D.I. (2008). Subsets of myeloid-derived suppressor cells in tumor-bearing mice. J Immunol *181*, 5791-5802.

Zhang, B., Wang, Z., Wu, L., Zhang, M., Li, W., Ding, J., Zhu, J., Wei, H., and Zhao, K. (2013). Circulating and tumor-infiltrating myeloid-derived suppressor cells in patients with colorectal carcinoma. PLoS One *8*, e57114.

Zhao, F., Falk, C., Osen, W., Kato, M., Schadendorf, D., and Umansky, V. (2009). Activation of p38 mitogen-activated protein kinase drives dendritic cells to become tolerogenic in ret transgenic mice spontaneously developing melanoma. Clin Cancer Res *15*, 4382-4390.

Zhou, L., Chong, M.M., and Littman, D.R. (2009). Plasticity of CD4+ T cell lineage differentiation. Immunity *30*, 646-655.

Zhou, Z., French, D.L., Ma, G., Eisenstein, S., Chen, Y., Divino, C.M., Keller, G., Chen, S.H., and Pan, P.Y. (2010). Development and function of myeloid-derived suppressor cells generated from mouse embryonic and hematopoietic stem cells. Stem Cells *28*, 620-632.

Ziegler, S.F. (2006). FOXP3: of mice and men. Annu Rev Immunol *24*, 209-226.

Zimmermann, T., Moehler, M., Gockel, I., Sgourakis, G.G., Biesterfeld, S., Muller, M., Berger, M.R., Lang, H., Galle, P.R., and Schimanski, C.C. (2010). Low expression of

chemokine receptor CCR5 in human colorectal cancer correlates with lymphatic dissemination and reduced CD8+ T-cell infiltration. Int J Colorectal Dis *25*, 417-424.

7 Abbreviation

A	
APC	allophycocyanin
APC	antigen-presenting cells
ARG-1	arginase-1
B	
BM	bone marrow
BSA	bovine serum albumin
C	
CCL	C-C chemokine ligand
CCR	C-C chemokine receptor
CD	cluster of differentiation
CTL	cytotoxic lymphocytes
CTLA-4	cytotoxic T lymphocyte antigen 4
Cy	cyanine
D	
DC	dendritic cells
DMSO	dimethyl sulfoxide
DNA	deoxyribonucleic acid
E	
EDTA	ethylene diamine-tetra-acetic acid
et al.	et alteri
F	
FACS	fluorescence activated cell sorting
FBS	fetal bovine serum
FITC	fluorescein-isothiocyanat
FMO	fluorescence minus one
FoxP3	forkhead box P3
FSC	forward scatter
G	
GM-CSF	granulocyte-macrophage colony-stimulating factor
H	
HLA-DR	human leucocyte antigen-DR
I	
IL	interleukin
IFN	interferon
iNOS	inducible nitric oxide synthase

L

LN	lymph nodes

M

MACS	magnetic-activated cell sorting
MDSC	myeloid-derived suppressor cells
MHC	major histocompatibility complex

N

NO	nitric oxide
Nf-κB	nuclear factor-kappa B

P

PBMC	peripheral blood mononuclear cells
PBS	phosphate buffered saline
PD-1	programmed death 1
PD-L1	programmed death ligand 1
PE	phycoerythrin
PerCp	peridinin-chlorophyll-protein complex
PRR	pattern recognition receptor

R

RBC	red blood cell
ret	human *ret* proto-oncogene
ROS	reactive oxygen species
rpm	rounds per minute
RPMI	Roswell Park Memorial Institute medium
RT	room temperature

S

SSC	side scatter

T

Tcon	conventional $CD4^+$ T cells ($FoxP3^-$)
TCR	T cell receptor
Teff	effector T cells
TGF-β	transforming growth factor beta
TIL	tumor infiltrating lymphocytes
TNF	tumor necrosis factor
Treg	regulator $CD4^+$ T cells ($CD25^+FoxP3^+$)
TRP	tyrosinase related protein

V

VEGF	vascular endothelial growth factor

8 List of Figures

Figure 1: Generation and accumulation of MDSC. IMC are generated in the BM. 6
Figure 2: Gating strategy of CCR5 expressing $CD11b^+Gr1^+$ cells (MDSC) in the BM of tumor bearing mice.....32
Figure 3: CCR5 expression on MDSC of *ret* transgenic tumor bearing mice.....33
Figure 4: Expression of CCR5 on Gr-MDSC and Mo-MDSC in tumor bearing mice.....36
Figure 5: Production of chronic inflammatory mediators in melanoma bearing mice. 37
Figure 6: Chronic inflammatory mediators during tumor progression. 39
Figure 7: Immunosuppressive phenotype of $CCR5^+$ MDSC in *ret* transgenic mice.. 41
Figure 8: Functional phenotype of $CCR5^+$ MDSC in melanoma lesions in course of tumor progression. 44
Figure 9: $CCR5^+$ MDSC from *ret* transgenic mice inhibit T cell proliferation. 45
Figure 10: CCR5 ligand-induced migration capacity of $CD11b^+Gr\text{-}1^+$ cells.....46
Figure 11: Gating strategy of CCR5 expressing T cell subsets in splenocytes of *ret* transgenic mice. 48
Figure 12: CCR5 expression on various T cell subsets of *ret* transgenic mice.. 50
Figure 13: $CCR5^+$ Treg in tumor bearing mice. 51
Figure 14: TRP-2 specificity of CCR5 expressing, $CD8^+$ T cells in melanoma bearing mice. 52
Figure 15: Survival of tumor bearing mice after mCCR5-Ig treatment. 53
Figure 16: mCCR5-Ig reduced the frequency of tumor-infiltrating MDSC in *ret* transgenic mice. 55
Figure 17: Reduced frequency of Treg in mCCR5-Ig treated *ret* transgenic mice.. 56
Figure 18: Gating strategy for $CCR5^+$ MDSC from melanoma patients. 58
Figure 19: Analysis of $CCR5^+$ MDSC of melanoma patients during course of tumor progression. 59
Figure 20: NO production of $CCR5^+$ MDSC in melanoma patients.....61
Figure 21: ROS production of $CCR5^+$ MDSC in melanoma patients. 62
Figure 22: ARG-1 expression on $CCR5^+$ MDSC in melanoma patients.....63
Figure 23: PD-L1 expression on $CCR5^+$ MDSC in melanoma patients. 64
Figure 24: CCR5 expression on immunosuppressive cells in melanoma patients.....65
Figure 25: Increased concentrations of chronic inflammatory factors for MDSC migration in skin tumors of melanoma patients of different stages. 66
Figure 26: Gating strategy of $CD45RA^-CCR5^+CD4^+$Treg. 68

Figure 27: Evaluation of Treg in melanoma patients during tumor progression. PBMC from the peripheral blood of melanoma patients and HD were analyzed by flow cytometry. 70

9 Acknowledgements

First of all, I would like to thank my primary supervisor Prof. Dr. Viktor Umansky for giving me the opportunity to perform my doctoral thesis in his group and supporting me throughout the last three years. Especially, I want to thank Viktor for his scientific guidance, continuous support and all his encouragement during my time in his group that have been absolutely essential for me.

I want to thank PD Dr. Adelheid Cerwenka and Prof. Dr. Stefan Schneider for being a part of my thesis advisory committee. I am grateful for their valuable input and critical advice. Moreover, I also want to acknowledge Prof. Dr. Markus Feuerer and Prof. Dr. Ana Martin-Villalba for enrolling as examiners in my disputation.

I want to thank Prof. Dr. Jochen Utikal and Dr. Christoffer Gebhardt for their clinical input and constructive comments during my work. I thank Prof. Dr. Hans-Peter Altevogt for sharing his scientific knowledge and giving supportive suggestions and ideas for further progress.

I want to acknowledge Stefanie Uhlig from the Core Facility “FlowCore Mannheim” for her technical support in cell sorting and Ludmila Umansky for helping me to perform bio-plex assays.

I would like to thank Bianca Himmelhan, Sara Becker and Eva-Maria Stork for their great help with my project and being my Master/ Bachelor students.

I want to thank all my lab colleagues for the great atmosphere, their helpful advices and their support in having coffees ☺ : Mareike Grees, Viktor Fleming, Xiaojing Hu, Loreen Kloss, Sonja Simon, Daniel Thomas and Christos Evangelou.

Furthermore, I would like to thank all my friends for sharing so many beautiful and unforgettable moments with me.

The greatest thank is addressed to my family. To my parents for their endless support, their motivation and for always being there and giving me strength. They gave me the opportunity to become who I am. No matter which decision I will take, I know that they will always be on my side and do everything for me that is possible. Without them I would have never reached so far. Finally, I want to thank Rico for being on my side and supporting me from the beginning on. Thank you for your care, your positive encouragement and for believing in me. I can always count on you.